A MICROPROCESSOR SYSTEM FOR INTERNAL COMBUSTION ENGINE PV DIAGRAM ANALYSIS

BY

YVES BOULANGER

A thesis submitted to the Faculty of Graduate Studies and Research in partial fulfillment of the requirements for the degree of Master of Engineering

Department of Mechanical Engineering
McGill University
Montréal, Canada

July 1988

ABSTRACT

An internal combustion engine was instrumented in view of developing automatic diagnosis methods based on the analysis of PV diagrams.

The pressure signal is unstable over successive cycles. Consequently, pressure must be averaged over several consecutive cycles to produce valid data.

Due to instrumentation problems the data obtained was insufficient to allow the development of diagnostics. The investigation reported in this work is thus limited to the development of a microprocessor-based system for the acquisition of pressure-volume data on high speed, spark ignition internal combustion engines.

Several instrumentation problems were identified and solutions applied or proposed. The information presented here can form the basis for further research on the original project.

SOMMAIRE

Un moteur fut équipé d'un microprocesseur pour l'acquisition et l'analyse de diagrammes PV dans le but de développer des méthodes diagnostiques.

Il existe une grande variabilité de la pression lors de cycles successifs. On doit calculer la moyenne des pressions sur plusieurs cycles consécutifs afin d'obtenir des données valables.

A cause de problêmes d'instrumentation, les données obtenues furent insuffisantes pour permettre le développement de méthodes diagnostiques. Les travaux présentés dans ce rapport se limitent au développement d'un système de microprocesseur pour l'acquisition de données p-v d'un moteur à combustion interne à haute vitesse et à allumage par bougie.

Plusieurs problêmes ont été identifiés et des solutions ont été adoptées ou suggérées. L'information contenue dans ce rapport peut former la base d'un projet de recherche sur le sujet original.

ACKNOWLEDGEMENTS

The work presented in this report was carried under the supervision of Dr. Paul J. Zsombor-Murray and of Mr. Louis J. Vroomen. The author wishes to express his deepest gratitude to them for their guidance and encouragement throughout the course of this project.

Special thanks are also due to Mr. George Dedic and staff for assistance with the instrumentation and computer equipment; to Mr. Jack Kelly and staff for assistance in the fabrication of the test bed; to Mr. Jean Fortin for assistance in debugging the instrumentation; to Mr. John Hoard of the Ford Company for sharing information on PV data acquisition and finally to Mr. Zhao Jien for his assistance during the experiments.

TABLE OF CONTENTS

LIST OF FIGURES

LIST OF TABLES

LIST OF SYMBOLS AND ABBREVIATIONS

PV: Pressure Volume (diagram)

TDC: Top Dead Center

IMEP: Indicated Mean Effective Pressure

IC: Internal Combustion (engine)

AEI: Automatic Engine Indicator

ADC: Analog to Digital Converter

PIA: Parallel Interface Adapter

p: pressure

U: internal energy

f: fraction by volume of burnt gas in intake mixture

T: temperature

Chart Quantity: the quantity of mixture containing 1 lb (454g) of air (*)

H: enthalpy

C: chemical energy (lower heating value) (*)

K: constant factor in equation: V=KT/p (derived from perfect gas equation) (*)

S_v: constant volume entropy

S: entropy

v: volume

x: position of piston relative to TDC

l: length of connecting rod between bearing centers

r: radius

v: angular position of connecting rod relative to piston axis

---

* as defined by ref. (15)

ϕ: angular position of crankshaft

λ: r/l

ω: angular speed of crankshaft

α: angular acceleration of crankshaft

F: force on piston pin

A: area of piston

w: reaction on cylinder wall

R_1: reaction in connecting rod small end

R_2: reaction in connecting rod big end

m: mass

m_r: mass of connecting rod

m_p: mass of piston

m_c: mass of crankshaft assembly

ρ: density

s: location of connecting rod center of gravity

d: location of crankshaft center of gravity

X_1, Y_1: displacement of connecting rod big end centroid

P_1, P_2, P: reactions at crankshaft rod bearing

$P_3 P_4$: reactions at crankshaft main bearing

R: radius of gyration

I: moment of inertia

I_{cg}: moment of inertia about center of gravity

M_f: friction load on crankshaft

M_l: external load on crankshaft

X_{cg}: position of center of gravity on X axis

Y_{cg}: position of center of gravity on Y axis

CHAPTER 1

EXPERIMENTAL SYSTEM STRUCTURE

1.1 General

Microcomputers can be applied to many control and data acquisition problems. Their flexibility, computation capacity, low cost and small size make them practical to replace custom-built analog instrumentation by microprocessor based digital circuits.

Internal combustion engines have until recently been controlled by mechanical control devices, such as carburettors and ignition distributors. These devices if simply replaced by microprocessor-based systems, would allow the implementation of superior control algorithms to improve the operation of the engine.

The pressure-volume (PV) diagram, also known as indicator diagram, has historically been used to observe the thermodynamic cycle taking place inside the engine.

The shape of this PV diagram depends on ignition, combustion, air-fuel mixture and also intake and exhaust systems including valve operation and piston sealing. The integral of the diagram is directly proportional to the work done inside the engine.

The PV diagram contains information that can be used for control feedback as well as to identify and quantify various parameters, for diagnostic purposes, if it is interpreted correctly.

Traditionally PV diagrams were obtained using a pen and drum mechanically linked to cylinder pressure and piston travel respectively. Such a system is hardly compatible with modern high speed machinery. Pressure transducers and crankshaft position encoders are used to display PV diagrams on an oscilloscope.

Today, PV diagrams can also be obtained with digital equipment which allows the implementation of software to analyse and use parameters of the diagrams for automatic control and/or diagnosis of engine operation.

1.2 Review of previous research

1.2.1 Application of computers to PV diagram acquisition

The fundamentals of internal combustion engine pressure measurement have been covered by several researchers.

In a paper published in 1967, W.L. Brown (3) analysed the requirements of the instrumentation used to measure pressure-volume diagrams and discussed several possible sources of error.

This problem was reexamined in 1975 by Lancaster, Krieger and Lienisch (11), taking into consideration the technological advances in computers and instrumentation. They also stress the importance of statistical fluctuations of the pressure curve over successive cycles.

In 1973 an early application of an analog computer to the task of acquiring PV data was reported by Brown. Fisher and Macey (6) reported in 1975 software developed for the same purpose on a mainframe computer. Young and Lienisch (22) reported in 1975 on the use of this system to obtain detailed combustion analysis from the measurement of pressure-time data.

Douaud and Eyzat (5) developed minicomputer software for PV diagram acquisition in 1977 and applied it to the experimental analysis of engine friction, cyclic variations and knock. They used a pressure transducer together with a crankshaft position encoder to trigger measurements every few degrees (or fraction of a degree) of crankshaft revolution. A second sensor is used to start measurements at TDC.

Kaplon and Hawrylkiewicz (10) developed a similar system with a PDP 11 in 1981 and applied the results to the calculation of heat release. Hayes, Savage and Sorenson (8) reported in 1986 the development of a system based on an Apple II computer; however, they indicate limitations on the ability of their

system to measure engine cycles at high RPM, due to computing speed.

This research project uses software based on the Automatic Engine Indicator (AEI) designed by Li Tian-Fu at McGill (14). This system, applied to a medium speed diesel engine, is different from those described above in that it uses only a top dead center (TDC) sensor, which greatly simplifies implementation.

1.2.2 Automatic control and diagnosis of IC engines

Werson and Stafford (21) developed in 1976 an analog closed-loop control system that could adjust ignition timing to maximize the work done by the engine (measured by the area of the PV diagram) while avoiding knock, also detected from the pressure measurements.

Bhot and Quayle (2) replaced the traditional mechanical ignition timing control system with an open-loop digital system in 1982. This permitted them to program an advance profile that is closer to the ideal than could be achieved with the traditional centrifugal mass-spring system. They also suggest using the angle of peak cylinder pressure for closed-loop ignition timing control.

Such a closed-loop system was built by Powell and Hosey (9) in 1979 with the addition of knock feedback to retard the

ignition timing when detonation occurs. Of particular interest is the piezoelectric "ring transducer" they developed and used to obtain the pressure signal. This transducer simply replaces the spark plug washer. Its ease of application and low cost make it ideal for eventual production applications requiring cylinder pressure feedback.

Visual inspection of PV diagrams with an oscilloscope has been used traditionally to observe engine condition in maritime applications. Warkman improved this technique (20) in 1983 by developing flow charts and fault finding tables for this purpose. These were used along with a dedicated mean indicated pressure calculator permanently installed to monitor engine performance in a systematic manner.

Uemukai, Higashino and Nomura (19) performed in 1982 statistical analysis of pressure data to detect piston ring failures and worn ignition points by comparing peak cylinder pressure and location of maximum combustion pressure rise with pre-determined values obtained from an engine in optimum operating condition.

In 1985 Sood, Fahs and Henein (16,17,18) developed a microprocessor device to identify faulty cylinders in the operation of a multi-cylinder engine. They achieved this by observing crank velocity fluctuations through an autocorrelation analysis.

Finally in 1982, Leung and Schira (12) described and demonstrated possible applications of engine speed and cylinder pressure measurement for control and diagnostics. Considering the fact that the cyclic variations of the pressure signal are dependant on the air-fuel ratio, they defined a mathematical indicator based on statistical observation of the unsteadyness of the engine operation to control the mixture in an electronic injection system.

Leung and Schira also used the fluctuations in engine velocity as a function of timing in order to balance the mixture equally between the cylinders. They also adapted Powell's concept of closed-loop control of ignition timing using the point of peak cylinder pressure to operate with velocity fluctuation feedback. Finally they suggested that the Fourier transform of the angular crankshaft speed will have harmonics at the engine speed and at the speeds of the various rotating accessories that are driven by the engine. Each coefficient would permit to identify the relative amount of power taken by each accessory. Historical changes could permit early detection of problems arising in the operation of these accessories.

1.3 Scope of the research project

This research project was originally intended to develop diagnostic methods for internal combustion engines. For this

task, it was expected that the Automatic Engine Indicator (AEI), as designed by Li-Tian Fu, could be used. However, the AEI had been developed for a medium speed Diesel engine. No existing instrumented spark-ignition engines were readily available. Apart from the task of developing an instrumented test bed, the adaptation of the AEI to a high speed spark ignition engine turned out to be more complicated than expected.

Eventually, due to instrumentation problems the data obtained was insufficient to allow the development of diagnostics. The investigation reported in this work is thus limited to the development of a microprocessor-based system for the acquisition of pressure-volume data on high speed, spark ignition internal combustion engines. The information presented here can form the basis for further research on the original project.

This report consists of five main sections. Chapter 2 describes the theoretical behavior of a spark ignition engine. Chapter 3 describes the construction of the test bed used in the tests. The instrumentation to measure the various parameters is descibed in Chapter 4. The computer hardware and software are presented in Chapters 5 and 6 respectively. Chapter 7 discusses the analysis of the experimental results. Conclusions are presented in Chapter 8.

CHAPTER 2

THEORETICAL BEHAVIOR

2.1 General

The various parameters of the Otto cycle (temperature, pressure, enthalpy, entropy) can be estimated at any point of the cycle if certain assumptions are made:

- -intake and exhaust are at atmospheric pressure,
- -isentropic compression,
- -constant volume combustion,
- -isentropic expansion.

This is defined as the ideal Otto cycle.

Calculations can be made using gas tables; however, charts known as Starkman-Newhall charts are available for this specific purpose. Details of the calculations can be found in Appendix A.

Note: The charts used for the calculations included in this part of the report can be found inm (15).

2.2 Stoichiometric, rich and lean mixtures

The calculations for these three cases have been made using all of the assumptions stated above. The mixture for the rich case has been set at 120% of the stoichiometric value; the lean case has been set at 80%. Results of the calculations are summarized in table 2.1.

Experimental results should not differ much from these calculations except the peak pressure area. The "constant volume combustion" assumption is the one which is the furthest away from reality. Flame propagation speed has to be taken in consideration and is one of the major limits on the performance of high speed internal combustion engines. Consequently, peak cylinder pressure will occur some time after TDC when the piston has moved and the volume is increasing. It follows that the peak cylinder pressure will be considerably lower than following a constant volume combustion.

In the absence of frictionless ducts, the intake and exhaust processes do not actually take place at atmopheric pressure. However, for an engine running at full load, the intake pressure can be very close to atmospheric and may even exceed it (*).

(*) Laboratory tests of production engines have shown that proper use of pressure waves in induction manifolds can permit a slight supercharging effect at specific engine speeds.

In the general case, it can be considered that both intake and exhaust pressures are close to atmospheric when the engine is operating at full load. The effect of varying these parameters will be examined in the next section.

The hypothesis of isentropic compression and expansion is fairly close to reality as can be seen from experimental data: drawing the log p-log v diagram is a good indicator of proper phasing of the PV data (11,23). By definition, the log-log diagram of an isentropic process is a straight line.

A comparative graph of the stoichiometric, rich and lean cases is shown in fig. 2.1; a graph introducing throttling and exhaust losses is shown in fig. 2.2.

Fig. 2.1 shows that the difference in peak pressure could be used to detect deviation from the ideal mixture ratio.

2.3 Intake throttling and exhaust back pressure

Calculations were made for two additional cases: in the first one, we assume an intake pressure 50% below atmospheric, due to throttling; in the second, we assume an exhaust back pressure in the order of atmospheric. The first case is typical of an engine operating under a light load, the second is exaggerated and intended to show the influence of back pressure on the ideal cycle calculations.

It is readily seen from the results in table 2.1 that throttling reduces peak pressure and work to a great extent. Throttling restricts the amount of fuel/air mixture admitted in the engine, reducing the work done during one cycle. For this reason, throttling has always been the means by which the power output of a spark ignition engine is controlled.

Back pressure seems to have considerably less effect on the cycle. However, exhaust back pressure will cause the fraction of burned gas remaining in the combustion chamber to increase; this could very well decrease the quality of the combustion to the point where calculations made from the charts are not realistic. It should be remembered that these charts are derived from experimental measurements.

A PV diagram showing the deviations between "real" and "ideal" cycles is included in fig. 2.3.

CALCULATION OF THE IDEAL OTTO CYCLE

	Normal	Rich	Lean	Throttled	w/Back Pressure
p_1(psi)	14.7	14.7	14.7	8.0	14.7
p_2(psi)	160.0	158.6	161.5	87.3	160.0
p_3(psi)	756	852	620	421	743
p_4(psi)	91.5	104.0	95.6	49.5	91.5
p_5(psi)	14.7	14.7	14.7	14.7	30.0
f	.038	.040	.046	.063	.068
u_1 (BTU/Cth.	111.4 Qty.)	113.1	109.5	119.7	111.4
u_2 (BTU/Cht.	214.0 Qty.)	205.0	211.5	214.0	214.0
u_3 (BTU/Cht.	1441 Qty.)	1687	1184	1409	1402
u_4 (BTU/Cht.	870 Qty.)	1085	745	860	860
T_1(^{o}R)	594	594	594	594	594
T_2(^{o}R)	1076	1068	1090	1076	1080
T_3(^{o}R)	4960	5345	4600	4890	4926
T_4(^{o}R)	3520	3650	3170	3480	3485
$IMEP_1$ (psi)	36.4	36.6	36.0	18.0	36.4
$IMEP_2$ (psi)	201.6	210.8	155.0	105.4	191.4
$IMEP_3$ (psi)	0	0	0	15.6	12.7
Net IMEP (psi)	165.2	174.2	119.0	71.8	142.3

TABLE 2.1

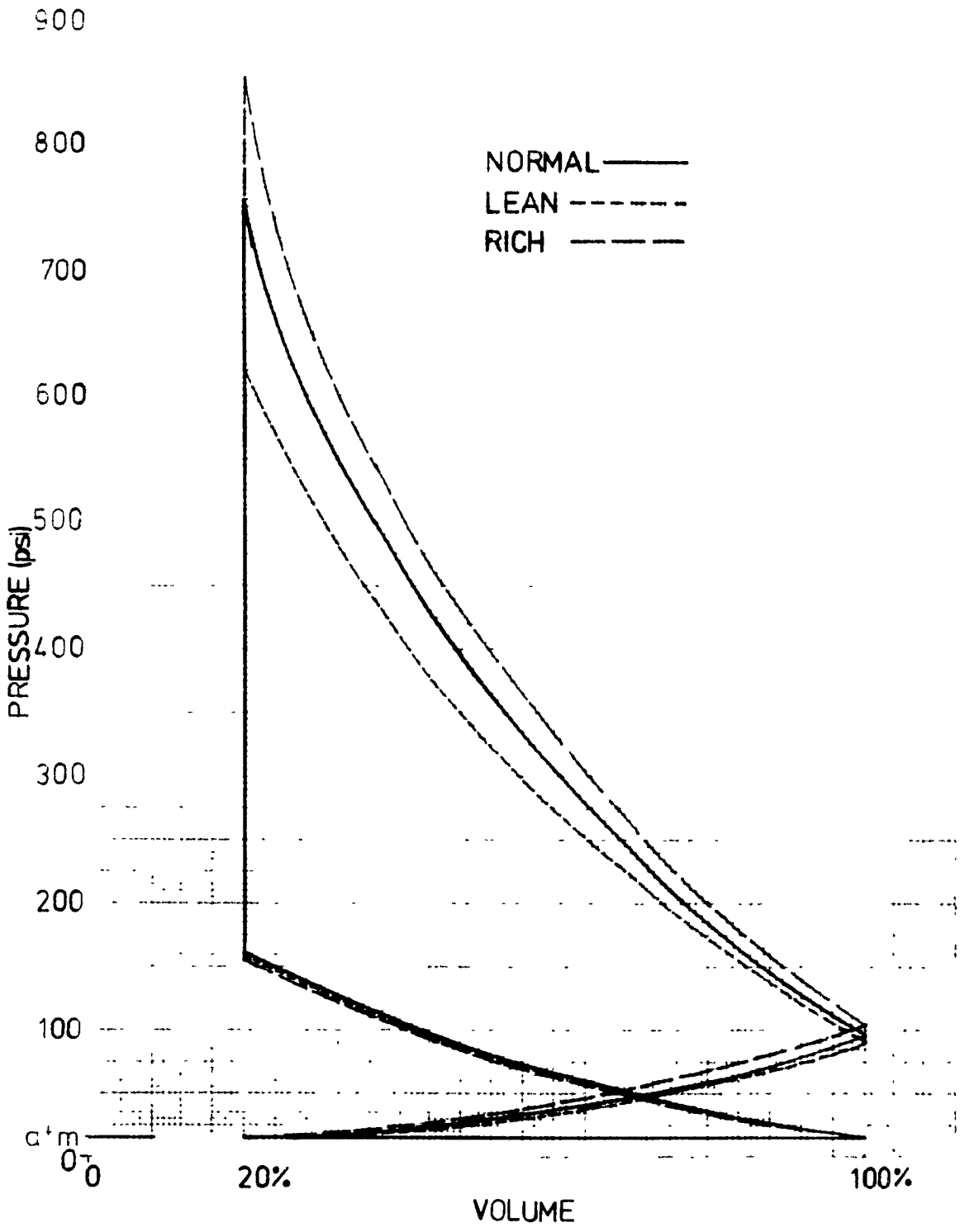

PV diagram of stoichiometric, rich and lean cases
Figure 2.1

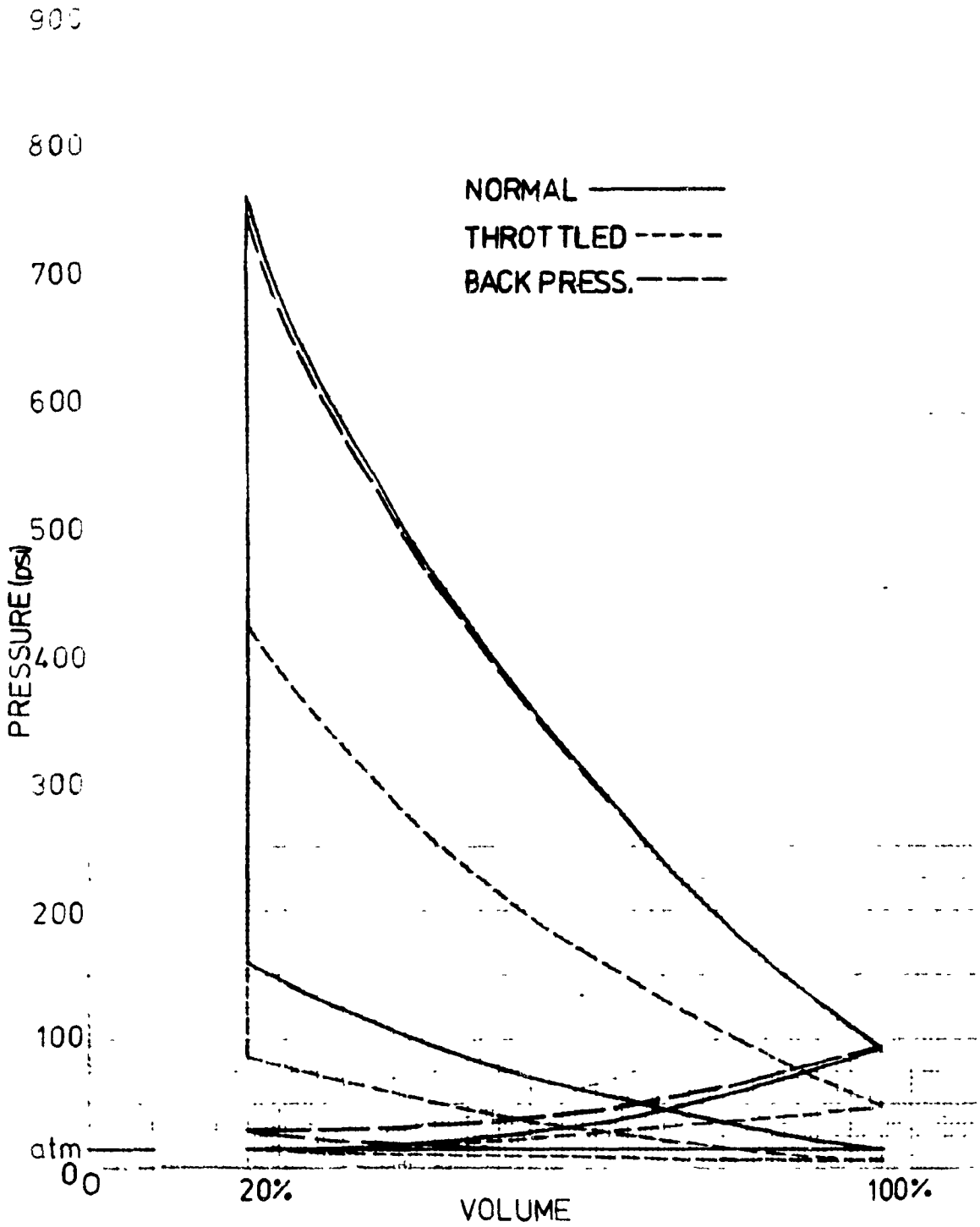

PV diagram of throttled and back pressure cases
Figure 2.2

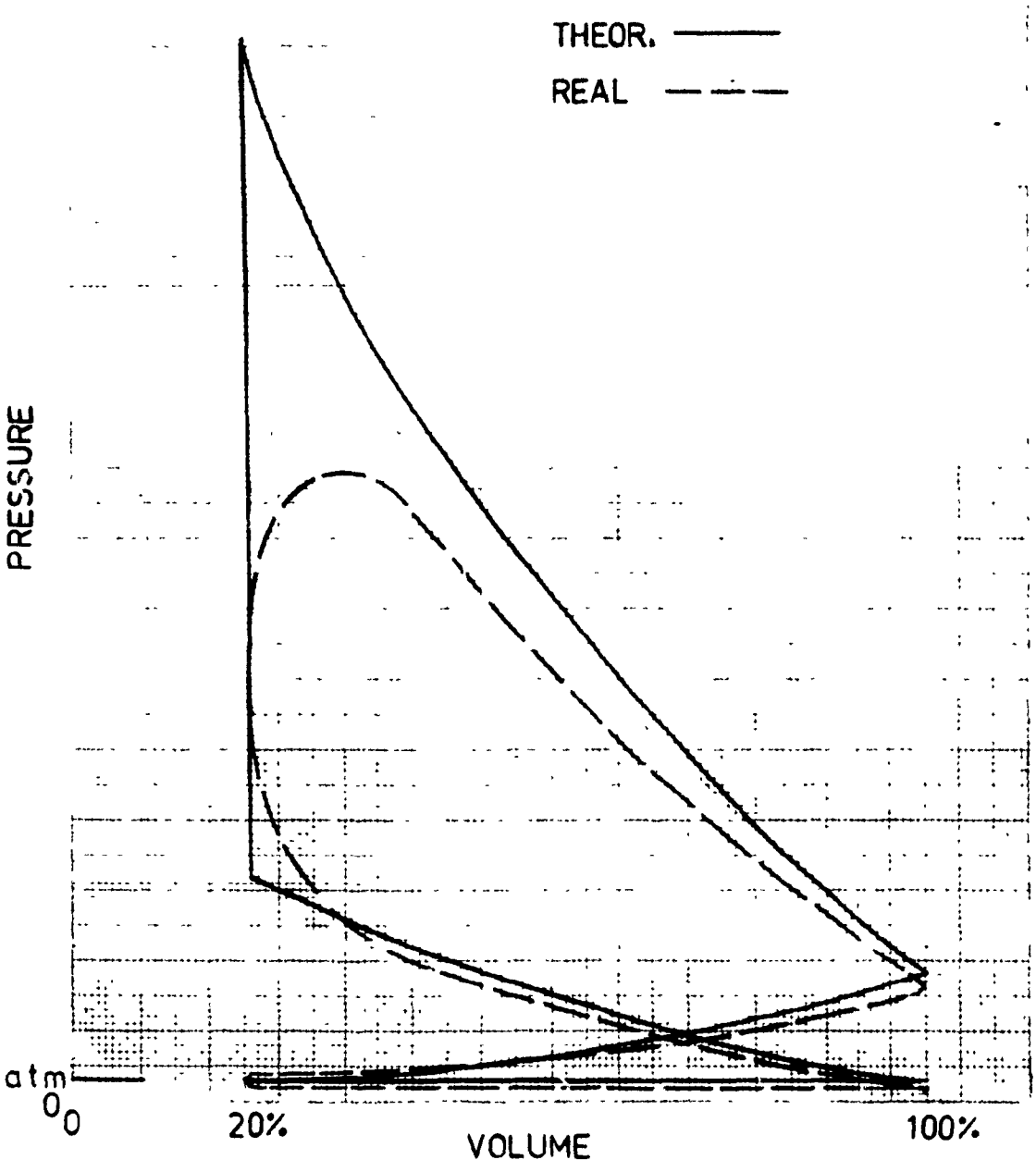

PV diagram, "ideal" and "real" cycles

Figure 2.3

CHAPTER 3

TEST BED DEVELOPMENT

3.1 General

To develop the data acquisition system described in this report, it was first necessary to design and fabricate a test bed on which an internal combustion engine could be installed and operated under controlled conditions.

It was desired to have a portable test bed which imposed the choice of a small engine. It was also decided to study a four-stroke Otto cycle engine as this is the most popular type of engine in marine, industrial and automotive applications.

The main purpose of the test bed is to provide a controllable brake loading so the engine behavior can be observed under unloaded as well as loaded conditions. The test bed must also provide cooling, noise reduction and fuel feed.

Measurement of the following parameters must be incorporated in the design:

-combustion chamber pressure,
-piston position,
-engine speed,
-torque load,
-fuel flow.

3.2 Design of the test bed

3.2.1 Experimental engine

The engine used for this study is a spark-ignition unit typically used in lawn-mowers. Its characteristics are described in Table 3.1. This engine is the smallest four stroke engine commonly available. It is air cooled and has an integrated fuel tank, which readily meets two of the requirements for the test bed.

The particular engine used for the experiments was obtained second-hand and disassembled for inspection. It was found to be in good condition and was reassembled without any component being replaced.

While disassembled, the various components were measured and weighed, and moments of inertia were calculated from this data. The details of the calculations can be found in Appendix B.

3.2.2 Test Bed

The engine was mounted on a frame made of 25mm x 25mm section steel tubing.

Noise reduction was achieved through the use of a standard muffler as supplied by the engine manufacturer. The test bed was installed near a window, to vent exhaust gases through a long exhaust pipe. The exhaust pipe was fitted with a valve to control the back pressure as an experimental parameter.

The frame was mounted on thick vibration absorbing pads. The whole assembly was firmly located to prevent vibrations from moving it on the workbench.

The test bed and engine are illustrated in Figures 3.1 and 3.2.

3.2.3 Engine loading

Torque loading is provided by a Prony brake. This brake was built by attaching a steel cylinder to the power take-off end of the crankshaft; friction is generated by mechanically tightening a brake lining which surrounds this cylinder. The brake cylinder was machined to press-fit on the crankshaft; it is located by a set-screw and power is transmitted by a Woodruff key.

The brake assembly was designed to minimize inertial load on the engine in order to better observe the fluctuation of velocity. No flywheel was installed to compensate for the inertia normally provided by the cutting blade. This turned out to be an unfortunate oversight.

The brake itself is a steel tube with a 13 mm thick lining on its internal surface. The lining was made of plywood discs. This assembly is slotted on one side; a tensioning screw is welded on the outside of the tube. The design allows for water cooling of the friction surfaces.

A 250 mm steel rod is welded perpendicularly to the wall of the brake tube and transmits the reaction torque from the brake to the engine frame through a cantilevered beam.

An angular contact ball bearing is mounted between the base of the brake cylinder and the engine frame. This bearing supports the vertical load that the weight of the brake cylinder would apply on the crankshaft. The brake assembly is shown in Figure 3.2.

The wooden brake lining was found to have inadequate wear characteristics. The lining was not adequately maintained in a concentric position relative to the brake cylinder; the resultant conical wear pattern caused the whole brake assembly to wobble at low settings, resulting in irregular loading and occasional stalling of the engine. A better type of brake (eg: electric) or at the very least a single piece lining made of hardwood or other friction material should be substituted in subsequent tests.

Water cooling of the brake friction surface helped the brake run smoothly but could not be used during testing because of the water spray from the unsealed brake assembly.

Consequently, the lining quickly overheated after a few minutes of engine operation under load. This severely limited the possibility of obtaining data under constant conditions. Test runs were kept short (1-2 min.) to avoid this problem.

Table 3.1 EXPERIMENTAL ENGINE MAIN CHARACTERISTICS

Make	Briggs & Stratton
Model	82902
Cycle	Four stroke
Nominal power	3.5 HP(2,5kW)@ 3500 rpm
Cooling	Air
Piston axis	Horizontal
Crankshaft axis	Vertical
Ignition	Magneto
Spark plug	Champion J8
Combustion chamber	Side valves (L-head)
Lubrication	Splash feed
Piston material	Aluminum
Cylinder material	Aluminum
Fuel feed	Vacuum pump
Carburettor	Sidedraft
Throttle control	Governor
Bore-nominal	60,325 mm
Stroke-nominal	44,450 mm
Displacement	0,127 l
Compression ratio	6/1
Mass of crankshaft	1341 g
Mass of piston (w/rings and pin)	178 g
Mass of connecting rod	87 g
Mass of magneto/cooling fan	1112 g
Mass of brake cylinder	1509 g

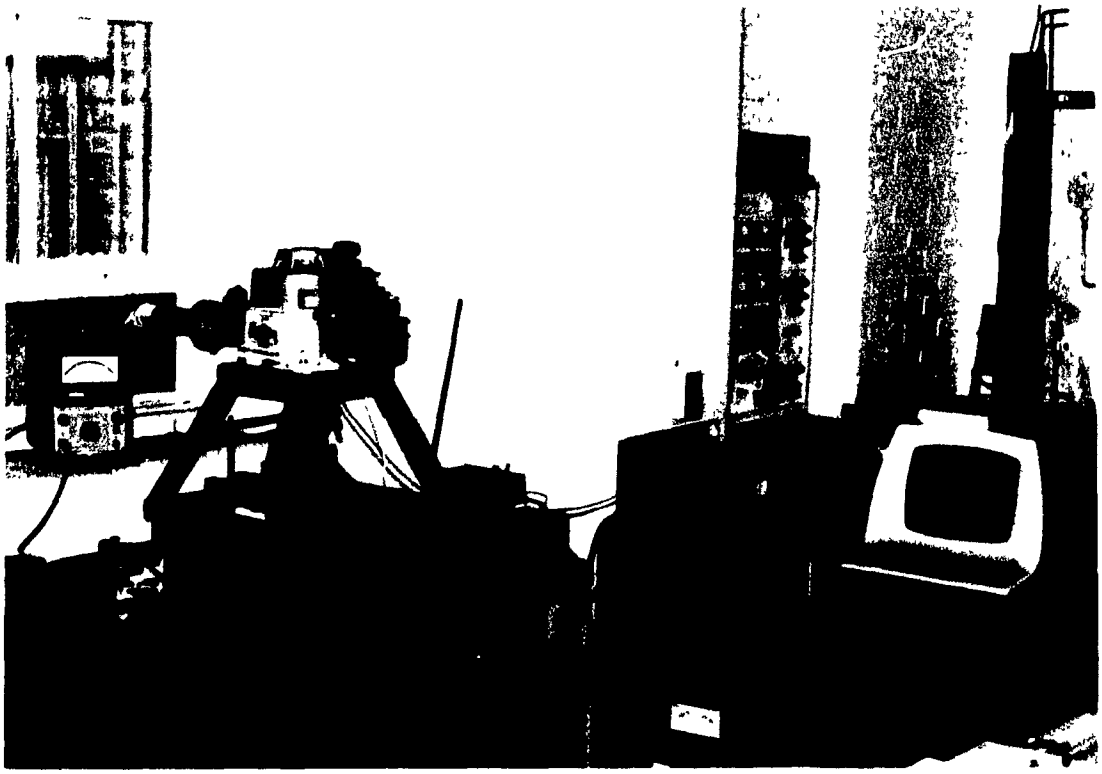

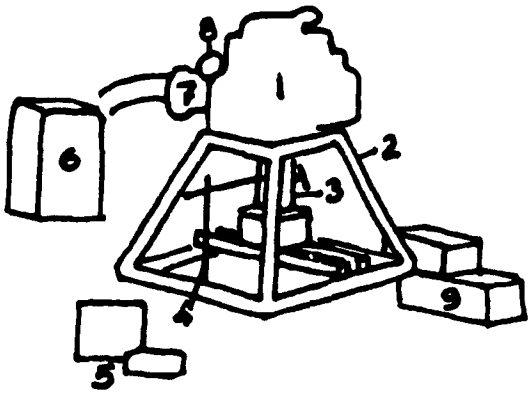

1 Engine
2 Test bed frame
3 Brake assembly
4 Strain gauge beam
5 Strain gauge bridge and battery
6 Microvoltmeter
7 Muffler and exhaust pipe
8 Back pressure control valve
9 Auxiliary power supplies

Experimental test bed
Figure 3.1

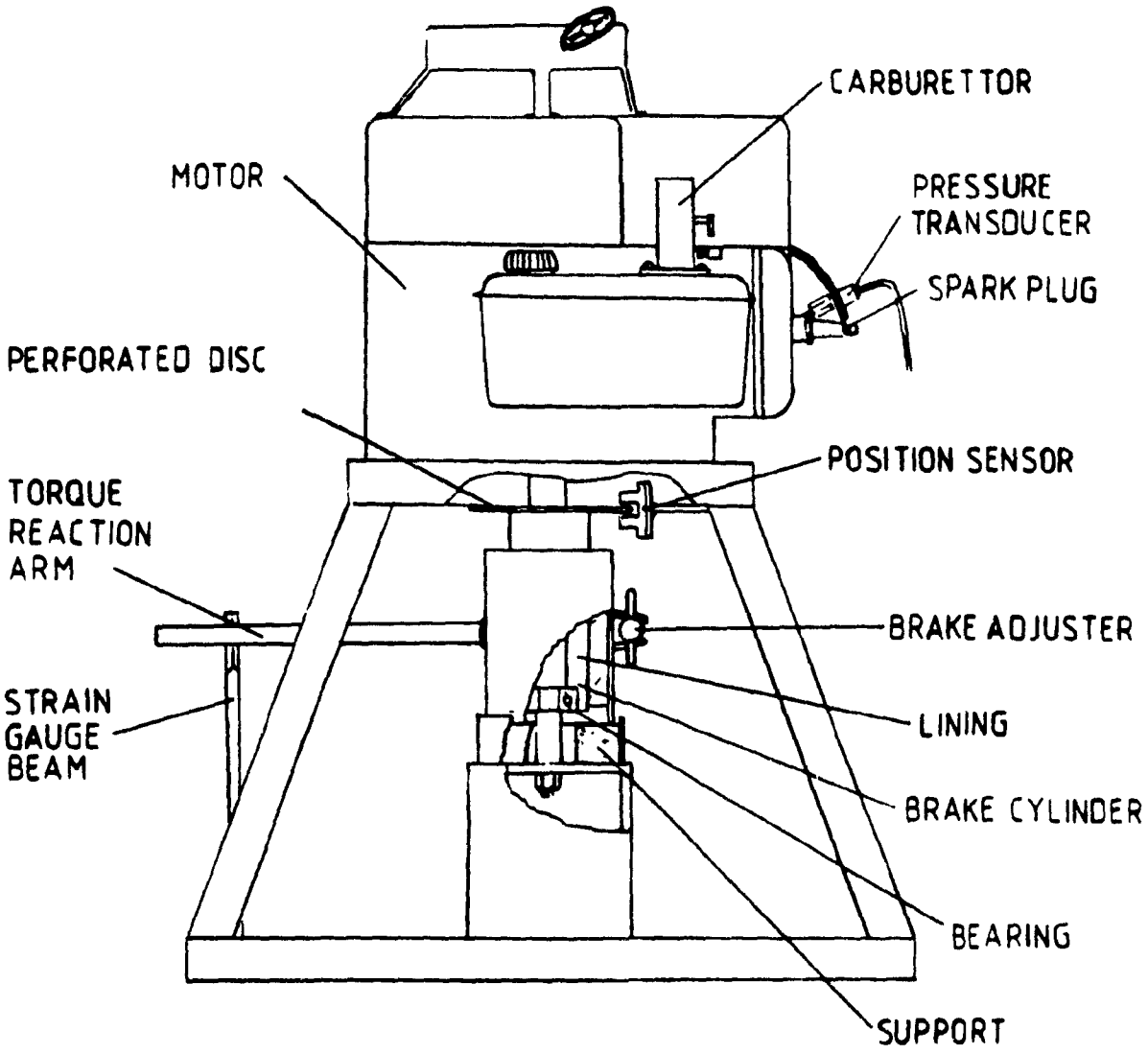

Experimental test bed
Figure 3.2

CHAPTER 4

INSTRUMENTATION

4.1 General

This chapter covers the development of the instrumentation used to measure the parameters enumerated in Section 3.1:

-combustion chamber pressure,

-piston position,

-engine speed,

-torque load,

-fuel flow.

4.2 Instrumentation selection and development

4.2.1 Combustion chamber pressure

Combustion chamber pressure is measured by a semiconductor strain-gauge type Kulite transducer, model ETM-375-1000 (*). The transducer is installed by the means of a special adapter spark plug such as the one shown in Figure 4.1.

Brown (3) made recommendations regarding the ideal characteristics for pressure transducers used to measure

(*) Two transducers were used for the experiments: serial numbers 3922-4-27 and 560-6-1.

combustion chamber pressure. These characteristics should guarantee reproducible measurements and were selected to reduce the error on IMEP measurements to about 1%, the maximum error level that can be tolerated for an accurate study.

The Kulite transducer is compared to Brown's "ideal transducer" in Table 4.1. It falls somewhat short of these recommendations. This transducer was used only because of its availability.

The other sources of error mentioned by Brown are: phasing error, mounting strains, thermal strains and noise.

Phasing errors have three major causes. The first one is a result of the inaccuracy of the sensors used to associate pressure measurements with crank angle. This will be covered in more detail in section 4.2.2. The crankshaft twist that can also contribute to the phasing error has, in the case of the single-cylinder test engine, been considered negligible particularly due to the very low inertial mass attached to the crankshaft.

The second cause of phasing error is the delay occuring while pressure waves travel along the passage in the spark plug adapter. While this passage causes some damping of the response, Brown points out that acoustic theory is currently unable to predict the resonant frequency of passages. It is

preferable to mount pressure transducers flush with the combustion chamber, but this was not done to reduce machining costs and delays. Keeping the passage as short and narrow as possible will however minimize this phasing error.

The third cause of phasing error is instrumentation lag as introduced by the transducer and the amplifiers used to bring the signal to the proper level for the microprocessor.

Mounting strains were not a problem: as pointed out by Lancaster, Krieger and Lienisch (11) such problems may be avoided by observing any changes in transducer output while the latter is tightened in its socket. No problem was observed on the test installation.

To prevent thermal strains, the transducer was provided with water cooling. Tap water was circulated in a jacket around the socket of the spark plug adapter.

The first experimental data sets obtained from the test bed were unrealistic. The pressure-time curve was offset in the Y-direction (pressure axis) by a DC voltage proportional to the load applied on the engine.

This phenomenon was observed on an oscilloscope. The offset would appear instantly when the load was increased but would decay logarithmically when the load was removed.

Elimination of possible causes suggested that this was caused by an abnormally high temperature of the gas at the pressure transducer.

A thermocouple was installed in the pressure transducer adapter. This confirmed that the problem was related to temperature. Measurements obtained at the transducer socket varied from 100°C at idle to more than 800°C at full load. The pressure transducer is designed for a maximum temperature of 125°C.

The water cooling provided to the transducer only lowered the maximum temperature to 600°C, which is still excessive.

The installation of a brass radiation shield at the bottom of the transducer adapter socket proved effective in controlling the temperature. With the shield in place, the maximum of 125°C was never exceeded. Details of the temperature measurements are shown in Table 4.2 and Figure 4.2.

We can therefore conclude that the problem was caused by radiation originating in the area of the tip of the spark plug, which is the hottest point in a combustion chamber.

The original pressure transducer was damaged by the overheating and failed completely shortly after the problem was found and solved. A new transducer was purchased to obtain further data.

Some drift of the pressure signal was still observed under loading conditions.

Thermal strain problems in pressure transducers are well documented by Brown (3) and Lancaster, Krieger and Lienisch (11). The standard method used to shield the transducer from radiation is to coat its face with silicon rubber. A detailed procedure to achieve a durable coating is included at Appendix A of Lancaster, Krieger and Lienisch's paper on "Measurement and Analysis of Engine Pressure Data" (11).

Ignition noise was another source of error that appeared during the experiments. Figure 4.3 is a photograph of the transducer output showing ignition noise. The spikes caused by magneto discharge appear at every revolution because the ignition system of the test engine is a simplified design that fires both at the end of the compression stroke and of the exhaust cycle.

These spikes are very narrow as seen on the pictures but their presence falsifies completely any IMEP calculations. If a pressure measurement happens to be triggered at or near the location of the spike, the corresponding pressure value stored in the computer's memory will be $FF (Hexadecimal notation). Numerical evaluation of IMEP nearly always includes a data point in the area of the spike. The resultant high pressure value recorded at this point times the volume

interval is often a number in the order of magnitude of the expected total IMEP.

This problem was solved through the normal methods of shielding the cables and transducer and also by providing the engine assembly with a proper ground connection common to the instrumentation. These measures were sufficient to eliminate the problem.

Transducer calibration data is provided in Appendix C.

4.2.2 Piston position and speed

A disc, with a row of evenly spaced holes along its perimeter, is attached to the exposed part of the crankshaft, just above the brake assembly. Optoelectronic sensors detect the passage of the holes and provide position signals. This arrangement is shown in Figure 4.4.

The disc is made of sheet steel with 64 evenly-spaced holes of 1.5mm dia. The spacing of the holes was obtained by using a standard machine-shop dividing head mounted on a drill-press.

For programming reasons, the number of measurement intervals must be a power of 2. A minimum distance of 3 mm between the holes is necessary for proper optoelectronics performance. Within these constraints, a disc with 64 holes provided the highest resolution within the available space.

The optoelectronic sensors used are Texas Instruments TIL 138. To obtain TTL-compatible output a 5V input voltage is applied to the phototransistor.

A second sensor is required to trigger the beginning of the measurements. A second TIL 138, installed to detect a slot located on the outside edge of the disc, is used for this purpose.

The position of the sensor can be adjusted to synchronize this event with a particular point of the rotation of the crankshaft (e.g..: Top Dead Center-*). The technique used to achieve proper synchronisation is described in Appendix C. The precision achieved with this system is about 0.1^{o}. This is adequate if we calculate the precision requirements according to the equation relating DMEP and Du developed by Brown (3). These calculations are included in Appendix C. This level of accuracy is also recommended by industrial researchers (23).

The position of the piston is related geometrically to the crank angle and can be deduced mathematically from the signals provided by the sensors.

(*) This sensor was actually set to trigger the beginning of the measurements 90^{o} before TDC for reasons of accuracy. It will nonetheless be refered to in the text as the "TDC sensor". Software adjustments are made for the proper phasing of the measurements.

The angular speed of the crankshaft can be obtained by measuring the elapsed time between the occurence of two position signals.

A bracket holds the TDC sensor at the proper peripheral location such that the start of the measurements is synchronized with TDC. The position sensor has to be maintained in a position such that its signal is in phase with that of the TDC sensor. At the same time, the position sensor must be held at the proper radial distance so that it is located exactly over the row of holes in the disc. Finally, both sensors must be centered over the disc (in the direction of the crankshaft axis).

In practice, the mode of adjustment of the bracket (slotted holes, bolts and shims) is very crude for the degree of accuracy required. This made the positioning of the sensors very tedious and the final settings obtained were always a compromise.

This even resulted in contact between the disc and the sensor. The friction eventually wore out the plastic matrix of the sensors to a point where their operation was obstructed by the plastic dust. This implied that the sensors had to be replaced occasionally.

Also, the best setting always puts the TDC sensor on the edge of the rotating disc. In principle this is not a problem as

the slot extended to the edge of the disc. In practice however, at high engine speeds, vibrations often caused the sensor to move slightly off the disc which resulted in a total loss of the TDC signal.

In general, the current equipment does not provide the reliability and accuracy of the position measurement as required, and must be improved in subsequent tests.

4.2.3 Torque measurement

A small cantilever beam is mounted vertically on the engine frame such that the reaction torque from the brake is transmitted through this beam. Strain gauges are mounted at the base of the beam; torque can be calculated from the strain-gauge output by geometry. To maximize readings, the dimension of the beam was chosen such that yield strength would correspond to the maximum nominal torque developed by the engine.

Details of the torque calculation using the output of this gauge beam are included in Appendix D.

A Hewlett-Packard model 425A microvoltmeter was used to measure the strain-gauge bridge output.

The cantilever beam and strain gauges worked smoothly and without problem throughout the experiment.

4.2.4 Fuel flow

The test engine has its carburator installed directly on the fuel tank. The tank has a constant-level bowl cast in its aluminum cover.

The rubber gasket between carburator and tank is partly exposed to intake vacuum and is used as the membrane of a vacuum pump. Two flaps cut in the rubber gasket act as one-way valves. This system pumps fuel from the main tank against a spring loaded section of the rubber gasket during the intake stroke; the fuel is pushed into the constant level bowl at the end of the stroke.

Overflow openings are provided to return fuel to the main tank when the correct level is reached. The carburator siphons fuel directly from the constant-level bowl.

It is not possible to install fuel flow measurement instrumentation in this very compact system. An attempt to measure fuel flow was made by removing the fuel tank. Only the cover with built-in constant-level bowl was being used. Fuel was fed to the constant-level bowl from a burette. The overflow from the constant-level bowl was also recovered in a second burette. The difference in fuel going in and fuel coming out over a measured time interval permitted to calculate net fuel consumption.

In practice, the system of burettes would either flood the carburator and prevent the engine from starting or would not supply enough fuel and stop the engine in the middle of a measurement.

This set-up proved to be extremely unpractical; the fuel flow would have had to be averaged over several minutes to be realistic.

In view of this, the fuel flow could not be measured. The fuel tank was reinstalled for the experiments.

One set-up that could have been used to measure fuel consumption is illustrated in fig. 4.5. This would have involved attaching a burette to the filler cap through a sealed tube. The fuel level would be kept above the filler cap, in the graduated portion of the burette. The fuel tank would need to be fitted with a vent tube and a drain cock to return the level below the cap while not experimenting. The difference in fuel level could be read at any time; along with a stop watch this would give a measure of fuel consumption.

IDEAL TRANSDUCER CHARACTERISTICS

	Suggested (3)	Actual
Linearity	<1%	±1% F.S. (*)
Change of pressure sensitivity with pressure: below 400 psi	<1%	n/a
above 400 psi	<3%	n/a
Repeatability, from room temp. to operating temperature	0.1%	±3% F.S. /100°F
Frequency response	DC-50 KHz	DC-8KHz
Thermal strain sensitivity	<0.01psi/°R	±.03%/°R
Acceleration sensitivity	<0.01psi/g	0.2psi/g
Signal to noise ratio	>3000:1	n/a
Hysteresis	<0.1%	±1% F.S. (*)
Mounting	Flush	Passage
Water cooling	Direct	Through adapter

(*) Combined non linearity and hysteresis

TABLE 4.1

TEMPERATURE AT TRANSDUCER HOUSING

Ambient temperature: 24°C
Water temperature: 10°C
Battery voltage: 6.21V

A) No cooling, no shield

RPM	Load	Torque (N-m)	HP	T(°C)
2739	0.2 mV	0.29	0.11	215
2648	1.5	2.16	0.80	550
2422	2.8	4.03	1.37	840

B) Water cooling, no shield

2751	0.2	0.287	0.11	180
2611	1.5	2.16	0.79	510
2363	2.7	3.88	1.29	670

C) Water cooling and shield

2747	0.2	0.29	0.11	15
2613	1.5	2.16	0.79	21
2318	3.2	4.60	1.50	49
2482	2.5	3.60	1.25	44

TABLE 4.2

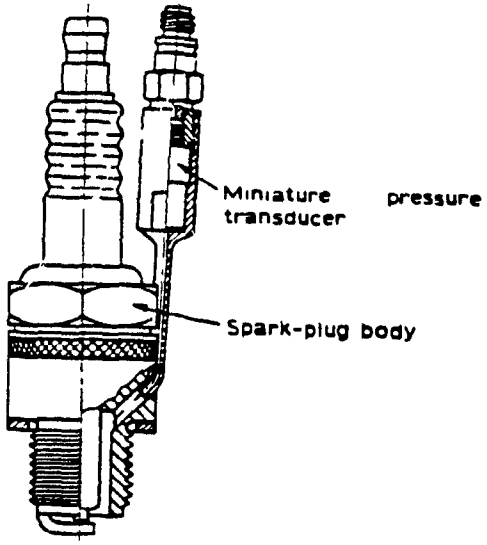

Figure 4.1: Pressure transducer adapter

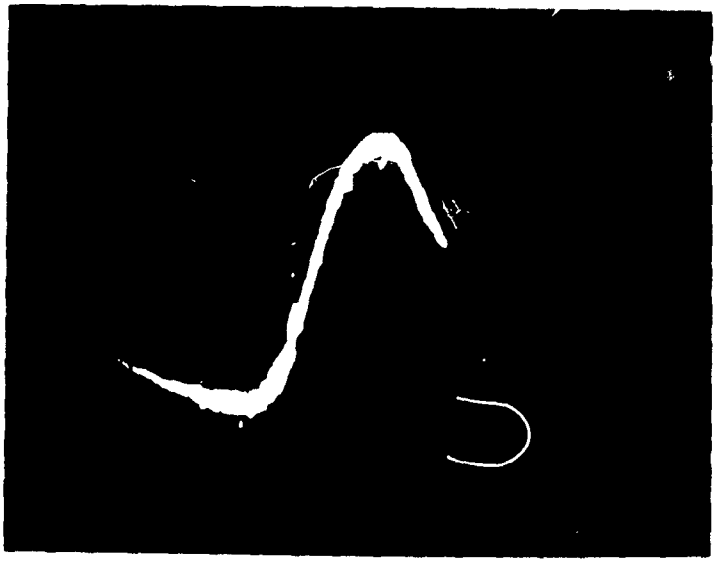

Figure 4.3: Pressure signal showing ignition noise

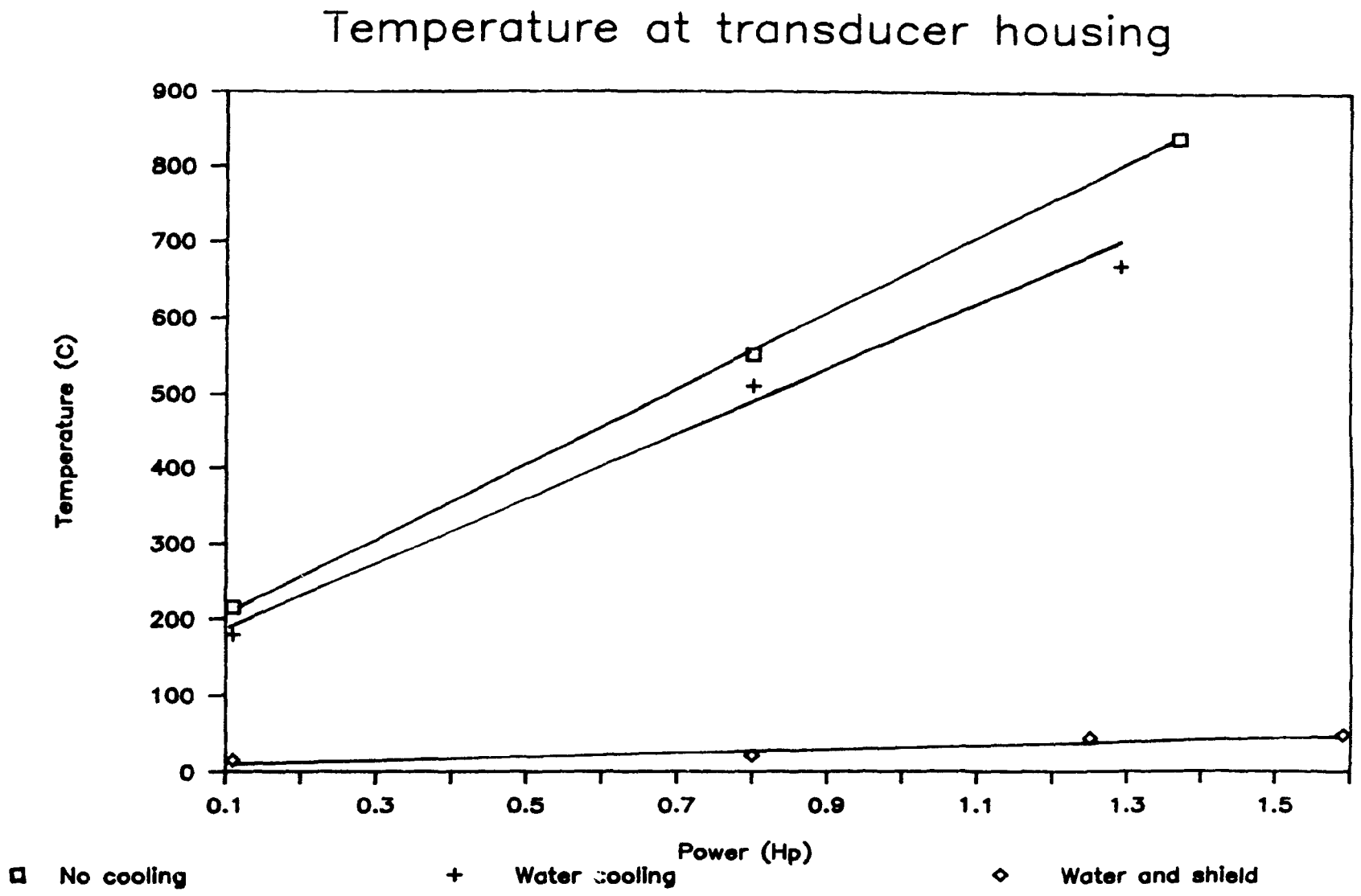
Temperature at transducer housing
900
800
700
600
500
400
300
200
100
0
Temperature (C)
0.1
0.3
0.5
0.7
0.9
1.1
1.3
1.5
Power (Hp)
No cooling
Water cooling
Water and shield

Figure 4.2

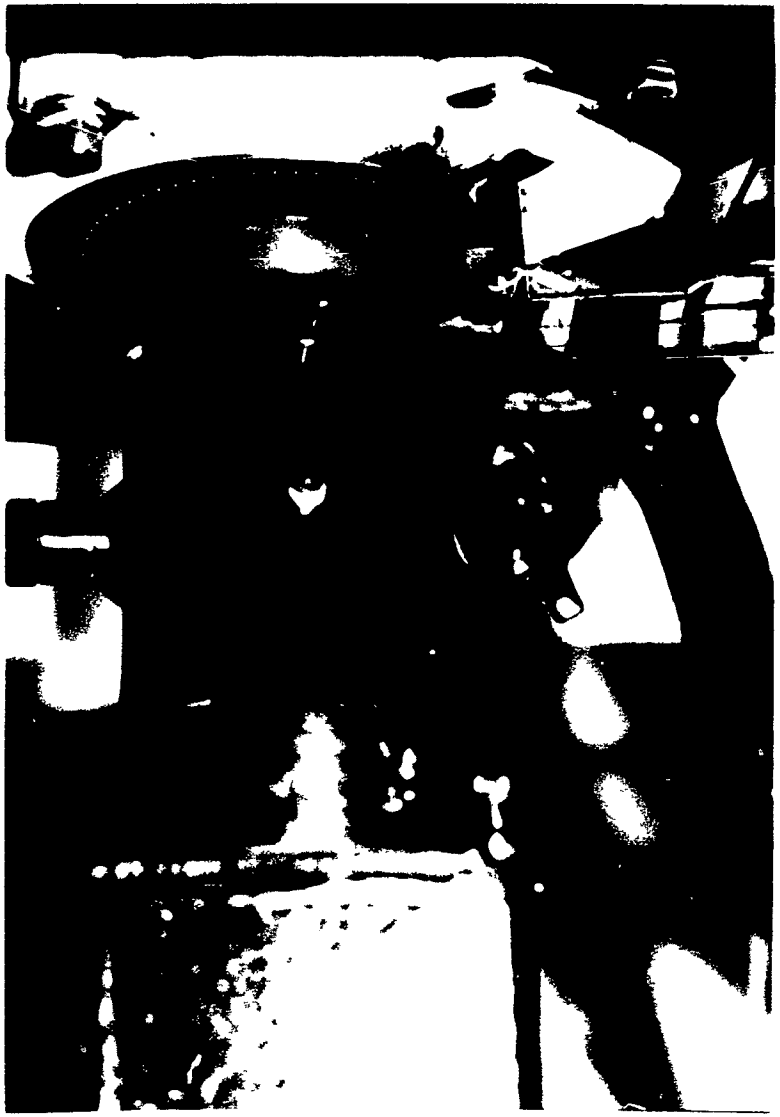

Figure 4.4: Arrangement of optoelectronic sensors

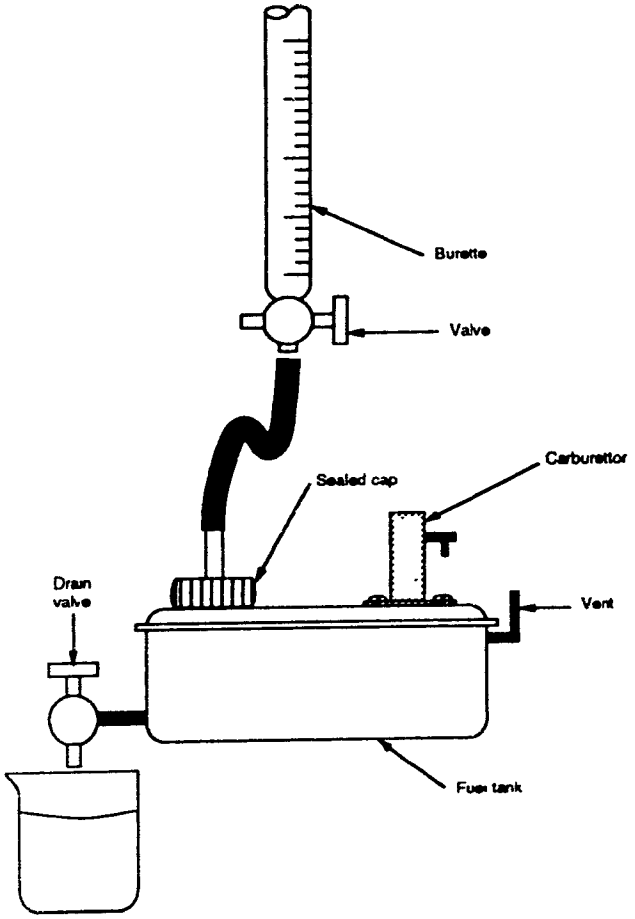

Figure 4.5: Proposed fuel measurement system

CHAPTER 5

COMPUTER HARDWARE

5.1 Microcomputer

Data acquisition in this project was performed using SWTP (South West Technical Products) Motorola 68xx based microcomputers. Initially a system consisting of a MC6800 was used, identical to the equipment used by Li Tian-Fu (14) for the Automatic Engine Indicator. It comprises of:

- 1MHz processor board with 4K EPROM,
- 8K RAM board,
- serial interface board,
- parallel interface board,
- custom built ADC,
- CRT Terminal and digital plotter.

It quickly became evident that mass storage would be required, as data sets had to be stored and later manipulated and compared, unlike the AEI where only one set of data for a single PV diagram had to be kept in memory at one time. The system was replaced by an SWTP 6809 system with 56K of memory, the same interfaces and dual floppy disc drives.

A block diagram and photograph of the 6809 system are shown in Figures 5.1 and 5.2.

5.2 Interface

Data is transmitted from the test bed sensors to the computer through a custom-built interface card located in slot 0 (slot 7 in the 6809) of the computer system. This interface card was designed by Li Tian-Fu for the original Automatic Engine Indicator (14) and was modified by the author to accomodate new and simplified data acquisition programs. Even though the card was designed for the 6800 system it was fully compatible with the 6809 system.

This card operates in the following manner:

The output of the pressure transducer is fed through an adjustable gain instrumentation amplifier and a sample-and-hold amplifier to an 8-bit successive approximation analog-to-digital converter (ADC).

The parallel output of the ADC and the amplified signals from the optoelectronic sensors are connected to a single MC6821 peripheral interface adapter (PIA). The interface circuit is shown in Figure 5.4.

The sequence of events that leads to a pressure measurement is as follows: (with reference to the block diagram of the interface, Figure 5.3)

1-PIA line CA2 is pulled low when a pressure measurement is required.

2-Single shot #6 generates a low pulse as a result of the low edge on CA2.

3-This low pulse toggles the output of the SN7400 which is wired as a flip-flop.

4-The sample-and-hold is then turned into "hold" mode.

5-The CA2 line is returned high by the next computer clock transition.

6-This causes the single-shot #7 to issue a "start of conversion" signal to the ADC.

7-Upon completion of conversion, the ADC issues an "end of conversion" signal to single-shot #5.

8-The single-shot generates a low pulse which toggles the flip-flop output and returns the sample-and-hold into "sample" mode.

A step-by-step procedure to operate the engine test bed appears in Table 5.1.

Table 5.1 Engine test bed starting and operation

1- Turn power on:
- microvoltmeter
- terminal
- main power supply
- instrumentation amplifier
- computer & disc drives
- ADC board power supply

2- Check oil and fuel level in engine.

3- Boot system and load data acquisition program (+++GET1.PRO4.BIN). Return to monitor (+++MON).

4- Plug pressure transducer on power supply (Cannon connector) and turn power on. Do not install transducer on engine.

5- Set program for measurement of one cycle (M0101:01).

6- Set Prony brake for minimal friction.

7- Start program (J0100).

8- Slowly pull engine start rope until teletype starts printing registers (indicating program has stopped).

Note: failure to stop after one or two pulls indicates software problems or problems with the optoelectronic TDC sensor.

9- Examine the pressure data in memory (M0400) and note.

Note: this output is a calibration measurement of atmospheric pressure. Non-constant output (memories 0400 to 048F) indicates hardware problems.

10- Adjust microvoltmeter zero with input to ground.

11- Connect 6V. battery to strain gauge bridge. Connect microvoltmeter to bridge. Balance bridge to zero output (make sure there is no load on the beam). Measure and note battery voltage using digital voltmeter.

12- Turn transducer power off. Unplug transducer from power supply. Screw transducer head into adapter spark plug socket taking care not to strain cable. Screw by hand until tight. Replug transducer to power supply and turn power on.

13- Turn on cooling water. Check for leaks and proper drainage.

14- Open back pressure valve completely. Start engine. Set speed, brake load and back pressure valve to desired conditions.

Note: to start cold engine, prime carburator with fuel or ether before closing choke.

15- Set program for desired number of measurement cycles (M0101:NN hex).

16- Take measurements (J0100) and note microvoltmeter output for load.

Note: do not leave engine running under load for more than two minutes at a time to prevent overheating of the brake lining.

17- Store contents of data memories: boot system (D) and save (+++SAVE 1.NAME.TXT 1000 128F).

18- Stop engine by shorting spark plug with insulated screwdriver.

19- Turn power off on all instruments.

20- Remove pressure transducer.

21- Turn cooling water off.

22- Measure 6V. battery voltage and note. Disconnect battery.

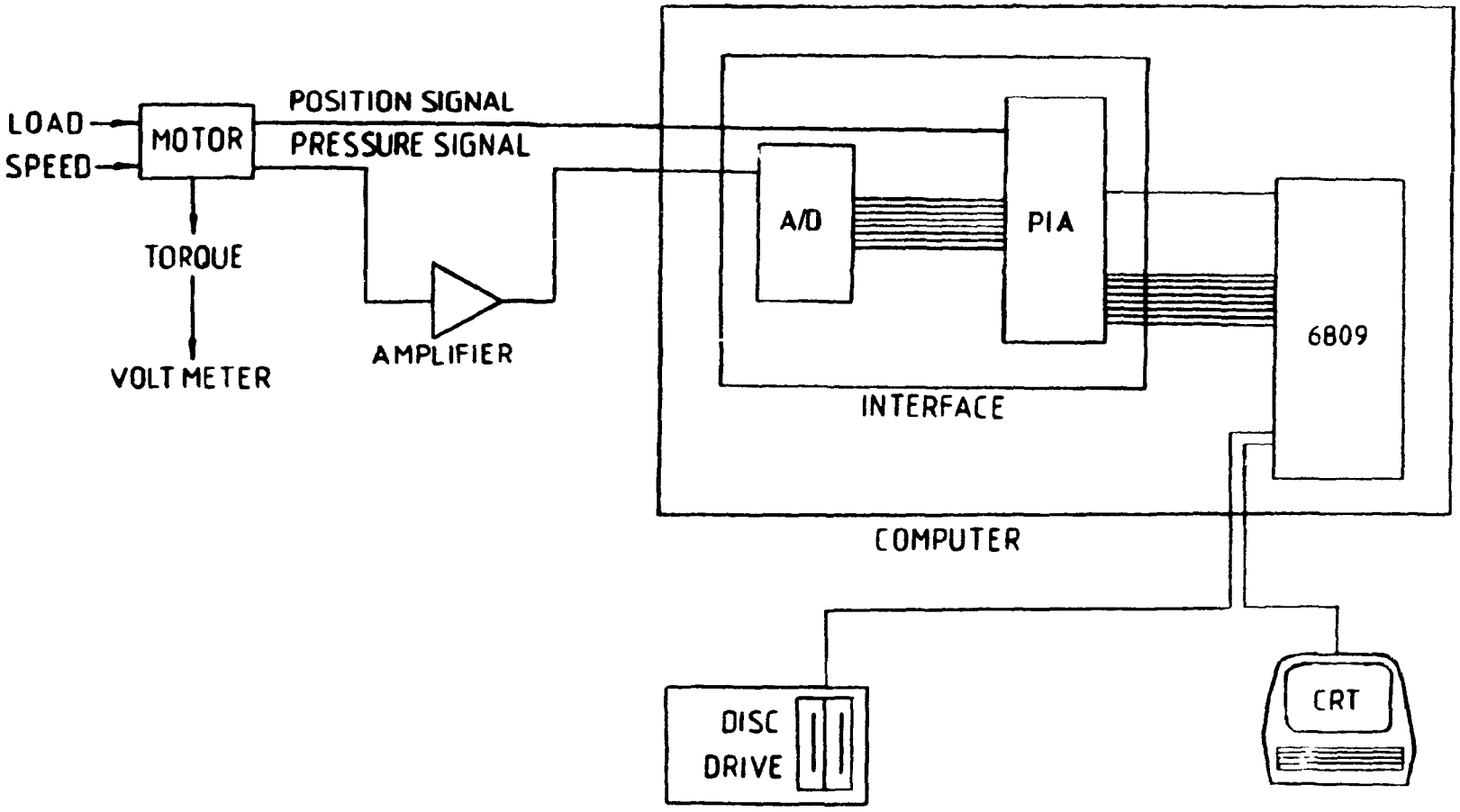

Block diagram of 6809 computer system
Figure 5.1

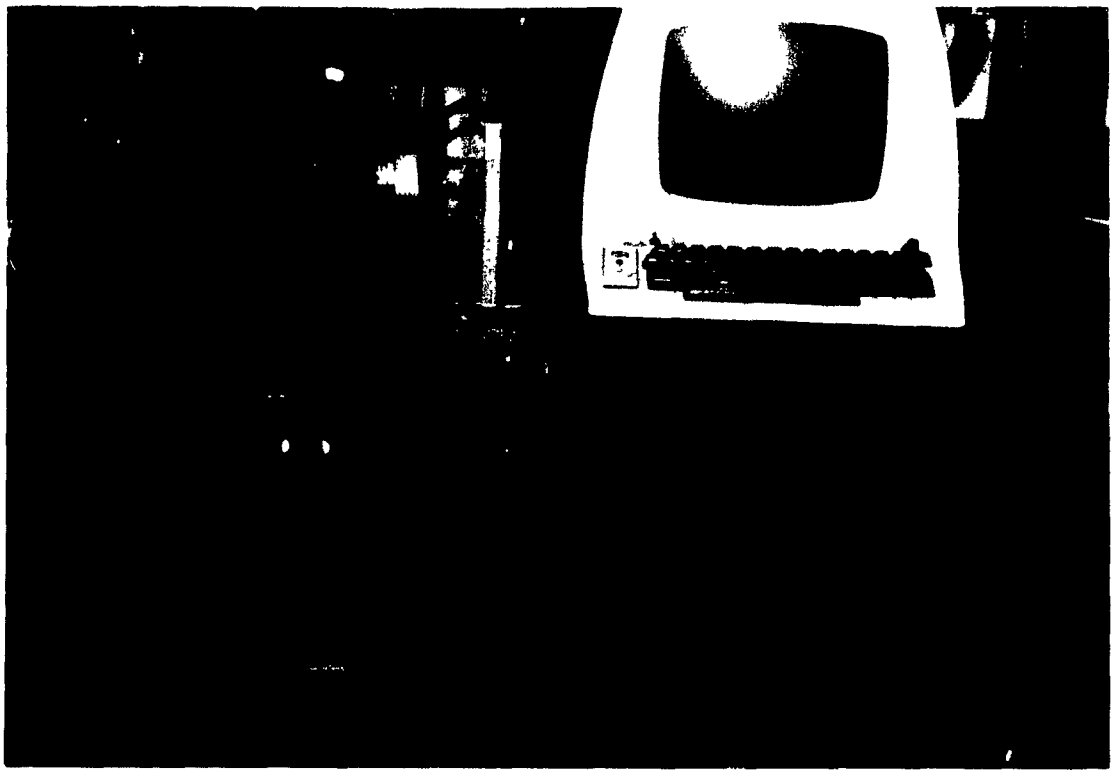

Figure 5.2: 6809 computer system

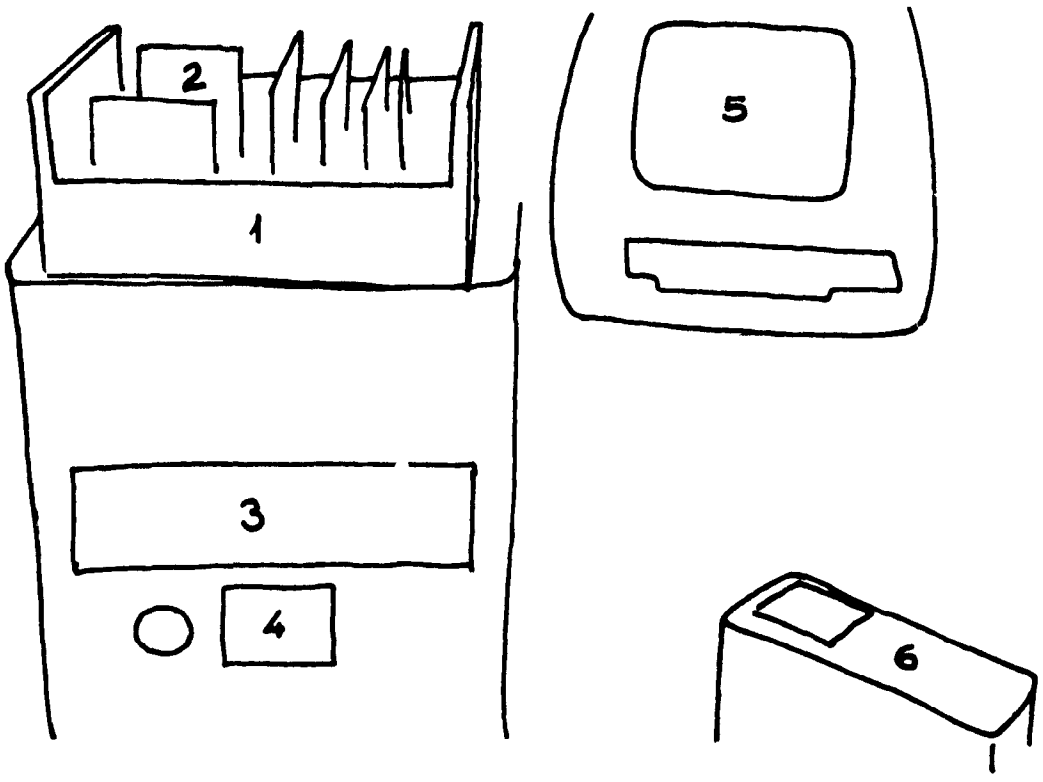

1 SWTP 6809 computer

2 ADC board

3 Instrumentation amplifier

4 Main power supply

5 Terminal

6 Oscilloscope

Legend of Figure 5.2

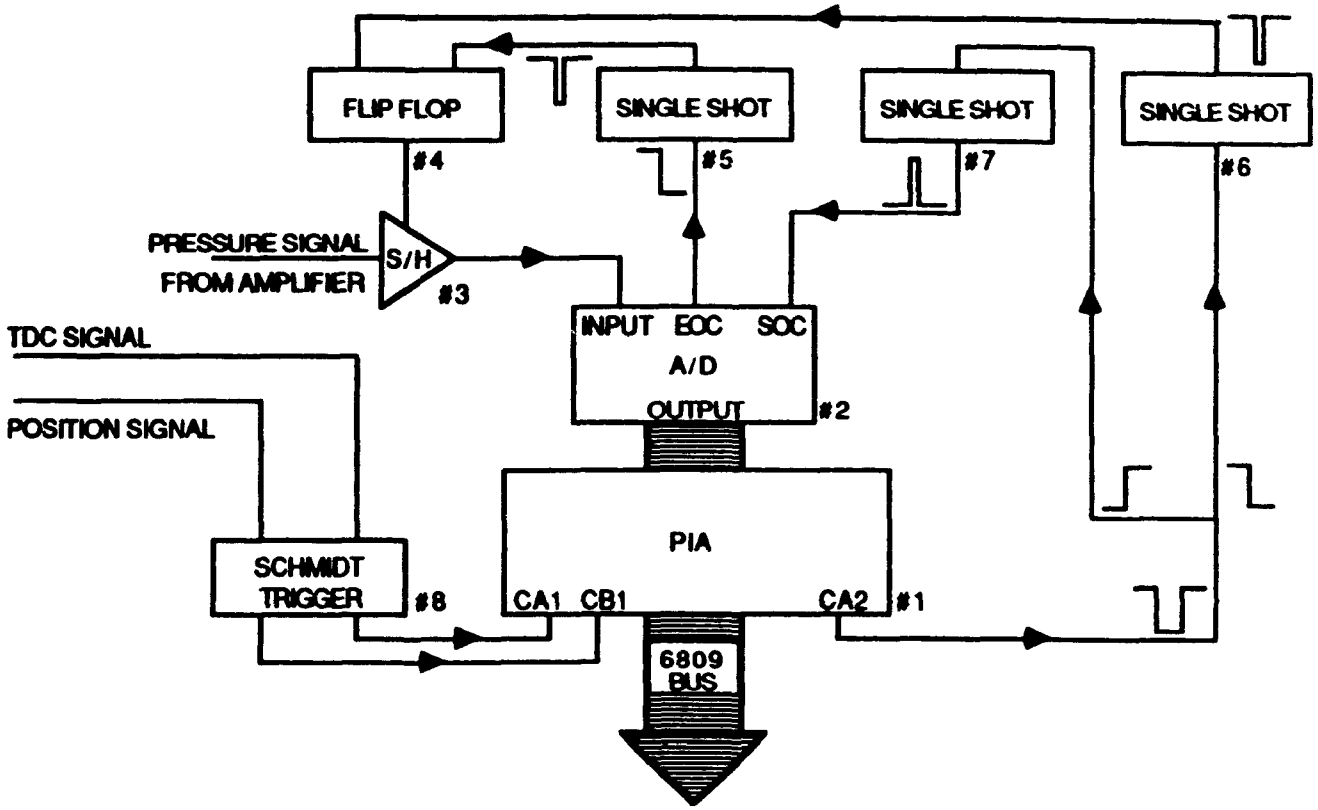

Block diagram of interface
Figure 5.3

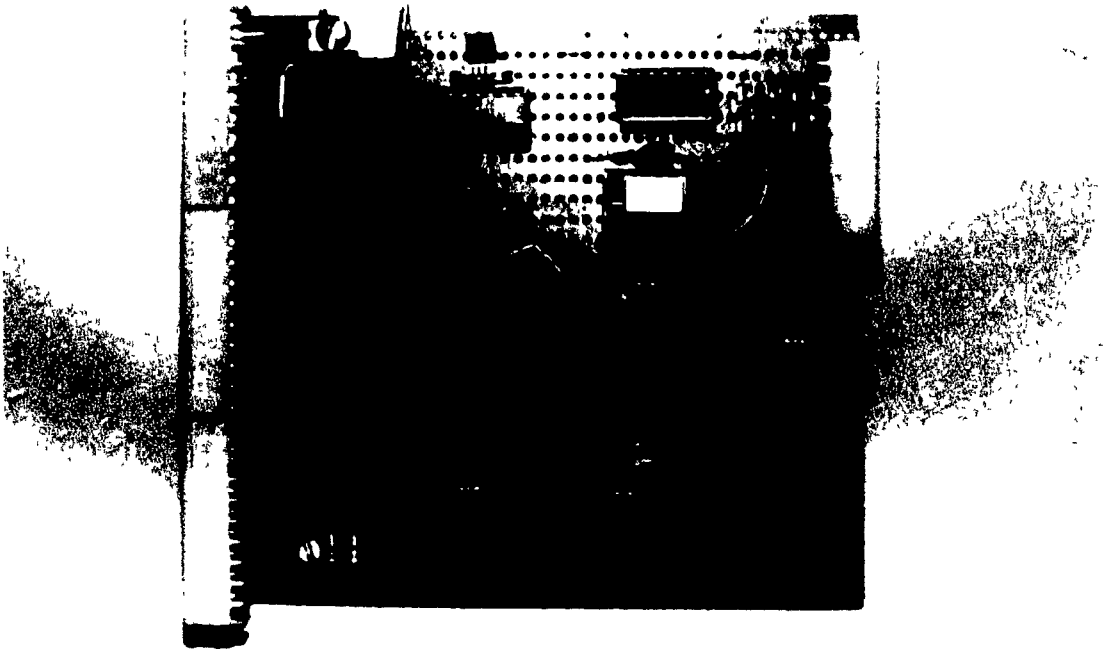

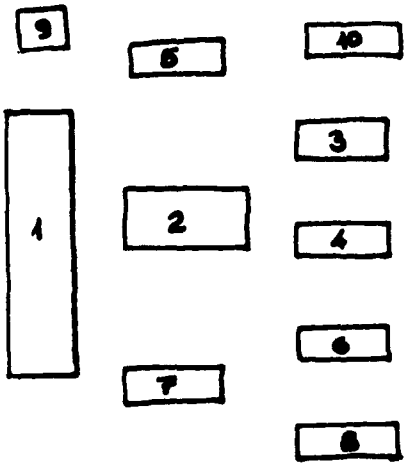

1 PIA
2 ADC
3 Sample and hold
4 SN4700
5 74121 single-shot
6 74121 single-shot
7 74121 single-shot
8 Schmidt trigger
9 Voltage regulator
10 Op. amplifier (not used)

Figure 5.4: ADC interface

CHAPTER 6

SOFTWARE DEVELOPMENT

6.1 General

A number of programs for data-acquisition, testing and debugging, and data analysis were written for this project.

Two data-acquisition programs were used with the experimental system. In the first one, the acquisition and storage of pressure data in memory is triggered by the position sensors . The second one is based on the original AEI data acquisition software (14), and requires only one position signal per revolution. Both programs were originally written in 6800 machine language and were later adapted to 6809 assembly language.

Also, a Fortran IV-G program and accompanying 6800 data acquisition program were written to simulate the velocity fluctuation of the crankshaft through a complete operating cycle. This program was also based on previous work done at McGill, in this case an Undergraduate Mechanical Laboratory project (7). This program was run on the McGill Computing Centre mainframe computer under MUSIC.

Finally, a group of Fortran programs were written to analyse the data. The printed output of the 6800 data acquisition system was transposed into MUSIC files through a keyboard.

It quickly became evident that this last procedure was not adequate to handle the amount of data necessary to obtain valid conclusions. The 6800 system was replaced by a SWTP 6809 system with dual floppy disc drives for data and program storage. Since BASIC was available on this machine, the data analysis programs were rewritten in this language. This allowed data acquisition, storage and processing to be performed by the same machine. The custom built data acquisition interface card (described at paragraph 5.1.2) was fully compatible with the 6809.

6.2 Data acquisition programs

6.2.1 Constant interval data acquisition

The original AEI software was designed to accept variable engine parameters as inputs. By setting these parameters as constants in a program written for the specific engine being tested, the amount of code was reduced by a factor of about 75%.

This program measures the average speed of the engine over one revolution and then stores pressure measurements triggered at specified time intervals. The time intervals are calculated to

correspond to an exact fraction (such as 1/64) of one revolution at the average speed. Measurements can be obtained for one or several consecutive cycles. A block diagram of this program is shown in Figure 6.1.

In the first step, the PIA is initialized for output. The CA2 line is used as an output to control the interface and is set in "handshake" mode. The CA1 line is used to receive the signal from the single-hole sensor.

Counters are set for the number of cycles to be measured and for the number of measurements per cycle. The storage files in memory are cleared.

The time interval between two succesive measurements is calculated by measuring the time between two subsequent CA1 signals. This, divided by 64, gives the number of computer clock cycles that have to elapse between measurements. Since the shortest delay loop that can be programmed is 6 cycles long, three different data acquisition subroutines are used, differing in length by 2 cycles. Thus, by selecting the proper subroutine, a precision of 1 cycle can be obtained in the timing of the measurements. At a typical engine speed of 2000 rpm, this amounts to an error of 0.22%.

When a cycle of measurements is completed, the time interval is stored, the data is transfered from the "work" memories to the main files and the counters are reset. It is then too late

to start a new cycle of measurements, therefore another delay loop synchronizes the next cycle of measurements by skipping two revolutions.

A listing of this program is shown in Appendix E, p.A-36.

6.2.2 Triggered data acquisition

This program triggers and stores a pressure measurement each time a signal is received from the position optoelectronic sensor. Measurements can be made for one engine cycle or for several consecutive cycles. A block diagram of this program is shown in Figure 6.2.

In the first step of the program, the PIA is initialized for input. The CA2 line is used as an output to control the interface and is set in "handshake" mode. The CA1 line is used to receive the signal from the single-hole sensor, while the CB1 line is used for the position sensor.

Counters are set for the number of cycles to be measured and for the number of measurements per cycle.

Once the "start" signal is received from the CA1 line, the program goes through a loop which triggers but does not store measurements for the 15 next signals (or 1/4 of a revolution, including the first signal). As the single-hole sensor is positioned such that it corresponds to a quarter of revolution

before TDC (see Appendix C), this delay is necessary to trigger the first measurement at TDC.

In the next loop, 128 pressure measurements are read and stored. Reading the ADC output through the PIA data register triggers the CA2 signal (see parag. 5.1.2), so reading a measurement triggers the next one. The pressure measurement that should actually be associated with TDC is thus the second one to be stored. Before stopping the program, the last measurement triggered has to be stored separately. Finally, a subroutine converts the data to ASCII characters for disc storage.

A listing of this program appears in Appendix E, p.A-40.

6.3 System debug programs

The interface card depends on software signals to issue the proper hardware control signals to the ADC and sample-and-hold circuitry (see parag. 5.1.2). A program must be active to examine the interface card for proper operation.

The program "1.PRO.TXT", included in Appendix E, p.A-42, was written to verify that the TDC signal is received by the interface card. The program waits for transitions to occur on the CB1 line connected to the TDC sensor. Upon such transitions, the program goes through a delay loop and issues a control pulse on the CB2 line which can be monitored with an

oscilloscope. The trace should show TTL pulses at a frequency equal to engine speed.

The program "1.PRO2.TXT", also included in Appendix E, p.A-43, was written to permit verification of the various triggering components of the interface card. While running, this program issues control pulses on the CA2 line at a frequency of about 50 KHz. This program does not depend for its operation on the reception of the TDC signal by the interface card.

6.4 Velocity fluctuation program

This program simulates the velocity fluctuation of the engine through a cycle of two revolutions by calculating the forces and acceleration of every moving component.

The velocity is calculated as a function of the crank angle by an iterative process starting at ignition top dead center (ITDC). A block diagram of this program is included in Figure 6.3.

Actual velocity measurements are used by this program for comparison. A machine language program was written for the acquisition of the required data. This program stores in computer memory the pressure signal and time elapsed for each position signal, starting at TDC for one engine cycle (two revolutions). The pressure and velocity data is converted into

decimal, taking into account the pressure transducer's calibration.

An initial value of the velocity at ITDC is assumed; rapid convergence is usually obtained if this value is assumed at 95% of the experimental average velocity. From this starting point, the energy balance is calculated for each increment of the crank angle. The resulting average value of the velocity is calculated and compared to the experimental value; if they do not correspond, the initial value of the velocity at ITDC is corrected and the program returns to the starting point and iterates until both average values are equal within a preset error.

Both the experimental and simulated velocity-versus-crank angle curves are plotted using the system subroutine "DDPLOT". As it was found that the experimental curve was very unsteady, a subroutine was written to smooth the data and the resulting curve was also including in the plot. Results of this analysis as well as sample outputs are included in the next chapter.

A listing of this program appears in Appendix E, p.A-48. Details of the force calculations are included in Appendix B.

6.5 Data analysis program

Two data analysis programs were written. The first was written in Fortran and ran on the McGill Computing Centre mainframe.

This program reads the digital pressure data and converts it to pressure units. A plot of pressure versus crank angle was then made through the system subroutine "DDPLOT". Pressure data is interpolated at constant volume intervals and separated into four series to correspond with the four strokes of the cycle. Plotting these four sets of data through DDPLOT draws a PV diagram. The diagram is integrated numerically to obtain the indicated work.

A second data analysis program was written in Basic for use with the 6809 data acquisition system. The program converts the pressure data converted to ASCII characters by the data acquisition program into pressure decimal values. Once again, an interpolation subroutine converts the data to constant volume interval values. This converted data is then separated into four sets corresponding to the four strokes of the cycle.

The subroutine Basgraph developed at McGill is used to plot the resultant PV diagram on the CRT. The plot can be observed to verify its validity. Several display options are incorporated in the program. It is possible to select log-log scales which permits detection of phasing errors. Other options affect the scale of the diagram on the screen.

A listing of this program appears in Appendix E, p.A-56.

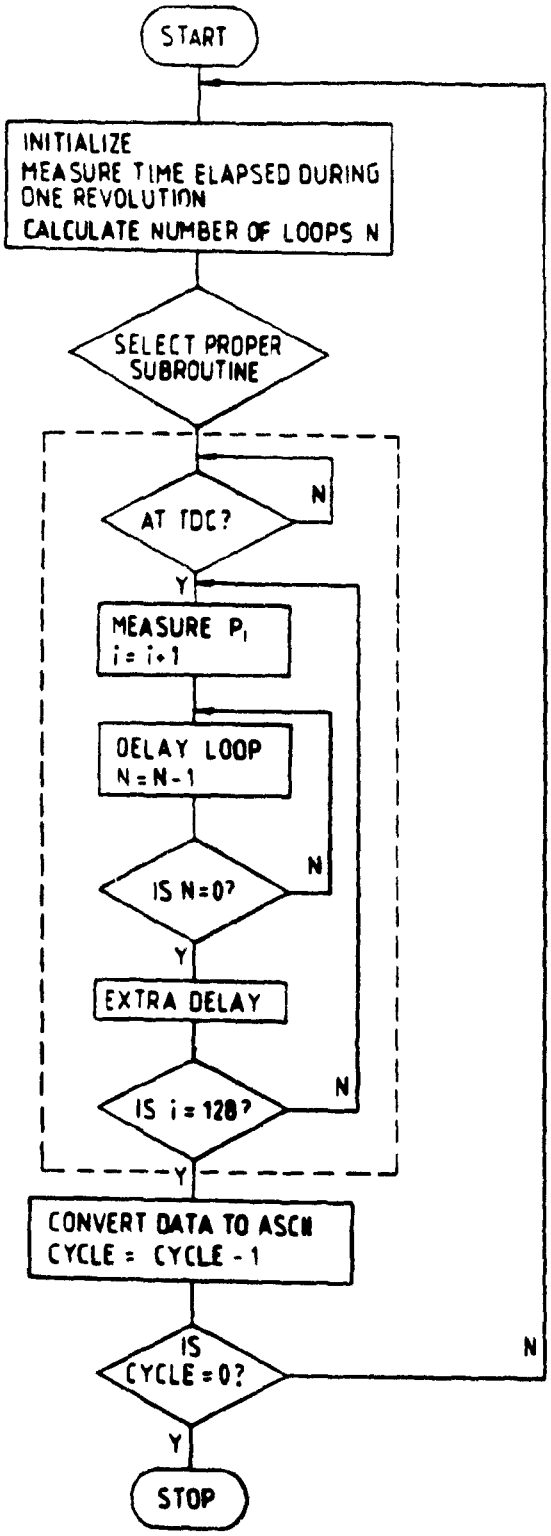

Block diagram of constant time interval data acquisition program
Figure 6.1

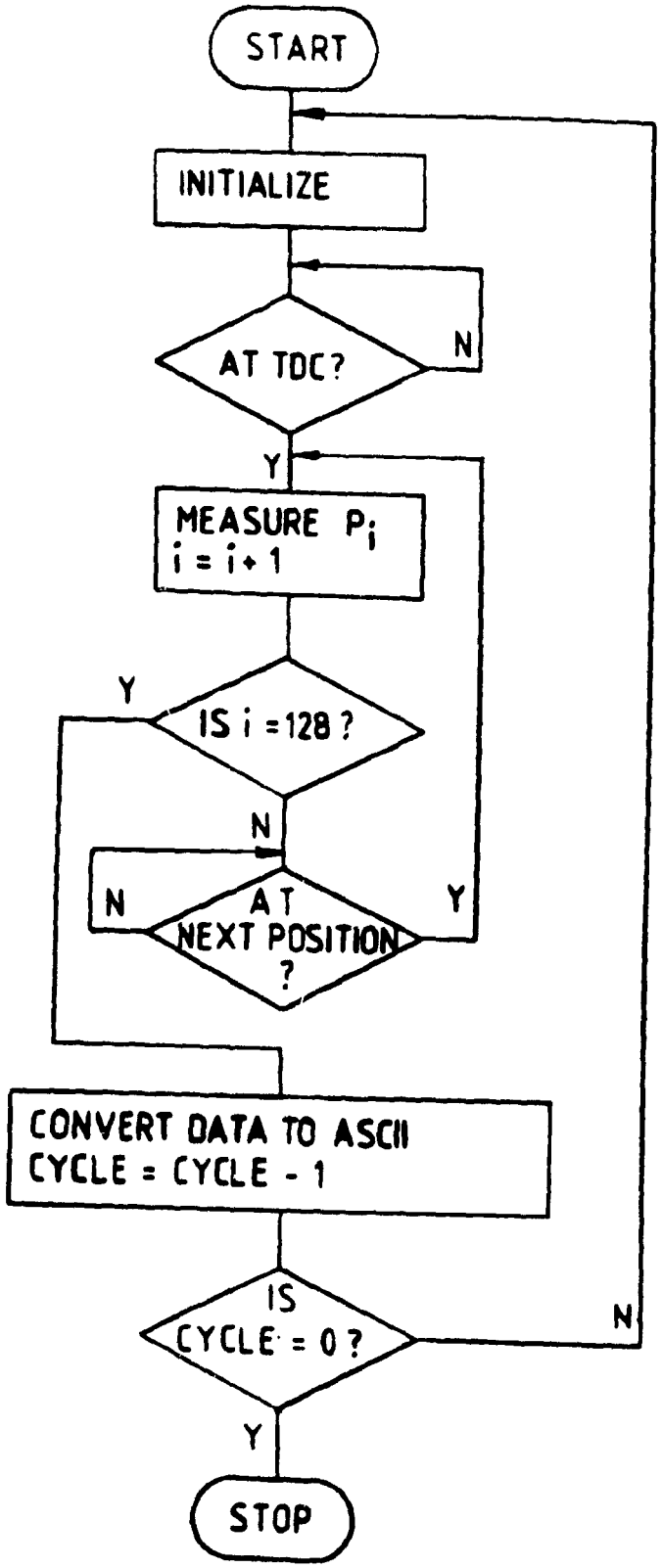

Block diagram of triggered data acquisition program
Figure 6.2

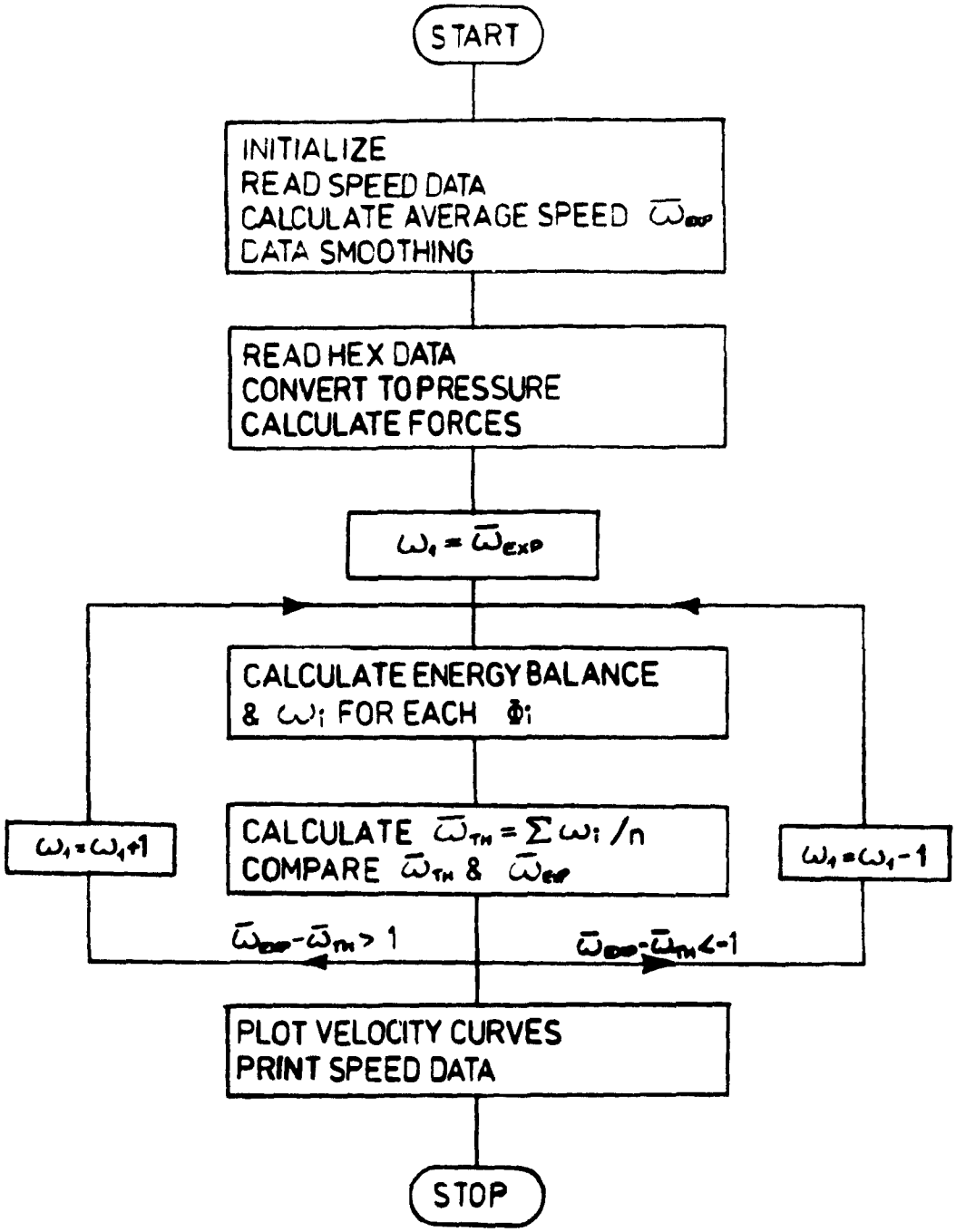

Block diagram of velocity fluctuation program
Figure 6.3

CHAPTER 7

EXPERIMENTAL ANALYSIS

7.1 General

The experimental analysis was planned to be presented in two separate parts. The first part evaluates the performance of the test equipment; the second part would present an analysis of the experimental data obtained under various operating conditions which would have resulted in the development of diagnostic methods.

The performance of the test equipment proved to be unsatisfactory. Instrumentation problems have been described in previous sections. Some other problems of a conceptual nature are described in this chapter.

The data abtained from the experiments were insufficient to be able to develop a set of diagnostic methods as originally foreseen. The description in this chapter is therefore limited to an analysis of the results pertaining to the concept of data acquisition on a high speed single cylinder reciprocating engine.

7.2 Velocity fluctuation analysis

The data sets obtained with the triggered data acquisition program resulted in plots with a high degree of dispersion

(Figure 7.1). Data sets were obtained that could be used with the velocity fluctuation program (see section 6.3) for three consecutive cycles. The plots shown in Figure 7.2 and measured velocities in Table 7.1 show that the dispersion pattern is repeated over successive cycles.

The obvious cause of this problem is that the holes in the perforated disc are not evenly spaced, due to the tolerance of the method used to drill these holes.

To compare this scattered data with the simulated curves, a data-smoothing routine was used.

This subroutine calculates a weighted average for a data point using both the previous and the following one. This algorithm does not change the average value of the data set. The data was smoothed twice by this process before the resulting curve was regular enough to allow comparison with the simulated curve.

It can be observed that the simulated curve agrees quite well, Figure 7.3, with the smoothed experimental data except at the end of the cycle. At this point, the simulated velocity is higher and does not match the initial velocity. This behavior of the model indicates that the calculated energy balance is higher at the end than at the beginning of the cycle. This could mean that the energy lost in friction is greater than estimated.

7.3 Constant time interval data acquisition

The assumption of a constant speed fails on this particular low-inertia, single cylinder engine: the average engine speed can fluctuate by as much as 15% between subsequent cycles.

As a result, if the time interval calculated from the average speed of one cycle is used to acquire data in a subsequent cycle, the measurements are not triggered at the right moment.

The resultant PV diagrams are distorted and cannot be used for analysis as shown in Figure 7.4. If the engine slows down after the speed has been measured by the computer, the subsequent pressure measurements will be associated with crank angle positions later than the real values, as the engine has not rotated by an angle as great as calculated from the average speed in the given time span. This results in a "fat" PV diagram where the peak pressure point is shown much later than TDC.

If the engine accelerates after the speed has been measured by the computer, the opposite error is incurred. This results in a PV diagram where the expansion curve crosses the compression curve as the peak pressure point is shown before TDC. Another symptom of speed fluctuation is the crank angle at which the compression and exhaust curves cross.The actual cross over should occur at a crank angle corresponding to about V= 2/3 V_{max}. In the case of the accelerating engine, the crossover is

shown at an earlier location, closer to V_{max}. In the case of a decelerating engine, the crossover is shown later, closer to V_{min}. This can be observed in the output of experimental data obtained using the constant speed data acquisition program, included in Figures 7.5 a, b and c.

This velocity fluctuation has been studied using a simple program measuring the time elapsed between the occurence of TDC signals. The engine speed was measured and stored for each of 255 consecutive revolutions.

The resulting data was then analysed to obtain average speed, variance and minimal as well as maximal speed within the data set. The test was repeated under different speed and loading conditions. The results are shown in Table 7.2. It appears that engine speed stability increases with higher speeds but decreases under load.

The source of instability is a function of the combustion process itself. The combustion is dependant on several factors: this is best summarised by Amann (1):

> "The susceptibility of an engine cylinder to combustion variability from cycle to cycle is influenced by a variety of factors, both chemical and physical. In a given engine, spark scatter (random variations in ignition timing) and inconsistencies in mixture composition and/or preparation from cycle to cycle have often been suspected. However, even when a single-cylinder

> engine was run at full throttle with carefully controlled spark timing on a stoichiometric mixture of propane and air that had been thoroughly mixed by passing it down a 3-m long pipe packed with marbles en route to the intake port, combustion variability persisted. It is generally acknowledged that after all other potential contributors to such variability have been brought under control, the remaining variation in combustion is attributable primarily to randomness in mixture motion in the vicinity of the spark plug at the time of ignition."

Consequently, the constant time interval data acquisition algorithm cannot be used on this particular engine. Since the error involved by using the triggered data acquisition method is known and constant, this method was chosen as the one more likely to permit the obtaining of valid experimental data.

It is thus necessary to average pressure data obtained over several consecutive cycles to obtain data sets that are usable for further analysis. Amann (1) suggests that a number of measurements in the order of 100 consecutive cycles is required to secure a reliable sample size.

Lancaster, Krieger and Lienisch (11) give typical values of 40 cycles for highly stable engine operating configurations, up to 300 for conditions of higher variability. Industrial researchers average measurements over as many as 500 consecutive cycles (24). This involves a great deal of confidence in the reliability of the instrumentation. The

current test equipment did not have this degree of reliability.

7.4 Validity of pressure data

Lancaster, Krieger and Lienisch (11), Brown (3) and other researchers (23) point out the need to validate the pressure data prior to analysis. They suggest obtaining "motored" (*) data that should be examined prior to the analysis of fired data. This can lend information regarding phasing and scaling error, because the pressure signal obtained from a mctored engine is not subjected to the instabilities that affect the fired signal.

Unfortunately, no provision had been incorporated in the test bed design to motor the engine. It is nonetheless necessary to examine carefully the pressure data to determine its validity. Brown (3) states: "consistency is no indication of accuracy", meaning that data that looks right is not necessarily right.

7.5 Data acquisition chronology

Several data sets were obtained before the thermal strain problem was identified and understood (see section 4.2.1). These data sets were submitted to the Fortran data analysis routine. The shape of the PV diagram was the only indication of the validity of the measurements.

* Pressure data obtained while the engine is rotated by an external source of power.

As was explained in section 4.2.1, one symptom of this problem was that the intake and exhaust pressure for datasets obtained under loading conditions did not correspond to atmospheric pressure. Sample outputs of the data analysis program are shown in Figure 7.5. These and other data sets obtained prior to the solution of the thermal strain problem were discarded.

By then it had become evident that the manual transfer of data between the data acquisition system and the mainframe computer for data processing was inadequate for the amount of data required for analysis. At this stage, the 6800 computer was replaced by the 6809 system, as described in section 5.1.1.

These and subsequent data sets were obtained using the constant time interval data algorithm and were thus subject to distortion, as shown in Figures 7.4 and 7.5. The position sensors are unreliable and their signals had to be upgraded through the use of Schmidt triggers before data sets could be obtained using the triggered data acquisition algorithm.

At this stage, the data sets provided seriously distorted and attenuated PV diagrams. A sample of such a diagram is included as Figure 7.6. This phenomenon delayed work for a few weeks but eventually disappeared. The source of the distortion was identified as the presence of liquid in the passage of the pressure transducer adapter. This problem is described by Brown (3). The liquid was most likely fuel condensed by the

low temperature of the water-cooled transducer adapter. At the time this problem occured, the water inlet temperature was about 10^{o} C.

Finally, an apparently correct data set was obtained. The PV diagram obtained from the single valid dataset is shown in Figure 7.7. The log-log plot of these data is shown in Figure 7.8.

It can be seen that the intake and exhaust strokes are represented by straight lines on the log-log plot, indicating a polytropic process. This corresponds to the theory of the four-stroke cycle. The slope of the compression curve is about 1.25, which is a realistic value of the polytropic exponent. The expansion curve has a slope of about 0.5, which is not correct.

The general shape of the diagram is correct (the four strokes are well defined) but the maximum pressure area close to TDC has a more pointed shape than typical PV diagrams. This cannot be explained by combustion phenomena.

Since the pressure transducer failed catastrophically (a burst diaphragm) after this data was obtained, the validity of this PV diagram is at best suspect as the transducer was very likely already damaged. Within the available time, a third transducer could not be obtained for further work.

TOTAL LENGTH 7258
ENTRY ADDRESS 118010

1 PHI	SPEED1	SPEED2	SPEED3
0	1859.0	1959.0	1833.7
5	1832.2	1832.2	1731.5
11	2003.2	2003.2	1942.8
16	1885.9	1885.9	1885.9
22	1942.8	1942.8	1885.9
28	2003.2	1942.8	1942.8
33	1942.8	1942.8	1942.8
39	1942.8	1942.8	1885.9
45	2209.4	2209.4	2209.4
50	1832.2	1885.9	1832.2
56	2003.2	2003.2	2003.2
61	2067.5	2003.2	2003.2
67	1885.9	1885.9	1885.9
73	2067.5	2067.5	2003.2
78	2003.2	2003.2	2003.2
84	2136.1	2067.5	2136.1
90	1942.8	1942.8	1942.8
95	2067.5	2067.5	2003.2
101	2067.5	2003.2	2067.5
106	2067.5	2067.5	2067.5
112	2136.1	2136.1	2136.1
118	2003.2	2003.2	1942.8
123	2067.5	2003.2	2067.5
129	2003.2	2003.2	2003.2
135	2463.0	2372.2	2372.2
140	1942.8	1942.8	1942.8
146	2209.4	2209.4	2136.1
151	2136.1	2067.5	2136.1
157	2136.1	2136.1	2136.1
163	2136.1	2136.1	2136.1
168	2067.5	2067.5	2067.5
174	1885.9	1832.2	1885.9
180	2287.9	2209.4	2209.4
185	2136.1	2209.4	2136.1
191	2136.1	2067.5	2067.5
196	2287.9	2287.9	2287.9
202	2067.5	2003.2	2003.2
208	1885.9	1885.9	1942.8
213	2067.5	2067.5	2067.5
219	2067.5	2003.2	2003.2
225	2136.1	2136.1	2067.5
230	1942.8	1942.8	2003.2
236	2136.1	2136.1	2057.5
241	2003.2	1942.8	2003.2
247	2287.9	2209.4	2209.4
253	1832.2	1832.2	1832.2
258	2372.2	2287.9	2372.2
264	1942.8	1942.8	1885.9
270	2003.2	2003.2	2003.2
275	2067.5	2003.2	2067.5
281	2003.2	2003.2	2003.2
286	2003.2	2003.2	2003.2
292	2136.1	2136.1	2067.5
298	2136.1	2067.5	2136.1
303	1885.9	1885.9	1885.9
309	2136.1	2136.1	2136.1
315	2067.5	2067.5	2003.2
320	2067.5	2003.2	2067.5
326	2136.1	2136.1	2136.1
331	2003.2	2003.2	2003.2
337	2136.1	2067.5	2067.5
343	2209.4	2209.4	2209.4
348	1942.8	1885.9	1942.8
354	2067.5	2003.2	2003.2

337	2136.1	2067.5	2067.5
343	2209.4	2209.4	2209.4
348	1942.8	1885.9	1942.8
354	2067.5	2003.2	2003.2
360	2209.4	2209.4	2209.4
365	1942.8	1942.8	1885.9
371	2067.5	2067.5	2136.1
376	2003.2	1942.8	1942.8
382	2067.5	2067.5	2067.5
388	2067.5	2067.5	2003.2
393	2067.5	2003.2	2067.5
399	2003.2	2003.2	2003.2
405	2287.9	2287.9	2287.9
410	1885.9	1832.2	1885.9
416	2067.5	2067.5	2003.2
421	2067.5	2067.5	2067.5
427	1942.8	1832.2	1885.9
433	2003.2	2067.5	2003.2
438	2003.2	1942.8	2003.2
444	2136.1	2067.5	2057.5
450	1885.9	1942.8	1885.9
455	2067.5	2003.2	2003.2
461	1942.8	1942.8	2003.2
466	2067.5	2003.2	2003.2
472	2067.5	2067.5	2067.5
478	1885.9	1885.9	1835.9
483	2003.2	1942.8	1942.8
489	1942.8	1942.8	1942.8
495	2287.9	2209.4	2287.9
500	1832.2	1832.2	1832.2
506	2136.1	2067.5	2057.5
511	2003.2	2003.2	2003.2
517	2003.2	2003.2	2003.2
523	2067.5	2067.5	2057.5
528	2003.2	1942.8	1942.8
534	1781.5	1781.5	1781.5
540	2136.1	2067.5	2136.1
545	2067.5	2067.5	2067.5
551	2003.2	1942.8	1942.8
556	2136.1	2209.4	2209.4
562	1942.8	1885.9	1885.9
568	1832.2	1832.2	1832.2
573	2003.2	1942.8	1942.8
579	1942.8	1942.8	1942.8
585	2003.2	2003.2	2003.2
590	1942.8	1885.9	1885.9
596	2003.2	2003.2	2003.2
601	1885.9	1832.2	1885.9
607	2209.4	2209.4	2136.1
613	1733.5	1733.5	1733.5
618	2287.9	2209.4	2287.9
624	1885.9	1832.2	1832.2
630	1942.8	2003.2	2003.2
635	1942.8	1885.9	1885.9
641	1942.8	1942.8	1942.8
646	1942.8	1885.9	1942.8
652	2067.5	2067.5	2003.2
658	2067.5	2003.2	2003.2
663	1832.2	1781.5	1832.2
669	2003.2	2067.5	2003.2
675	2003.2	1942.8	2003.2
680	1942.8	1942.8	1885.9
686	2067.5	2003.2	2067.5
691	1942.8	1885.9	1885.9
697	2003.2	1942.8	1942.8
703	2067.5	2067.5	2067.5
708	1832.2	1832.2	1781.5
714	1885.9	1885.9	1885.9
720	1859.0	1859.0	1833.7

Velocity over three consecutive cycles
as a function of crank angle "phi"

Table 7.1

Load	RPM	Std. dev.	Slowest	Fastest
No	1550	6%	-16%	+11%
No	2500	2%	-4%	+5%
Yes	2280	3%	-8%	+6%
No	3430	1%	-2%	+2%
Yes	2765	3%	-5%	+4%

Average speed variation
Table 7.2

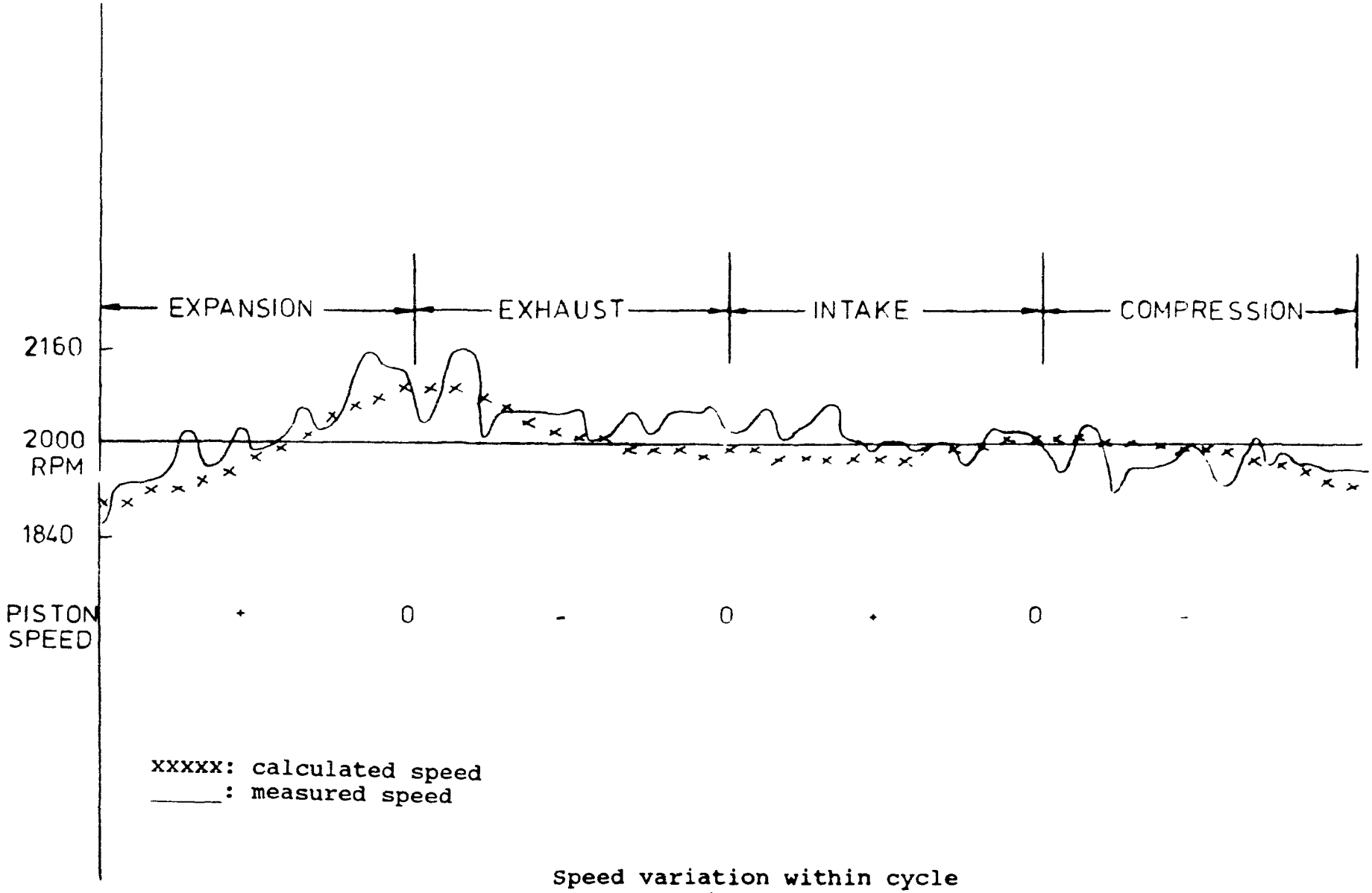

Speed variation within cycle
Figure 7.1

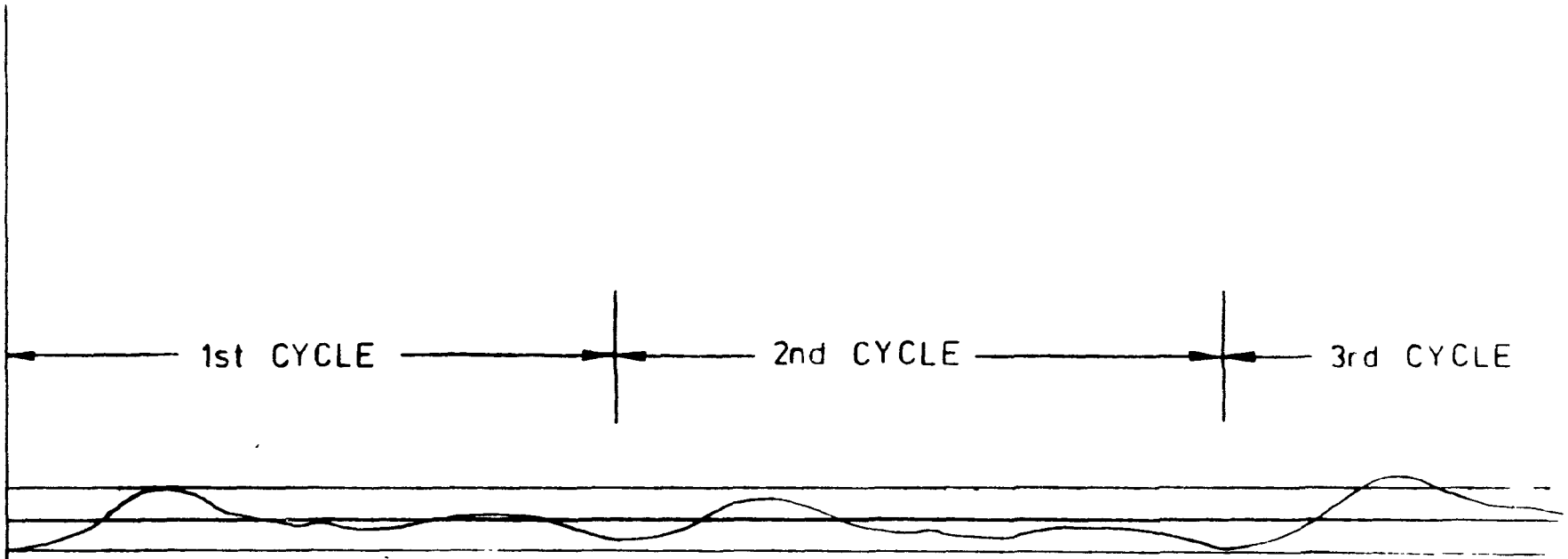

Speed variation over consecutive cycles
Figure 7.2

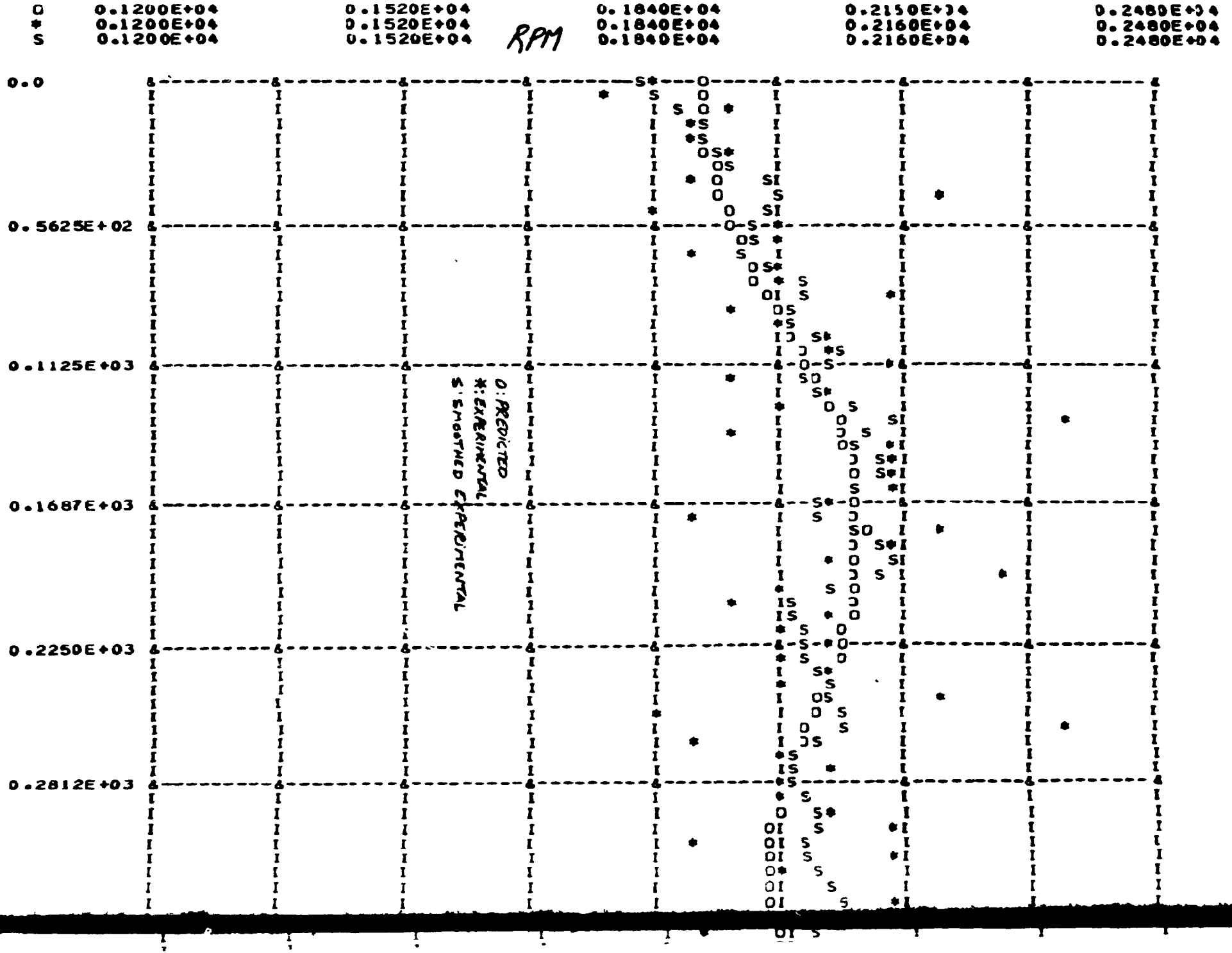
O 0.1200E+04 0.1520E+04 0.1840E+04 0.2160E+04 0.2480E+04
* 0.1200E+04 0.1520E+04 0.1840E+04 0.2160E+04 0.2480E+04
S 0.1200E+04 0.1520E+04 0.1840E+04 0.2160E+04 0.2480E+04
RPM
0.0
0.5625E+02
0.1125E+03
0.1687E+03
0.2250E+03
0.2812E+03
O: PREDICTED
*: EXPERIMENTAL
S: SMOOTHED EXPERIMENTAL

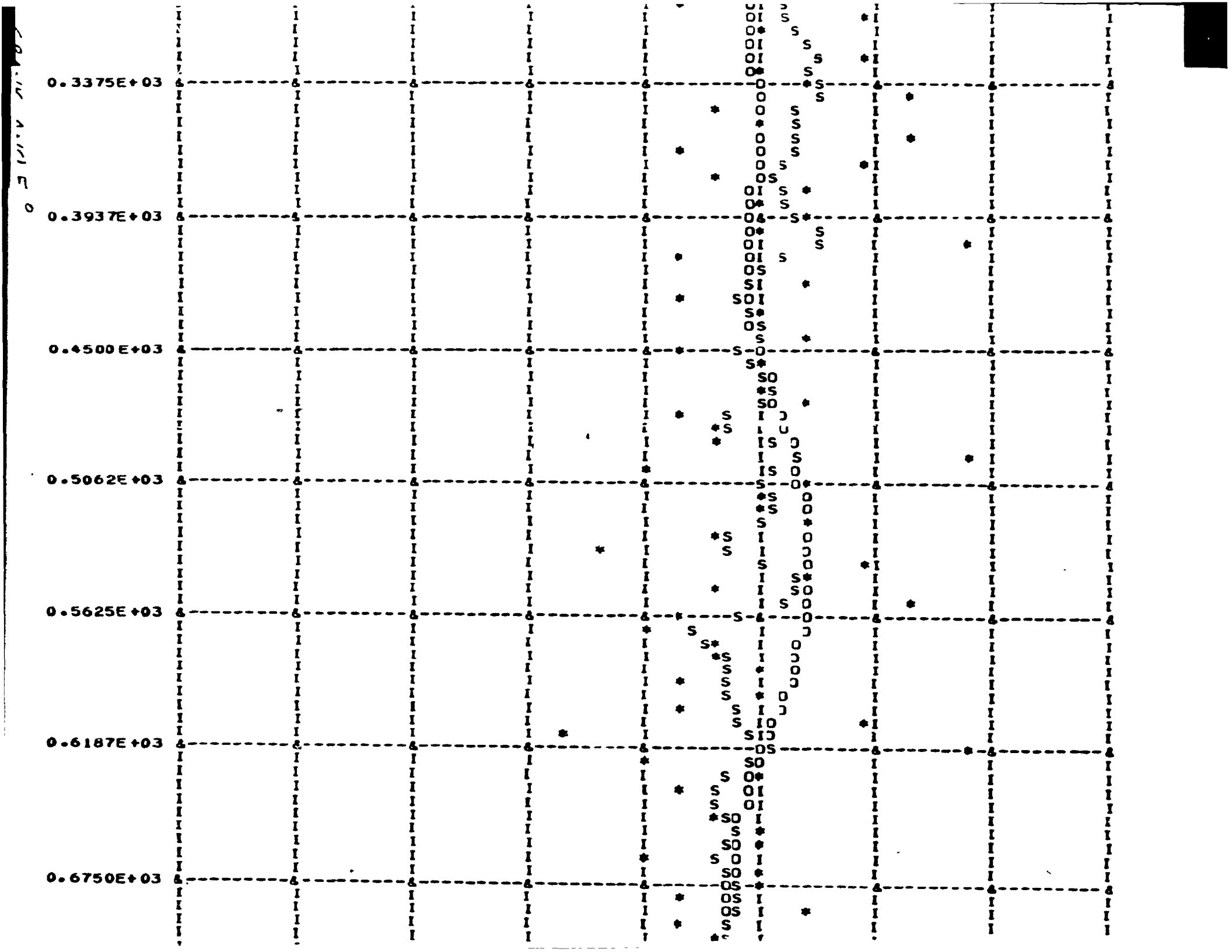
0.3375E+03
0.3937E+03
0.4500E+03
0.5062E+03
0.5625E+03
0.6187E+03
0.6750E+03

Velocity fluctuation analysis
program output

Figure 7.3

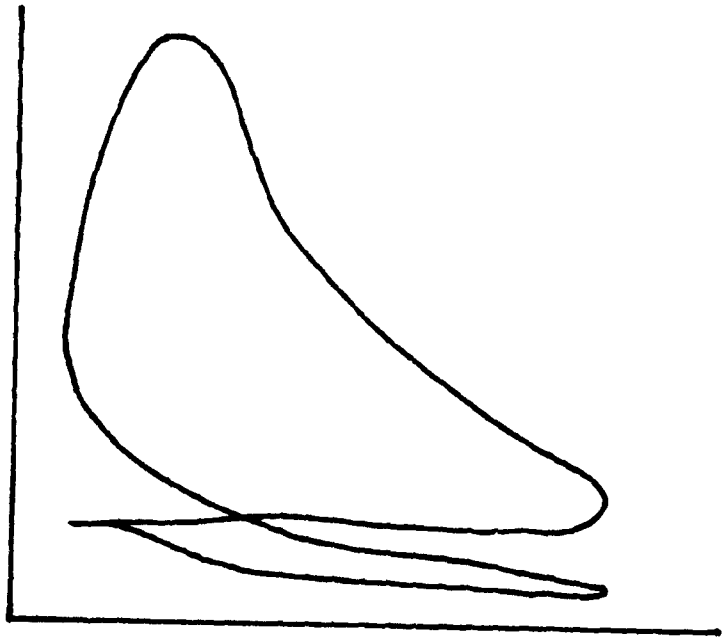

Engine running slower than average speed

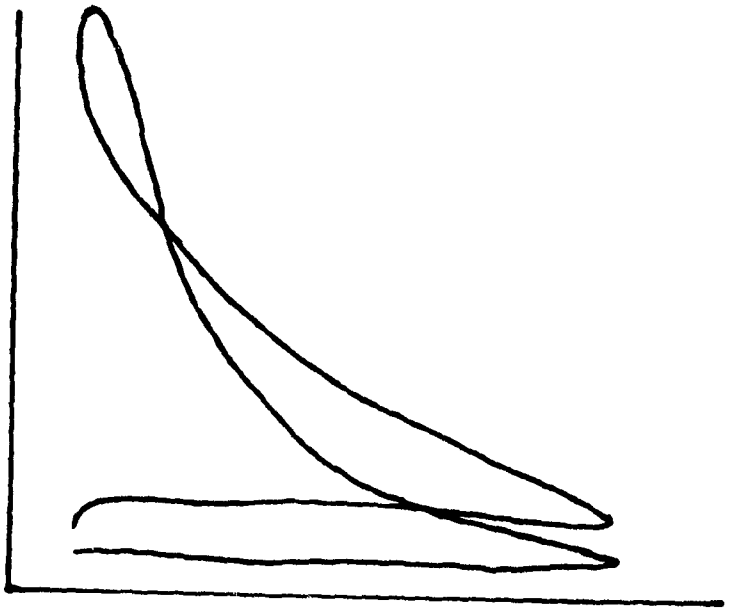

Engine running faster than average speed

PV diagrams distorted by average speed variation
Figure 7.4

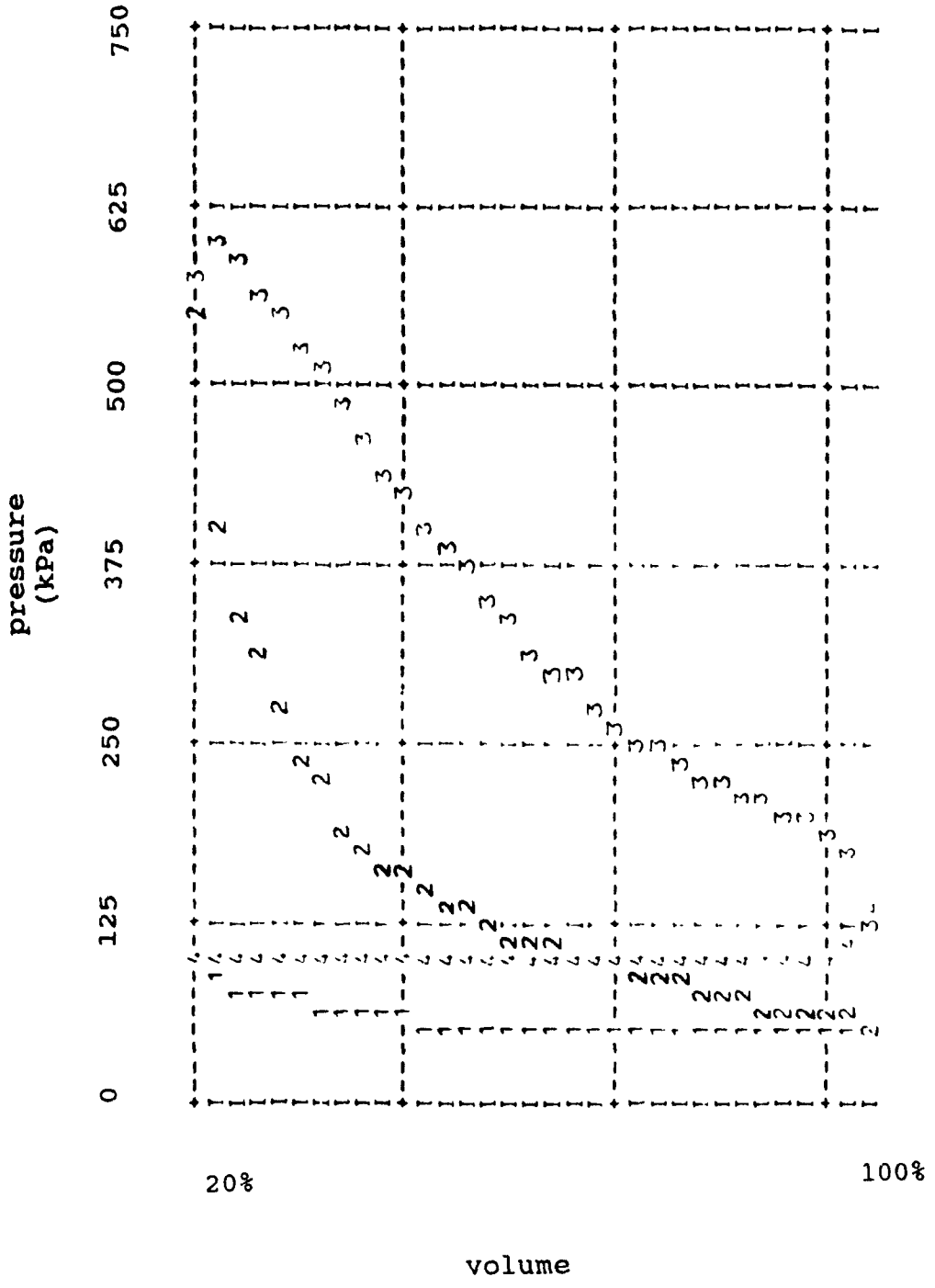

Engine running close to average speed
PV diagram from data analysis program
Figure 7.5a

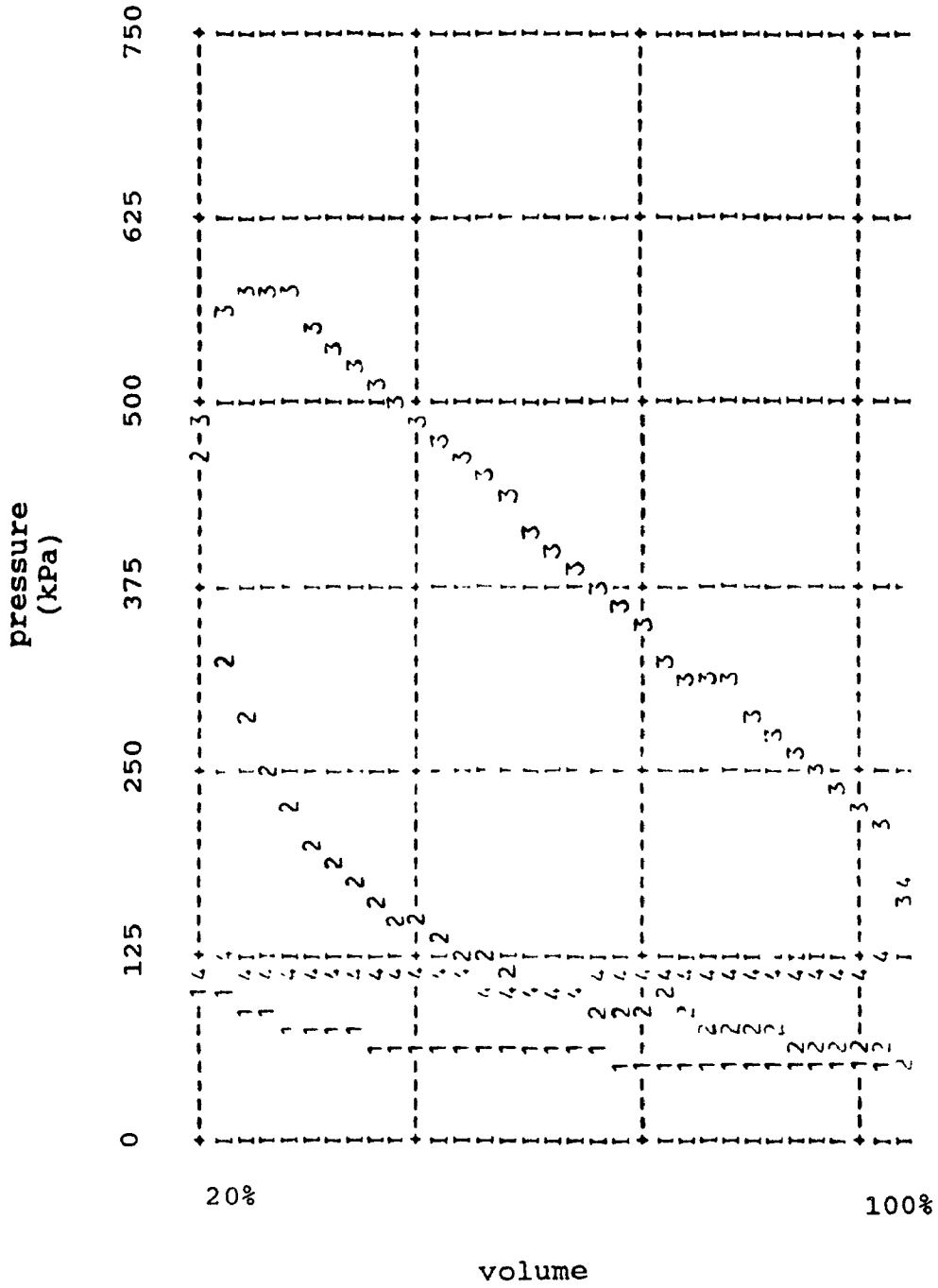

Engine running slower than average speed
PV diagram from data analysis program
Figure 7.5b

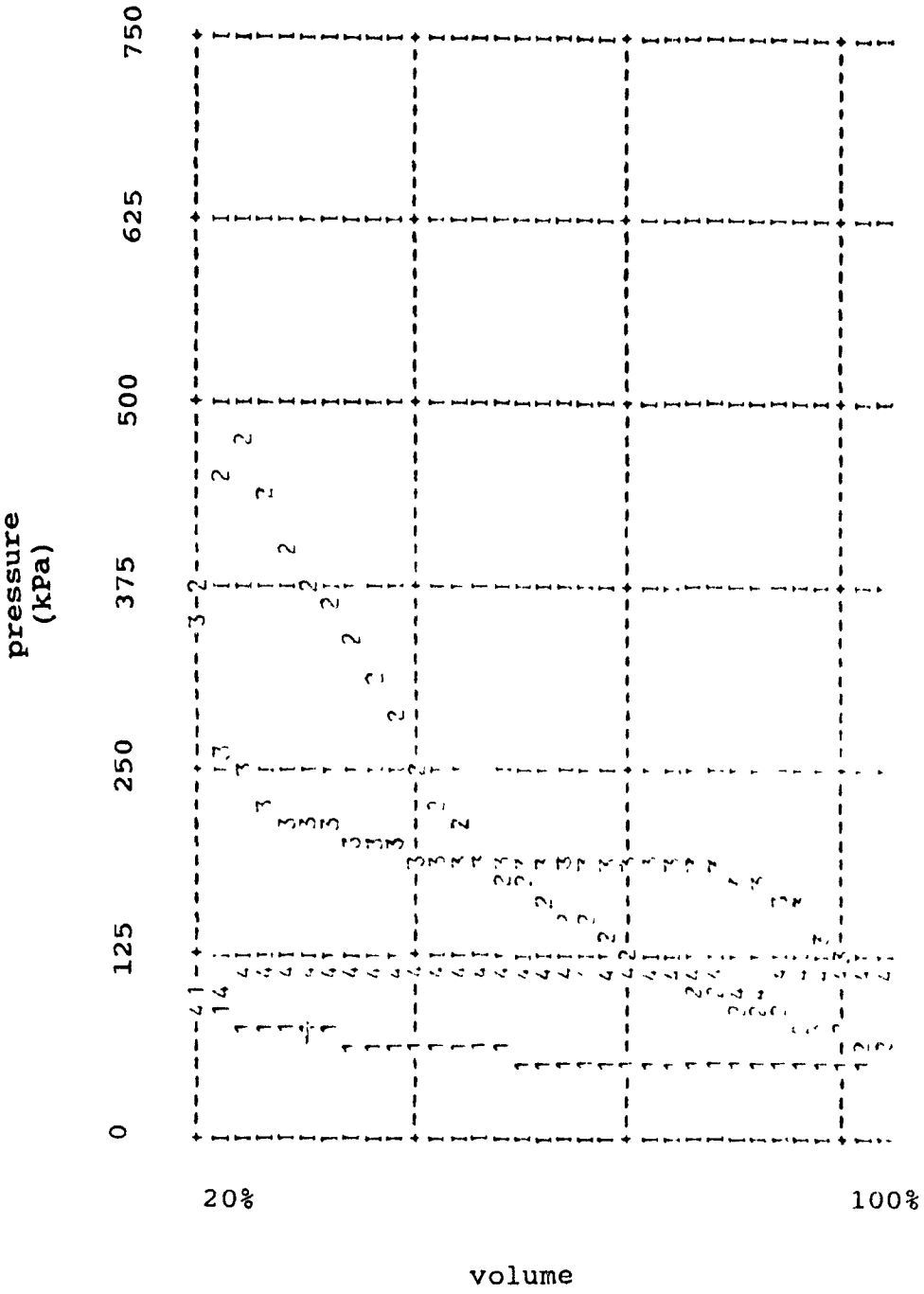

Engine running faster than average speed
PV diagram from data analysis program
Figure 7.5c

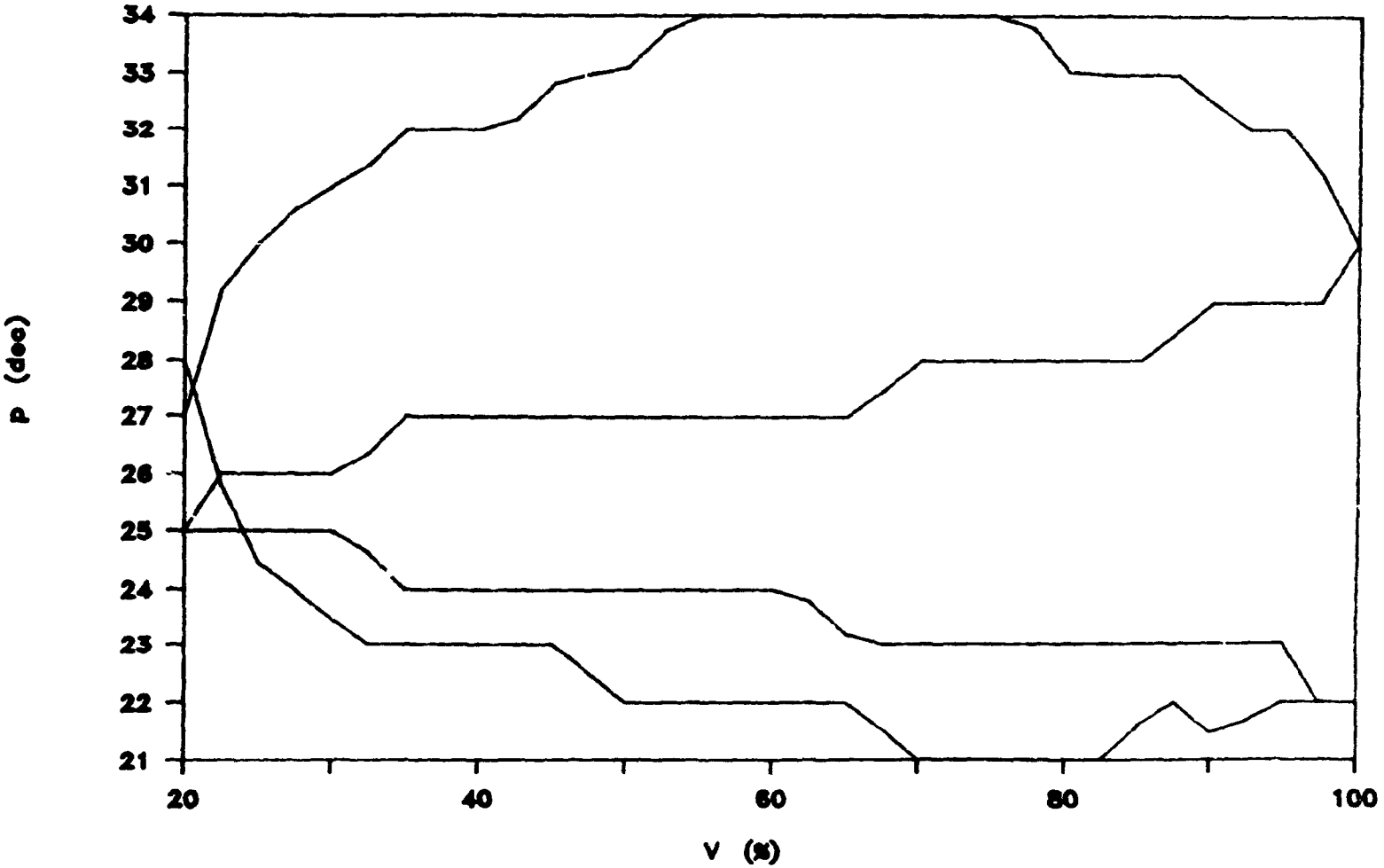

PV diagram distorted by fuel condensation
in transducer adapter passage
Figure 7.6

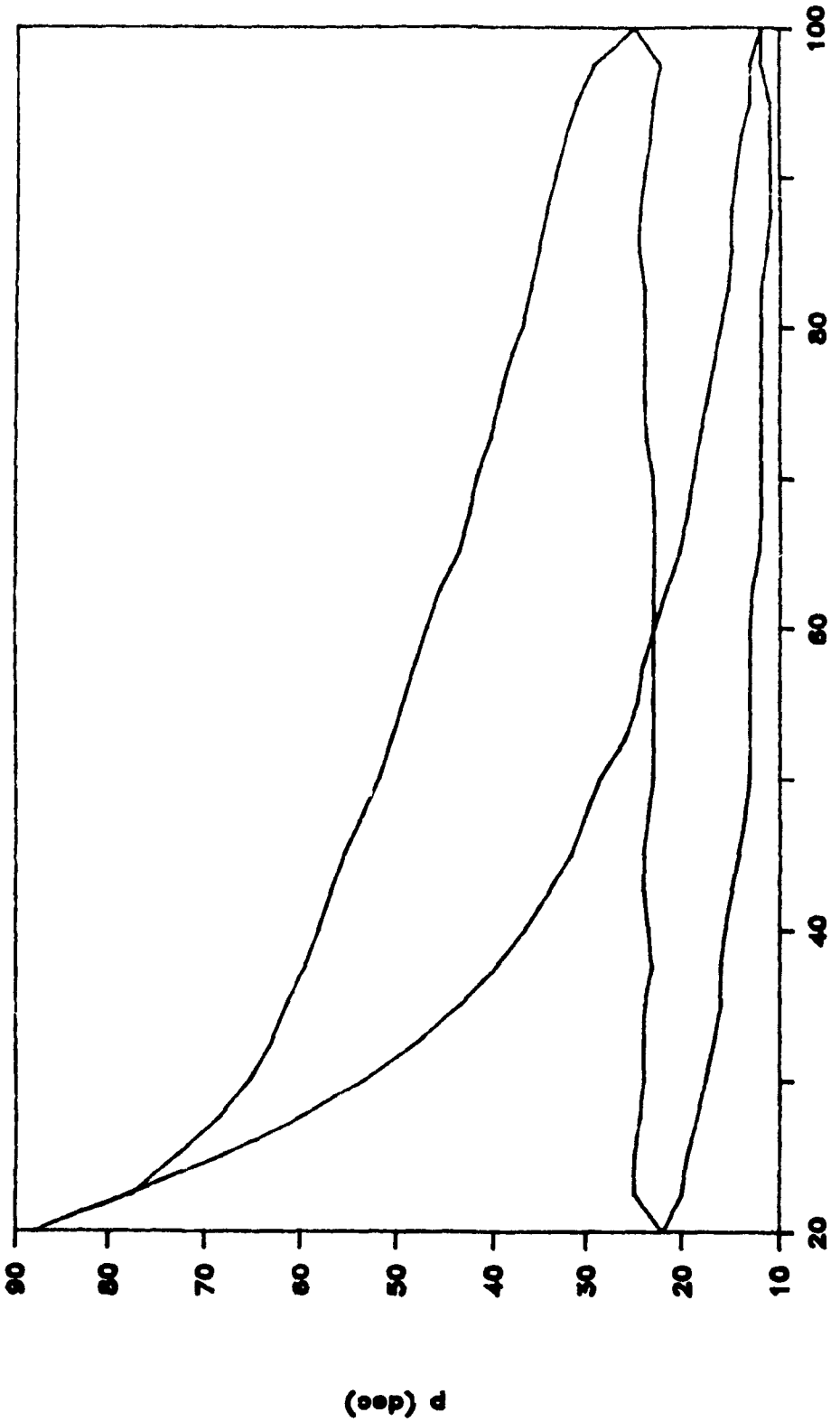

PV diagram from final data set
Figure 7.7

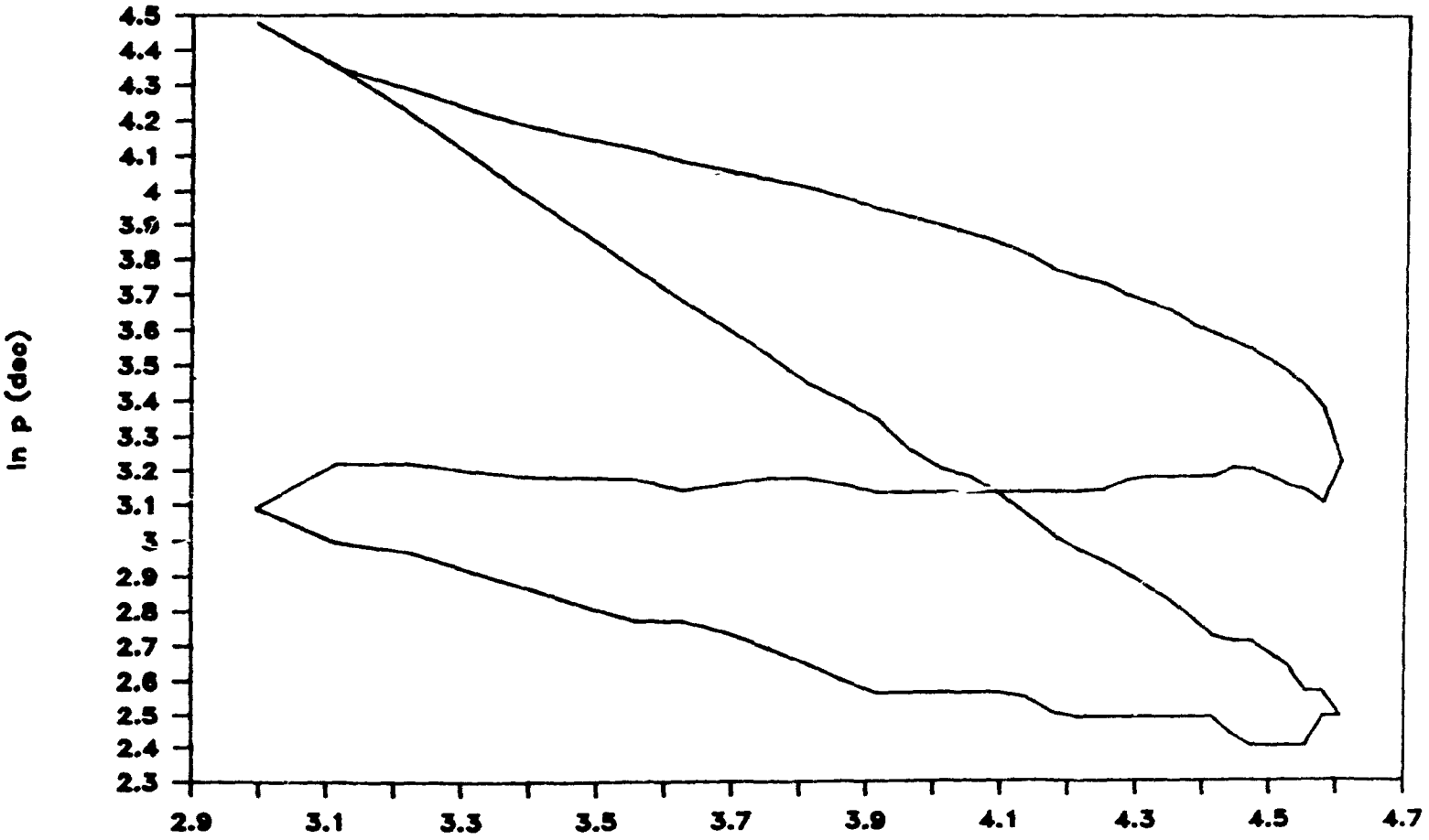

ln P-ln V diagram from final data set
Figure 7.8

CHAPTER 8

CONCLUSION AND RECOMMENDATIONS

8.1 General

The goal of this research project, to establish diagnostic methods for a combustion engine via the PV diagrams has not been reached. The major cause was that the task of instrumenting a spark ignition internal combustion engine had been severely underestimated.

The problems that were encountered while attempting to obtain experimental data have, for the most part, been well documented by professional researchers. However, as this was originally thought of as a straightforward task, the literature survey was limited to topics regarding automatic engine diagnosis and pressure volume diagram analysis. A new survey covering internal combustion engine instrumentation was done only after a considerable time was spent in understanding data acquisition problems and after acquiring much invalid data.

As was stated earlier, this report is intended to assist future researchers who would like to continue work on the original project.

8.2 Recommendations for future work

The reliability of the test equipment has been the major problem in obtaining experimental data. The pressure signal from a spark ignition, internal combustion engine has a random character. To make valid observations on the pressure-volume diagram as a tool for engine diagnosis, several hundreds of data sets consisting of averages of at least one hundred successive engine cycles each are required. To obtain reliability to such an extent that such an amount of data can be acquired, a few aspects of the apparatus need to be revised. These will be described in this section.

8.2.1 Test bed

The test bed itself has been reliable throughout the test period. The brake lining needs to be replaced with a more heat resistant material in view of the need to average measurements over several consecutive cycles. The current lining overheats after a few seconds of operation at high load and the resultant engine condition is not stable as the brake load decreases gradually.

Validating the data is recognized by professional researchers as an extremely important task. An electric motor should be incorporated in the test bed such as to allow the acquisition of motored pressure data. The power rating of this electric motor should be high enough so that the speed of the engine

remains fairly constant through the four strokes. A large inertia, auxiliary, declenchable flywheel on the motoring unit is also deemed advisable in this regard.

8.2.2 Instrumentation

The pressure transducer recommended by most researchers is the piezo-electric type. Specific transducers are manufactured by Kistler and AVL for internal combustion engine applications. Such transducers can provide reliable data within the required margins of accuracy. These transducers are provided with integral internal water cooling, which permits their installation directly in the cylinder head. It should be noted however that the capillary cooling tubes have a tendency to plug up. Ideally, a recirculating water cooling system should be designed, allowing the use of distilled water as a coolant.

In view of the problems inherent in the passage type of installation, modifying the cylinder head to install the pressure transducer directly should be considered.

The possibility of using the "ring transducer" described by Powell and Hosey (9) should also be investigated.

The design of the position sensors needs improvement. It is suggested that the position sensor and TDC sensor be installed on separate brackets mounted on different sides of

the test bed frame. The designer should ensure that the brackets are sufficiently rigid to resist motion due to engine vibrations. The new brackets could retain the current adjustment techniques for height (shims) and radial position (slotted holes). However, slotted holes are not adequate for the adjustment of the angular position of the sensors. Some form of screw adjustment should be provided to ensure proper synchronization of the sensors.

Commercial shaft encoders are available and may be cost effective compared to the fabrication of accurate mounting brackets. Their accuracy is better than that of the locally fabricated perforated discs. There does not seem to be a simple way to incorporate such a position encoder in the current test bed design. The benefits to be derived from accurate position measurements may justify an extensive rebuilding of the test bed.

8.2.3 Computer system

The SWTP 6809 system has adequate capacity for the data acquisition tasks; however, it is essentially an obsolete machine. The existing systems at McGill are little used any more and are replaced by IBM PC, or compatible, systems.

Replacing the 6809 with a PC should be considered in view of standardizing the type of equipment not only for use in the laboratory but also to be compatible with external

installations. This will involve redesigning the custom interface card.

8.2.4 Laboratory space

Any further work should be performed in a more reliable environment. The test bed was installed throughout the experiments in room 263B, an Undergraduate laboratory mainly used for the "Measurement Laboratory" course. This room was not adequate for experiments involving the operation of an internal combustion engine. The location of the engine and test equipment should be guided also by safety considerations something that due to the lack of adequate space was ignored in this set-up.

8.3 Conclusion

Internal combustion engines are subject to severe cycle-to-cycle combustion variability. Obtaining pressure measurements for the development of diagnostic methods will involve some form of statistical analysis to even out this variability. This, in turn, implies a rigorous approach where each data set used is an average obtained over several consecutive cycles.

Consequently, the experimental apparatus has to have a very high level of reliability: the Prony brake must control engine loading to a constant level over long periods; the

pressure transducer must survive a harsh environment and has to be immune from errors such as caused by thermal strain or ignition noise. The pressure measurement system has to be coupled to a reliable and accurate crank angle sensor as errors in the association of crank angle and pressure measurements cancel the care with which the pressure measurements were obtained.

The test bed built for this research project did not have the reliability required for the obtention of the required data. Several problems relating to the accuracy and the reliability of the pressure and crank angle measurements have been identified and possible solutions proposed.

This project was an extension of research done at McGill on an Automatic Engine Indicator. Adaptation of this system to a high-speed spark ignition engine revealed a conceptual problem in the data acquisition algorithm. A different algorithm was used to overcome the error caused by the high cyclic variation of the revolution speed of this type of engine. The Automatic Engine Indicator software was also simplified in view of a future single-chip computer implementation.

The author is confident that once the reliability problems have been resolved, the original task of developing the diagnostic methods will be a straightforward one.

REFERENCES

1 Amann,C.A. Cylinder Pressure Measurement and its use in Engine Research SAE paper 852067, 1985.

2 Bhot,S. Quayle,R. Microprocessor Control of Ignition Advance Angle. Microprocessors and Microsystems, vol. 6-7: pp. 355-359, 1982.

3 Brown,W.L. Methods for evaluating requirements and errors in Cylinder Pressure Measurements. SAE paper 670008, 1967.

4 Brown,W.L. The Caterpillar imep Meter and Engine Friction. SAE paper 730150, 1973.

5 Douaud,A. Eyzat,P. DIGITAP-An On-Line Acquisition and Processing System for Instantaneous Engine Data- Applications. SAE paper 770218, 1977.

6 Fischer,R.V. Macey,J.P. Digital Data Acquisition with Emphasis on Measuring Pressure Synchronously with Crank Angle. SAE paper 750028, 1975.

7 Goldman,A. Kaskavaltzis,C. Rubenstein,B. A Study of Velocity Fluctuations in Internal Combustion Engines. Undergrad. Mech. Lab. II Report, McGill University, 1984.

8 Hayes,T.K. Savage,L.D. Sorensen,S.C. Cylinder Pressure Data Acquisition and Heat Release Analysis on a Personal Computer. SAE paper 860029, 1986.

9 Hosey,R.J.
Powell,J.D.
Closed Loop, Knock Adaptive Spark Timing Control Based on Cylinder Pressure.
ASME Journ.Dyn.Syst.,Meas. Ctrl.,
vol. 101 1979: pp. 64-70.

10 Kaplon,A.
Hawrylkiewicz,A.
A Computer system for measurement and calculation of combustion process in an internal combustion engine.
Proceedings ISATA 1981 : pp. 499-510.

11 Lancaster,D.R.
Krieger,R.B.
Lienesch,J.H.
Measurement and Analysis of Engine Pressure Data.
SAE paper 750026, 1975.

12 Leung,C.K.
Schira,J.J.
Digital Analyzer for Internal Combustion Engines.
SAE paper 820207, 1982.

13 Lienisch,J.H.
Using Microwaves to phase Cylinder Pressure to Crankshaft Position.
SAE paper 790103, 1979.

14 Li Tian-Fu
Vroomen,L.J.
Zsombor-Murray,P.J.
An Automatic Engine Indicator.
Proceedings 1983 ASEE Conference,
pp. 431-442.

An Automatic Engine Analyzer.
ASEE "Computers in Education" Journal
vol. IV-4: pp. 15-24, 1984.

15 Lichty, L.C.
Internal Combustion Engines Principles
McGraw-Hill, New York, 1967

16 Sood,A.K.
Fahs,A.A.
Henein,N.A.
A Real-Time Microprocessor-Based System for Engine Deficiency Analysis.
IEEE Trans. Ind. Elec.,
vol. 30-2: pp. 159-163, 1983.

17 Sood,A.K.
Fahs,A.A.
Friedlander,C.
Engine Fault Analysis:
Part 1, Statistical Methods
IEEE Trans. Ind. Elec.,
vol. 32-4: pp. 294-300, 1985.

18 Sood,A.K.
Fahs,A.A.
Henein,N.A.
Engine Fault Analysis:
Part 2, Parameter Estimation Approach.
IEEE Trans. Ind. Elec.,
vol. 32-4: pp. 301-307, 1985.

19 Uekumai,T.
Higashino,I.
Nomura,T.
Gasoline Engine Diagnosis by Statistical Analysis.
Bulletin of JSME,
vol. 25-206: pp. 1281-1288, 1982.

20 Warkman,D.C.
Performance Monitoring based on an MIP calculator.
Mar. Eng. Rev., March 1983: pp. 8-11.

21 Werson,W.J.
Stafford,E.M.
Self-Adaptive Ignition Timing System.
Int. Conf. Autom. Elec.,
IEE London 1976: pp. 51-55.

22 Young,M.B.
Lienesch,J.H.
An Engine Diagnostic Package (EDPAC)-Software for Analyzing Pressure-Time Data.
SAE paper 780967, 1978.

23
Ford Car Product Development Inter-Office Memo, 12-9-1986.

24
Personal conversation with J. Hoard, Supervisor, Combustion and Induction Optimization Section, Ford Advanced Powertrain Engineering, 07-03-1987.

Appendix A

Calculation of ideal Otto cycle

These calculations are based on the ideal cycle assumptions made in Chapter 2. The objective is to observe PV behaviour when specific parameters of the cycle are changed:

- fuel-air mixture
- intake air pressure
- exhaust back pressure

The calculations are made following the procedure in reference (15). Thermodynamic data is from the Starkman-Newhall charts supplied in this reference.

Calculation are included for the following cases:

stoichiometric mixture
rich mixture (20% excess fuel)
lean mixture (25% excess air)
throttled
excessive exhaust back pressure

Case # 1: stoichiometric mixture

assume f = 0.038
compression ratio: 6:1
intake temperature: $57°C = 594°R$
intake pressure: 14.7 psia

From chart "B" (15) :

$$V_1 = \frac{K_{1.0}T_1}{P_1} = \frac{.379 \times 594}{14.7} = 15.3 \frac{\text{cu.ft.}}{\text{cht.qty.}}$$

$$u_1 = 111.4 \text{ BTU/cht.qty.}$$

$1 \rightarrow 2$ compression (isentropic)

$$n(S_v)_{594} = .076 \text{ BTU/}° \text{ R-cht.qty.}$$

$$n(S_v)_{T_2} = .076 + .0701ln(6) = .202 \text{ BTU/}°\text{R-cht.qty.}$$

From chart "B" :

$$T_2 = 1076°R, u_2 = 214 \text{ BTU/cht.qty.}$$

$$P_2 = \frac{KT_2}{V_2} = .379 \times \frac{1076}{15.3/6} = 160 \text{ psia}$$

$2 \rightarrow 3$ constant volume combustion

$$C_3 = (1 - .038)1275 = 1227 \text{ BTU/cht.qty.}$$

$$u_3 = C_3 + u_2 = 1227 + 214 = 1441 \text{ BTU/cht.qty.}$$

$$V_3 = V_2 = 15.3/6 = 2.55 \text{ cu.ft./cht.qty.}$$

From chart "D" :

$$P_3 = 756 \text{ psia}, T_3 = 4960^\circ R$$

$$S_3 = 2.218 \text{ BTU}/^\circ R \text{ cht.qty.}$$

$3 \rightarrow 4$ isentropic expansion

$$V_4 = V_1 \quad S_4 = S_3$$

From chart "D" :

$$P_4 = 91.5 \text{ psia}, T_4 = 3520^\circ R$$

$$u_4 = 870 \text{ BTU/cht.qty.}$$

$4 \rightarrow 5$ isentropic exhaust

$$S_5 = S_4 \quad P_5 = 14.7 \text{ psia}$$

From chart "D" :

$$V_5 = 66.6$$

$$f = \frac{2.55}{66.6} = .038 \text{ as assumed}$$

Summary

compression work

$$u_2 - u_1 = 214 - 111 = 103 \text{ BTU/cht.qty.}$$

expansion work

$$u_3 - u_4 = 1441 - 870 = 571 \text{ BTU/cht.qty.}$$

Conversion to indicated mean effective pressure (IMEP)

$$w\left(\frac{\text{BTU}}{\text{cht.qty.}}\right) \times \frac{1}{V}\left(\frac{\text{cht.qty.}}{\text{cu.ft.}}\right) \times \frac{778\ \text{lb-ft}}{1\text{BTU}} \times \frac{1\text{sq.ft.}}{144\text{sq.in.}} = \text{IMEP}\frac{16}{\text{sq.in.}}$$

$$\text{Compression IMEP} = \frac{103}{15.3} \times \frac{778}{144} = 36.4\ \text{psi}$$

$$\text{expansion IMEP} = \frac{571}{15.3} \times \frac{778}{144} = 201.6\ \text{psi}$$

$$\text{net IMEP} = 201.6 - 36.4 = 165.2\ \text{psi}$$

Case # 2 : rich mixture (1.2)
assume f = .040
other conditions as # 1

From chart "B" :

$$V_1 = \frac{.382 \times 594}{14.7} = 15.43 \text{ cu.ft./cht.qty.}$$

$$u_1 = 113.1 \text{ BTU/cht.qty.}$$

$1 \rightarrow 2$ isentropic compression

$$n(S_v)_{594} = .0792 \text{ BTU/°R-cht.qty.}$$

$$n(S_v)_{T_2} = .0792 + .0706ln(6) = .205 \text{ BTU/°R cht.qty}$$

From chart "B" :

$$T_2 = 1068°R, u_2 = 217.5 \text{ BTU/cht.qty.}$$

$$P_2 = \frac{KT_2}{V_2} = \frac{.382 \times 1068}{15.43/6} = 158.6 \text{ psia}$$

$2 \rightarrow 3$ constant volume combustion

$$C_3 = (1 - .040)1530 = 1469 \text{ BTU/cht.qty.}$$

$$u_3 = C_3 + u_2 = 1469 + 217.5 = 1687 \text{ BTU/cht.qty.}$$

From chart "E" :

$$P_3 = 852 \text{ psia}, T_3 = 5345°R$$

$$S_3 = 2.326 \text{ BTU/°R cht.qty.}$$

3 → 4 isentropic expansion

$$V_4 = V_1 \quad S_4 = S_3$$

From chart "E" :

$$P_4 = 104 \text{ psia}, T_4 = 3650°R$$

$$u_4 = 1085 \text{ BTU/cht.qty.}$$

4 → 5 isentropic exhaust

$$S_5 = S_4 \quad P_5 = 14.7 \text{ psia}$$

Form chart "E" :

$$V_5 = 64.9 \text{ cu.ft./cht.qty.}$$

$$f = \frac{2.57}{64.9} = .040 \text{ as assumed}$$

Summary

compression work

$$u_2 - u_1 = 217.5 - 113.1 = 104.4 \text{ BTU/cht.qty.}$$

expansion work

$$u_3 - u_4 = 1687 - 1085 = 602 \text{ BTU/cht.qty.}$$

Conversion to IMEP

$$\text{Compression IMEP} = \frac{104.4}{15.43} \times \frac{778}{144} = 36.6 \text{ psi}$$

$$\text{expansion IMEP} = \frac{602}{15.43} \times \frac{778}{144} = 210.8 \text{ psi}$$

$$\text{net IMEP} = 210.8 - 36.6 = 174.2 \text{ psi}$$

Case # 3 : lean mixture (0.8)
assume f = .046
other conditions as for # 1

From chart "B" :

$$V_1 = \frac{.378 \times 594}{14.7} = 15.3 \text{ cu.ft./cht.qty.}$$

$$u_1 = 109.5 \text{ BTU/cht.qty.}$$

$1 \rightarrow 2$ isentropic compression

$$n(S_v)_{594} = .075 \text{ BTU/°R cht.qty.}$$

$$n(S_v)_{T_2} = .075 + .0698 \ln(6) = .200 \text{ BTU/°R cht.qty.}$$

From chart "C" :

$$T_2 = 1090°\text{R}, u_2 = 211.5 \text{ BTU/cht.qty.}$$

$$P_2 = \frac{KT_2}{V_2} = .378 \times \frac{1090}{15.3/6} = 161.5 \text{ psia}$$

$2 \rightarrow 3$ constant volume combustion

$$C_3 = (1 - .046)1020 = 972 \text{ BTU/cht.qty.}$$

$$u_3 = C_3 + u_2 = 972 + 211.5 = 1184 \text{ BTU/cht.qty.}$$

From chart "C" :

$$P_3 = 620 \text{ psia}, T_3 = 4600°\text{R}$$

$$S_3 = 2.140 \text{ BTU/°R cht.qty.}$$

3 → 4 isentropic expansion

$$V_4 = V_1 \quad S_4 = S_3$$

From chart "C" :

$$P_4 = 95.6 \text{ psia}, T_4 = 3170^\circ \text{R}$$

$$u_4 = 745 \text{ BTU/cht.qty.}$$

4 → 5 isentropic exhaust

$$S_5 = S_4 \quad P_5 = 14.7 \text{ psia}$$

From chart "C" :

$$V_5 = 55 \text{ cu.ft./cht.qty.}$$

$$f = \frac{2.55}{55} = .046 \text{ as assumed}$$

Summary

compression work

$$u_2 - u_1 = 211.5 - 109.5 = 102 \text{ BTU/cht.qty.}$$

expansion work

$$u_3 - u_4 = 1184 - 745 = 439 \text{ BTU/cht.qty.}$$

Conversion to IMEP

$$\text{Compression IMEP} = \frac{102}{15.3} \times \frac{778}{144} = 36.0 \text{ psi}$$

$$\text{expansion IMEP} = \frac{439}{15.3} \times \frac{778}{144} = 155.0 \text{ psi}$$

$$\text{net IMEP} = 155 - 36 = 119 \text{ psi}$$

Case # 4 : stoichiometric mixture, throttled
assume f = .063
intake pressure : 8 psia
other conditions as Case # 1

From chart "B" :

$$V_1 = \frac{.379 \times 594}{8} = 28.14 \text{ cu.ft./cht.qty.}$$

$1 \rightarrow 2$ isentropic compression

$$n(S_v)_{594} = .076 \text{ BTU/°R cht.qty.}$$

$$n(S_v)_{T_2} = .076 - .0701 \ln(6) = .202 \text{ BTU/°R cht.qty.}$$

From chart "B" :

$$T_2 = 1076°\text{R}, u_2 = 214 \text{ BTU/cht.qty.}$$

$$P_2 = \frac{.379 \times 1076}{28.14/6} = 87 \text{ psia}$$

$2 \rightarrow 3$ constant volume combustion

$$C_3 = (1 - .063)1275 = 1195 \text{ BTU/cht.qty.}$$

$$u_3 = C_3 + u_2 = 1195 - 214 = 1409 \text{ BTU/cht.qty.}$$

$$V_3 = V_2 = 28.14 = 4.69 \text{ cu.ft./cht.qty.}$$

From chart "D" :

$$P_3 = 421 \text{ psia}, T_3 = 4890°\text{R}$$

$$S_3 = 2.259 \text{ BTU/°R cht.qty.}$$

3 → 4 isentropic expansion

$$V_4 = V_1 \quad S_4 = S_3$$

From chart "D" :

$$P_4 = 49.5 \text{ psia}, T_4 = 3480^\circ\text{R}$$

$$u_4 = 860 \text{ BTU/cht.qty.}$$

4 → 5 isentropic exhaust

$$S_5 = S_4 \quad P_5 = 14.7 \text{ psia}$$

From chart "D" :

$$V_5 = 74.4 \text{ cu.ft./cht.qty.}$$

$$f = \frac{4.69}{74.4} = .063 \text{ as assumed}$$

$$u_5 = 630 \text{ BTU/cht.qty.}$$

$$u_1 = (1 - \mathrm{f})(\mathrm{H_{air}} + (\mathrm{F/A})\mathrm{H_{fuel}})_{\mathrm{ATM}} + f u_5 - P_1(V_1 - V_2)$$

$$\mathrm{F/A} = .066$$

From table A (15) :

$$\mathrm{H_{air}} = 124 \text{ BTU/lb}$$
$$\mathrm{H_{fuel}} = -24 \text{ BTU/lb}$$

$$u_1 = (1 - .063)(124 - .066 \times 24) - .063 \times 630 - \frac{8(28.14 - 4.69)}{778} \times 144$$

$$= 119.7 \text{ BTU/cht.qty.}$$

Summary

compression work

$$u_2 - u_1 = 214 - 120 = 94 \text{ BTU/cht.qty.}$$

expansion work

$$u_3 - u_4 = 1409 - 860 = 549 \text{ BTU/cht.qty.}$$

pumping work (intake)

$$(V_1 - V_2)\ (P_5 - P_1)$$

$$(28.14 - 4.69) \times (14.7 - 8.0) \times \frac{144}{778} = 29.1 \text{ BTU/cht.qty.}$$

Conversion to IMEP

$$\text{Compression IMEP} = \frac{94}{28.14} \times \frac{778}{144} = 18.0 \text{ psi}$$

$$\text{expansion IMEP} = \frac{549}{28.14} \times \frac{778}{144} = 105.4 \text{ psi}$$

$$\text{pumping IMEP} = \frac{29}{28.14} \times \frac{778}{144} = 5.6 \text{ psi}$$

$$\text{net IMEP} = 105.4 - 18.0 - 5.6 = 71.8 \text{ psi}$$

Case # 5 : stoichiometric mixture, back-pressure
assume f = .068
other conditions as Case # 1

From chart "B" :

$$V_1 = \frac{.379 \times 594}{14.7} = 15.3 \text{ cu.ft./cht.qty.}$$

$$u_1 = 111.4 \text{ BTU/cht.qty.}$$

$1 \rightarrow 2$ isentropic compression

$$n(S_v)_{594} = .076 \text{ BTU/°R cht.qty.}$$

$$n(S_v)_{T_2} = .076 - .0701 \ln(6) = .202 \text{ BTU/°R cht.qty.}$$

From chart "B" :

$$T_2 = 1076°\text{R}, u_2 = 214 \text{ BTU/cht.qty.}$$

$$P_2 = \frac{.379 \times 1076}{15.3/6} = 160 \text{ psia}$$

$2 \rightarrow 3$ constant volume combustion

$$C_3 = (1 - .068)1275 = 1188 \text{ BTU/cht.qty.}$$

$$u_3 = C_3 + u_2 = 1188 + 214 = 1402 \text{ BTU/cht.qty.}$$

From chart "D" :

$$P_3 = 743 \text{ psia}, T_3 = 4927°\text{R}$$

$$S_3 = 2.215 \text{ BTU/°R cht.qty.}$$

$3 \rightarrow 4$ isentropic expansion

$$V_4 = V_1 \quad S_4 = S_3$$

From chart "D" :

$$P_4 = 91.5 \text{ psia}. T_4 = 3485^\circ \text{R}$$

$$u_4 = 860 \text{ BTU/cht.qty.}$$

$4 \rightarrow 5$ isentropic exhaust

$$S_5 = S_4 \quad P_5 = 30 \text{ psia}$$

From chart "D" :

$$V_5 = 37.4 \text{ cu.ft./cht.qty.}$$

$$f = \frac{2.55}{37.4} = .068 \text{ as assumed}$$

Summary

compression work

$$u_2 - u_1 = 214 - 111.4 = 102\,6 \text{ BTU/cht.qty.}$$

expansion work

$$u_3 - u_4 = 1402 - 860 = 542 \text{ BTU/cht.qty.}$$

pumping work

$$(V_1 - V_2) \quad (P_5 - P_1) =$$

$$(15.3 - 2.55) \frac{\text{cu.ft.}}{\text{cht.qty.}} \times (30 - 14.7) \frac{\text{lb}}{\text{sq.in.}} \times 144 \times \frac{1}{778}$$

$$= 36.1 \text{ BTU/cht.qty.}$$

net work

$$542 - 103 - 36 = 403 \text{ BTU/cht.qty}$$

Conversion to IMEP

$$\text{Compression IMEP} = \frac{103}{15.3} \times \frac{778}{144} = 36.4 \text{ psi}$$

$$\text{expansion IMEP} = \frac{542}{15.3} \times \frac{778}{144} = 191.4 \text{ psi}$$

$$\text{pumping IMEP} = \frac{36}{15.3} \times \frac{778}{144} = 12.7 \text{ psi}$$

$$\text{net IMEP} = 191.4 - 36.4 - 12.7 = 142.3 \text{ psi}$$

Appendix B

Physical properties of engine components

In the first section, the moments of inertia of the internal engine components are calculated from the geometry of the parts. The dimensions have been obtained by measurements of the actual components.

In the second section, the dynamic equations of the reciprocating / rotating components (piston, connecting rod, crankshaft) are developed

Moments of inertia and dynamic equations are required for the velocity fluctuation program (see section 6.4).

Calculation of Moments of Inertia

Connecting Rod

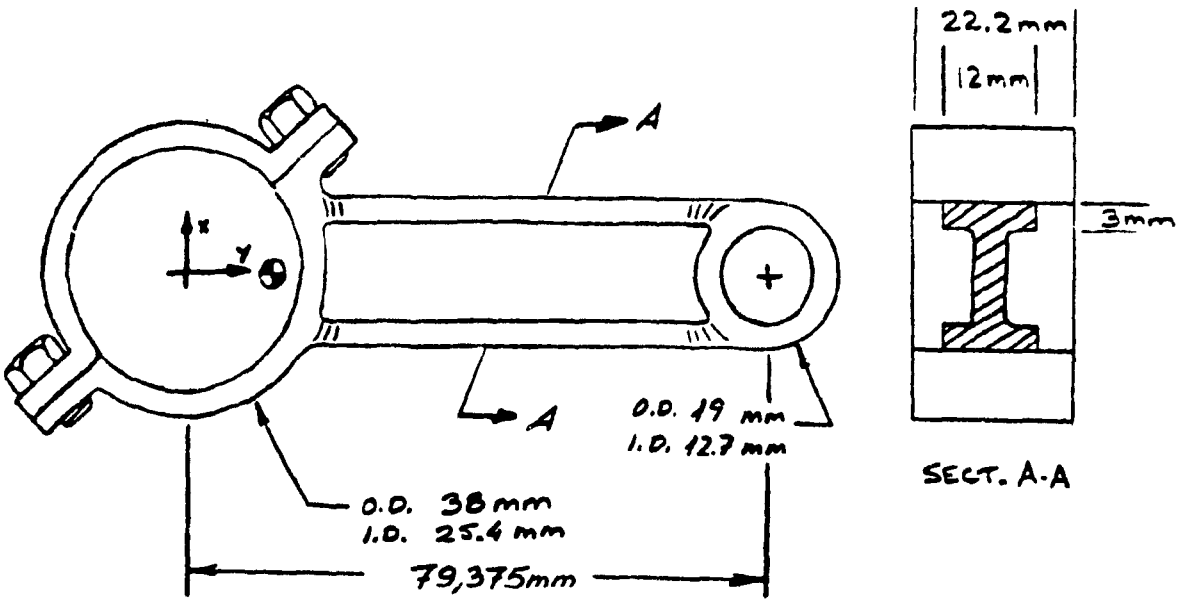

Material: Aluminum Mass (W/Bolts) 87g

Part 1 (Base) $m = \rho t(r_o^2 - r_i^2)\pi$ $I_{CG} = \frac{m}{2}(r_o^2 + r_i^2)$

$$m_1 = 2,711 \times 10^{-3} g/mm^3 \times 22.2mm \times \left[(38/2)^2 - (25.4/2)^2\right]mm^2 = 37.8g$$

$$I_{CG_1} = 37.8g/2 \times \left[(38/2)^2 + (25.4/2)^2\right]mm^2 = 9862gmm^2$$

Part 2 (Rod) $m = \rho lA$ $I_{CG} = ml^2/12$

$$l = 79,375 - \left[(38/2) + (19/2)\right] = 50,875mm$$

$$A = 2 \times (3 \times 12)mm^2 + 3mm \times (19mm - (2 \times 3mm)) = 111mm^2$$

$$m_2 = 2,711 \times 10^{-3} g/mm^3 \times 111mm^2 \times 50,875mm = 15,3g$$

$$I_{CG_2} = 1/12(15.3g \times 50,875mm^2) = 3300g - mm^2$$

Part 3 (Head) $\quad m = \rho t(r_o^2 - r_i^2)\pi \quad I_{CG} = \frac{m}{2}(r_o^2 + r_i^2)$

$$m_3 = 2,711 \times 10^{-3} g/mm^3 \times 22.2mm \times \left[(19/2)^2 - (12,7/2)^2\right]mm^2 = 9,5g$$

$$I_{CG_3} = 9,5g/2 \times \left[(19/2)^2 + (12,7/2)^2\right]mm^2 = 620g - mm^2$$

Part 4 (Bolts)

$$2m_4 = m_{total} - (m_1 + m_2 + m_3) = 87 - (37,8 + 15,3 + 9,5) = 24.4g$$

$$m_4 = 12,2g \quad I_{CG} = 0$$

Summary - Connecting Rod

Location of C.G.

Part	Mass	X_{CG}	Y_{CG}	Mass × X	Mass × Y
1	37,8 g	0	0	0	0
2	15,3 g	0	44.4 mm	0	679,32 g-mm
3	9,5 g	0	79,4 mm	0	754,30 g-mm
4-1	12,2 g	-16,3 mm	-16,3 mm	-198,86	-198,86 g-mm
4-2	12,2 g	16.3 mm	16.3 mm	198,86	198,86 g-mm
Total	87 g			0	1433,62 g-mm

$$Y_{CG} = \frac{1433,62g - mm}{87g} = 16,5mm \quad X_{CG} = 0$$

Moment of Inertia

Part	I	X	Y	$X - X_{CG}$	$Y - Y_{CG}$	R	mR^2
1	9862	0	0	0	-16,5	16,5	10291
2	3300	0	44.4	0	27,9	27,9	11907
3	620	0	79,4	0	62,9	62,9	37586
4-1	0	-16.3	-16,3	-16,3	32,8	36,6	16343
4-2	0	16,3	16,3	16,3	0,2	16,3	3241
	$g - mm^2$	mm	mm	mm	mm	mm	$g - mm^2$

$$R^2 = (X - X_{CG})^2 + (Y - Y_{CG})^2$$

$$I_{total} = \sum I + mR^2 = 93160g - mm^2 = 9316 \times 10^{-6} Kg - m^2$$

$$\text{Radius of gyration} \sqrt{\frac{I}{m}} = 0,0327\text{m}$$

Brake Cylinder

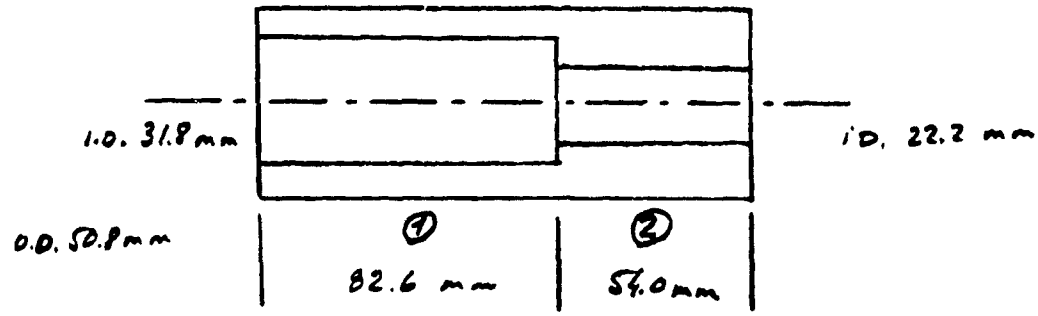

Material: Steel Mass: 1509g

Part 1 $m = \rho l(r_o^2 - r_i^2)$ $I_{CG} = \frac{m}{2}(r_o^2 + r_i^2)$

$$m_1 = 7,813 \times 10^{-3} g/mm^3 \times 82,6mm \times (25,4^2 - 15,9^2)mm^2 \times \pi = 796g$$

$$I_{CG_1} = 796g/2 \times (25,4^2 + 15,9^2)mm^2 = 357392g - mm^2$$

Part 2 $m = \rho l(r_o^2 - r_i^2)$ $I_{CG} = \frac{m}{2}(r_o^2 + r_i^2)$

$$m_2 = 7,813 \times 10^{-3} g/mm^3 \times 54,0mm \times (25,4^2 - 11,1^2)mm^2 \times \pi = 713g$$

$$I_{CG_2} = 713g/2 \times (25,4^2 + 11,1^2)mm^2 = 273924g - mm^2$$

$$I_{CG_{Total}} = 631316g - mm^2$$

Flywheel

Aluminum - Mass = 1112g

Part 1 Disc $r = 70mm$ $t = 6mm$ $m = \rho t r^2 \pi$ $I_{CG} = \frac{mr^2}{2}$

$$m_1 = 2,711 \times 10^{-3} g/mm^3 \times 6mm \times (70mm)^2 = 250g$$

$$I_{CG_1} = 250g \times (70mm)^2/2 = 612500g - mm^2$$

Part 2 Ring $r_o = 70mm$ $r_i = 5/mm$ $I_{CG} = \frac{m}{2}(r_o^2 + r_i^2)$

$$m_2 = m_{Tot} - m_1 = 1112 - 250 = 862g$$

$$I_{CG_2} = 862g/2 \times (70^2 + 51^2)mm^2 = 3232931g - mm^2$$

$$I_{CG_{Total}} = 3232931 + 612500 = 3844431g - mm^2$$

Crankshaft

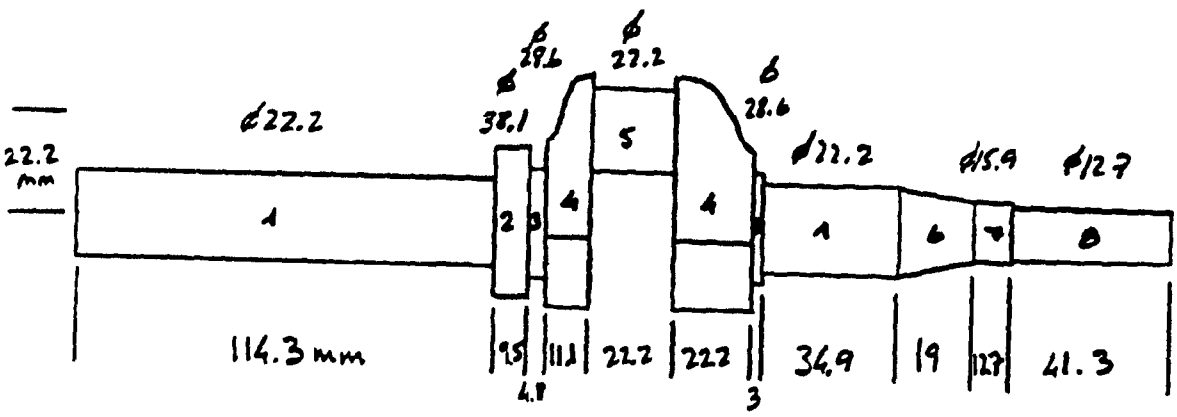

Mtl : Steel Mass = 1341 g

All cylindrical sections: $m = \rho\pi r^2 l$ $I_{CG} = mr^2/2$

1 - $m = 7,813 \times 10^{-3} g/mm^3 \times \pi \times (22,2/2)^2 mm^2 \times (114,3+34,9)mm = 451g$

$$I_{CG} = 451g \times (22,2/2)^2 mm^2/2 = 27797g - mm^2$$

2 - $m = 7,813 \times 10^{-3} g/mm^3 \times \pi \times (38,1/2)^2 mm^2 \times 9,5mm = 85g$

$$I_{CG} = 85g \times (38,1,2)^2 mm^2/2 = 15355g - mm^2$$

3 - $m = 7,813 \times 10^{-3} g/mm^3 \times \pi \times (28,6/2)^2 mm^2 \times (4,8 + 3,0) mm = 39g$

$$I_{CG} = 39g \times (28,6/2)^2 mm^2/2 = 4003g - mm^2$$

5 - $m = 7,813 \times 10^{-3} g/mm^3 \times \pi \times (22,2/2)^2 mm^2 \times 22,2mm = 67g$

$$I_{CG} = 67g \times (22,2/2)^2 mm^2/2 = 4134g - mm^2$$

$$I = I_{CG} + md^2 = 4134g - mm^2 + 67g \times 22.2^2 mm^2 = 37224g - mm^2$$

7 - $m = 7,813 \times 10^{-3} g/mm^3 \times \pi \times (15,9/2)^2 mm^2 \times 12,7mm = 20g$

$$I_{CG} = 20g \times (15,9/2)^2 mm^2/2 = 623g - mm^2$$

6 - $m = \frac{\rho l \pi}{12}(D^2 + dD + d^2)$ $I_{CG} = \frac{3m}{10}\frac{R^5 - r^5}{R^3 - r^3}$

$$m = \frac{7,813 \times 10^{-3}}{12}\frac{g}{mm^3} \times 19mm \times (22,2^2 + 22,2 \times 15,9 + 15,9^2) mm^2 = 43g$$

$$I_{CG} = \frac{3 \times 43g}{10} \times \frac{(22,2/2)^5 - (15,9/2)^5}{(22,2/2)^3 - (15,9/2)^3} mm^2 = 2025g - mm^2$$

4 - Treated as two separate parts:

1 - a sector of a cylinder (v = 22.2) covering an arc of 160°

$$m = \frac{160°}{360°} \times 7,813 \times 10^{-3} g/mm^3 \times \pi \times (11,1 + 22,2) mm \times 22,2^2 mm^2 = 179g$$

$$I = \frac{mr^2}{2} = 179g \times 22,2^2 mm^2/2 = 44118g - mm^2$$

2 - remaining portion considered parallepiped 38 mm high

$$m = 1341g - \sum m_i = 417g$$

location of CG is 17 mm from crankshaft axis

$$I = \frac{m}{12}(h^2 + t^2) + md^2 = 417g \times \frac{((11,1 + 22,2)^2 + 38^2)}{12} + 17^2 mm^2$$

$$= 209025g - mm^3$$

$$I_{crankshaft} = \sum I_i = 340994g - mm^3$$

$$\text{Radius of gyration} \quad R = \sqrt{\frac{I}{m}} = 15,95mm$$

$$Y_{CG} = 0 \quad X_{CG_{4-1}} = \frac{2r}{3}\frac{\sin x}{x} = -1,81mm \quad X_{CG_{4-2}} = +17mm$$

$$X_{CG_{Total}} = \frac{1}{1341g}(179 \times (-1,81) + 417 \times 17)g - mm = +5,04mm$$

Dynamics of engine components

Kinematics

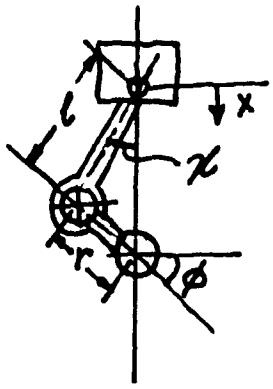

define $\lambda = \frac{r}{l}$

$\sin\chi = \lambda\sin\phi$

$\cos\chi = \sqrt{1 - \lambda^2\sin^2\phi}$

$x = (l + r) - (l\cos\chi + r\cos\phi)$

$= (1 - \cos\phi) + l(1 - \sqrt{1 - \lambda^2\sin^2\phi})$

$\dot{x} = \omega R\,(\sin\phi + \frac{\lambda}{2}\sin 2\phi)$

$\ddot{x} = \omega^2 R\,(\cos\phi + \lambda\cos 2\phi)$

where $\omega = \dot{\phi}$

Piston Reaction

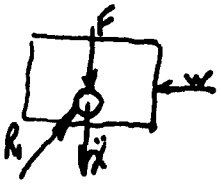

$F = pA - (F_R + F_W)$

$F_W = \mu\sqrt{W^2 + (mpg)^2} \cong \mu W$

$W = R_1\sin\chi$

$MpẌ = F - R_1\cos\chi$

use $R_1\cos\chi \simeq R_1$

$R_1 = F - MpẌ = pA - (F_R + \mu W) - MpẌ$

$= pA - F_R - \mu R_1\sin\chi - MpẌ$

$R_1(1 + \mu\sin\chi) = pA - F_R - MpẌ$

$\frac{R_1 = pA - F_R - MpẌ}{(1+\mu\sin\chi)} = \frac{pA - F_R - MpẌ}{1+\mu\lambda\sin\phi}$

Reaction in Connecting Rod

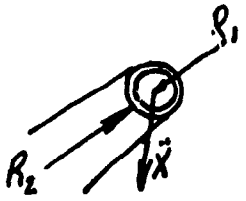

$$M_R\left(\frac{s}{l}\right)\ddot{X} = R_1\cos\chi - R_2\cos\chi$$

$$R_2 = R_1 - M_R\left(\frac{s}{l}\right)\ddot{X} \quad (\cos\chi \simeq 1)$$

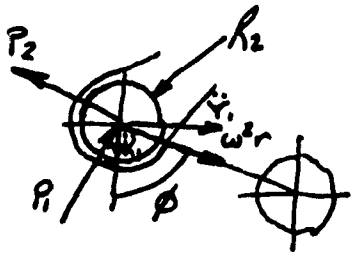

$$\ddot{Y}_1 = w^2 r\sin\phi$$

$$\ddot{X}_1 = w^2 r\cos\phi$$

$$m\ddot{Y}_1 = -R_2\sin\chi + P_1\cos\phi - P_2\sin\phi$$

$$m\ddot{X}_1 = R_2\cos\chi - P_1\sin\phi - P_2\cos\phi$$

$$m\ddot{Y}_1\sin\phi = mw^2 r\sin^2\phi =$$
$$-R_2\sin\chi\sin\phi + P_1\cos\phi \quad \phi - P_2\sin^2\phi$$

$$m\ddot{X}_1\cos\phi = mw^2 r\cos^2\phi =$$
$$R_2\cos\chi\cos\phi - P_1\sin\phi\cos\phi - P_2\cos^2\phi$$

$$mw^2 r = mw^2 r\sin^2\phi + mw^2 r\cos^2\phi =$$
$$R_2(\cos\chi\cos\phi - \sin\chi\sin\phi) - P_2$$

$$P_2 = -mw^2 r + R_2(\cos\chi\cos\phi - \sin\chi\sin\phi)$$
$$= -mw^2 r + R_2(\cos\phi - \lambda\sin^2\phi)$$

using $\cos\chi \cong 1 \quad \sin\chi = \lambda\sin\phi$

$$m\ddot{Y}_1\sin\phi\cos^2\phi = mw^2 r\sin^2\phi\cos^2\phi =$$
$$-R_2\sin\chi\sin\phi\cos^2\phi + P_1\cos^3\phi\sin\phi$$
$$-P_2\sin^2\phi\cos^2\phi$$

$$m\ddot{X}_1\cos\phi\sin^2\phi = mw^2 r\cos^2\phi\sin^2\phi =$$
$$R_2\cos\chi\cos\phi\sin^2\phi - P_1\sin^3\phi\cos\phi$$
$$-P_2\cos^2\phi\sin^2\phi$$

$$m\ddot{Y}_1\sin\phi\cos^2\phi - m\ddot{X}_1\cos\phi\sin^2\phi = 0 =$$
$$-R_2(\sin\chi\sin\phi\cos^2\phi + \cos\chi\cos\phi\sin^2\phi)$$
$$+P_1\sin\chi\cos\phi$$

$$P_1 = R_2\sin\phi(1 + \lambda\cos\phi)$$

Reaction at Crankshaft

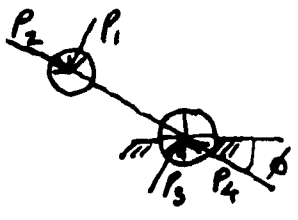

$$P_3 = P_1$$

$$m_c dw^2 = P_4 - P_2$$

$$P_4 = P_2 + m_c dw^2$$

$$I \propto = P_1 r - M_f - M_l$$

Appendix C

Synchronization of TDC Sensor and Error Calculation

In the first section is shown that crank position $\phi = 90°$ before TDC can be located with greater accuracy, with the same instruments, than position $\phi = 0°$ (TDC).

In the second section, calculations are made from an equation developed by reference (3) relating position signal accuracy and error in IMEP calculatins. The values obtained are compared to the author's (3) recommendations.

Precision required from TDC and position signals

From Brown (3) :

$$\Delta mep = 1.25 \times 10^{-2} \Delta\phi p_i r\left(\frac{p_m}{p_c} + 1\right)$$

where:

p_i = intake pressure, psia

Δmep = error in mep, psi

p_m = maximum cylinder pressure, psia

p_c = maximum compression pressure, psia

r = compression ratio

To obtain valid imep measurements, Δmep must be kept below 1.0%.

Using data from Appendix "A"

(case 2):

$$\frac{\Delta mep}{\Delta\phi} = 1.25 \times 10^{-2} \times 6 \times 14.7\left(\frac{852}{159} + 1\right) = \frac{7psi}{1°}$$

$$\frac{\Delta mep}{netimep} = \frac{7}{174} = 4\% \Rightarrow error of .25° tolerable$$

(case 4):

$$\frac{\Delta mep}{\Delta\phi} = 1.25 \times 10^{-2} \times 6 \times 8.0\left(\frac{421}{49.5} + 1\right) = \frac{5.7psi}{1°}$$

$$\frac{\Delta mep}{netimep} = \frac{5.7}{71.8} = 8\% \Rightarrow error of .125° tolerable$$

Using a "worst case" approach, it is concluded that an accuracy of better than 0.125° is required.

Synchronization of TDC Sensor

Error on TDC location

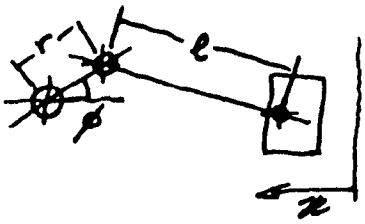

$r = .875''$ (22.225 mm)

$l = 3.125''$ (79.375 mm)

$x = l + r - r\cos\phi - \sqrt{l^2 - r^2\sin^2\phi}$

at	$\phi = 0$	$x = 0$
with	$\Delta\phi = 0.1°$	$\Delta x = .0000017''(43.2 \times 10^{-9} m)$
	$\Delta\phi = 1°$	$\Delta x = .00017''(43.2 \times 10^{-6} m)$
	$\Delta\phi = 2°$	$\Delta x = .0006''(15.2 \times 10^{-6} m)$

The accuracy with which TDC can be located using a dial gauge having a precision of .001" (.025 mm) is worse than 2°. This is not acceptable.

at	$\phi = 90°$	x = 1"
	$\Delta\phi = 0.1°$	$\Delta x = .0015''(38.1 \times 10^{-6} m)$

It is then possible to locate crank angle $\phi = 90°$ with an accuracy of better than 0.1° using the same dial gauge.

The sensor will then be synchronized with this crank angle since it can be measured more accurately.

"TDC" Sensor synchronization technique

The TDC sensor will actually be set to issue a signal at a crank angle $\phi = 90°$ before TDC, to optimize the accuracy of the setting. Adjustments will be made within the data acquisition software to properly phase the pressure data with TDC.

Procedure:

- Install dial gauge (50 mm stroke) with extension stem and special adapter in place of spark plug.
- Connect oscilloscope (twin trace) to the outputs of TDC and position sensors.
- Bring engine to TDC by hand, observing dial gauge indication. Adjust dial to zero at TDC.
- Turn engine backwards by hand one fourth of a revolution, until dial gauge reads 1.000" (25.4 mm)
- Adjust position of both sensors such that they are both triggered at this exact crankshaft position.

Appendix D

This section contains calibration data on the instrumentation

- theoretical and experimental calibration of the strain gauge beam used to measure torque
- calculation of torque from strain gauge output
- calibration data on A/D converter and instrumentation amplifier
- calibration data on pressure transducer.

Calibration of strain gauge beam

Theory

Cantilever beam $\varepsilon_{th} = 6\frac{FL}{bH^2E}$

where:

F = force applied on beam, N

L = 178 mm

b = H = 6.3 mm

E = 206×10^6 N/mm^2 (mildsteel)

Experimental

Two active arms brige $\varepsilon_{exp} = \frac{2E_{AC}}{E_{BAT}GF}$

where:

E_{AC} = bridge output, V

E_{BAT} = battery voltage = 6.07V

GF = gauge factor = 2

Results

Load	Force	E_{AC}	$\varepsilon_{th} \times 10^6$	$\varepsilon_{exp} \times 10^6$	$\Delta\varepsilon\%$
100g	.98N	.125mV	20.3	20.6	+1.5
200g	1.96N	.240mV	40.6	39.5	−2.8
300g	2.94N	.360mV	60.9	59.3	−2.7
400g	3.92N	.480mV	81.2	79.1	−2.7
500g	4.90N	.590mV	101.5	97.1	−4.5
1000g	9.81N	1.20mV	203.1	197.6	−2.8
1500g	14.71N	1.78mV	304.7	293.2	−3.9
2000g	19.62N	2.35mV	406.3	387.1	−5.0
2500g	24.52N	2.95mV	507.9	485.9	−4.8

Calculation of the resultant torque

$$T = Fd$$

$$\text{where } F = \frac{EbH^2\varepsilon}{6L}$$

d = length of reaction arm = 190mm

Combining with ε:

$$T = \frac{EbH^2}{6}\frac{d}{L}\frac{2}{GF}\frac{E_{AC}}{E_{BAT}}$$

applying the proper values

$$T = \frac{206\times10^6\times(6.3)^3}{6}\left(\frac{190}{178}\right)\frac{E_{AC}}{E_{BAT}}$$

$$= 9.1637\times10^9\,\frac{E_{AC}}{E_{BAT}}\,N-mm$$

Calibration of A/D converter & amplifier

Input V	Amplifier output V	A/D output HEX	Decimal value	Equivalent V
0.000	0.000	00	0	0
0.123	0.999	19	25	1.00
0.249	2.00	32	50	2.00
0.498	3.99	64	100	4.00
0.375	3.00	48	75	3.00
0.624	5.00	70	125	5.00
0.751	6.01	96	150	6.00
0.876	7.01	AF	176	7.04
1.000	8.00	C8	200	8.00
1.126	9.01	E1	225	9.00
1.122	8.98	E0	224	8.96
1.247	9.99	F9	249	9.96
1.270	10.17	FE	254	10.16
1.273	10.19	FF	255	10.20
1.271	10.18	FE	254	10.16
1.249	10.00	FA	250	10.00
0.873	7.00	AF	176	7.04
0.872	6.99	AE	175	7.00
1.000	0.123	19	25	1.00

The A/D converter has a range 0 - 10.20V in FF or 255 steps of 0.04V.

Calibration of pressure transducer

Equipment used: Dead Weight Tester

psi	V
0	0.147
20	0.251
40	0.350
60	0.450
80	0.549
100	0.649
120	0.749
140	0.850
160	0.950
180	1.050
200	1.150
220	1.250
240	1.351
260	1.451
280	1.552
300	1.653
320	1.754
340	1.855
360	1.956

$$V = (psig \times .005) + .147$$

Appendix E

This section contains listings of the programs written for this project:

- Constant time interval data acquisition program
- Triggered data acquisition program
- System test and debug programs
- Velocity fluctuation program
- Data analysis program

Constant time interval data acquisition program

```
0100 FE 0600   LDX #$0600      Set first transfer address
0103 FF 031E   STX $031E
0106 5F        CLR B
0107 F7 8001   STA B PIA AC    Set PIA for DDR access
010A F7 8000   STA B PIA AD    Set DDR as input
010D 86 3E     LDA A #$3E      00111110
010F B7 8001   STA A PIA AC    Reset CA2
0112 86 2E     LDA A #$2E      00101110
0114 B7 8001   STA A PIA AC    Set CA1 and CA2 control
0117 86 18     LDA A #$18      24
0119 B7 0310   STA A #0310     Store number of cycles
011C CE 03FF   LDX #$03FF      Set first storage address
011F 6F 00     CLR 0,X         Clear memory
0121 08        INX             Increment memory address
0122 8C 0526   CMP X $048F     Compare with last address
0125 26 F8     BNE (011F)      Return if not finished
0127 CE 0000   LDX #0000       Clear X register
012A B6 8000   LDA A PIA AD    Reset CA1
012D B6 8001   LDA A PIA AC    Check for CA1-TDC signal
0130 2A FB     BPL (012D)      Return if no signal
0132 C6 0F     LDA B #$0F      Set B for delay loop
0134 5A        DEC B           Decrement B
0135 26 FD     BNE (0134)      Return if not zero
0137 B6 8000   LDA A PIA AD    Reset CA1
013A 5F        CLR B           Clear B for counting loop
013B B6 8001   LDA A PIA AC    Check for CA1-TDC signal
013E 2B 0C     BMI (014C)      Continue if signal
0140 5C        INC B           Count number of loops
0141 C1 FF     CMP B #$FF      Compare B reg. with max. value
0143 26 F6     BNE (013B)      Return if less
0145 08        INX             Count major loops
0146 8C 05DD   CMP X #$05DD    Compare X reg. with max. value
0149 26 EF     BNE (013A)      Return if less
014B 3F        SWI             Stop if too slow
014C 7F 0300   CLR #$0300
014F F7 0301   STA B $0301     Store counters
0152 FF 0302   STX $0302
0155 CE 0300   LDX #$0300      Load X with address of B count
0158 86 00     LDA A #$00      Load A and B with 0016
015A C6 10     LDA B #$10
015C BD 0330   JSR MULT        Multiply B count*16
015F FF 0300   STX $0300       Store result
0162 B6 0300   LDA A $0300
0165 F6 0301   LDA B $0301     (B count*16)+114
0168 CB 72     ADD B #$72      B+114
016A 89 00     ADC A #$00      A+carry
016C B7 0300   STA A $0300     Store result
016F F7 0301   STA B $0301
0172 CE 0302   LDX #$0302      Load X with address of X count
```

```
0175 86 0F      LDA A #$0F      Load A and B with 4093
0177 C6 FD      LDA B #$FD
0179 BD 0330    JSR MULT        Multiply X count*4093
017C FF 0304    STX $0304       Store result (last two bytes)
017F CE 0300    LDX #$0300      Load X with address of
                                (B count*16)+114 result
0182 A7 02      STA A 2,X       Store result (first two bytes)
0184 E7 03      STA B 3,X
0186 A6 04      LDA A 4,X       (4093*X)+((16*B)+114)
0188 E6 05      LDA B 5,X
018A EB 01      ADD B 1,X
018C A9 00      ADC A 0,X
018E A7 04      STA A 4,X       Store result (last two bytes)
0190 E7 05      STA B 5,X
0192 A6 02      LDA A 2,X
0194 E6 03      LDA B 3,X
0196 C9 00      ADC B #$00
0198 89 00      ADC A #$00
019A A7 02      STA A 2,X       Store result (first two bytes)
019C E7 03      STA B 3,X
019E 86 00      LDA A #$00      Load A and B with 0064
01A0 C6 40      LDA B #$40
01A2 CE 0302    LDX #$0302      Load X with address of last
                                result
01A5 BD 0359    JSR DIVIDE      (4093*X)+((16*B)+114)/64
01A8 B6 0323    LDA A $0323     Load A with rest
01AB 81 20      CMP A #$20      Compare rest with 32
01AD 2D 01      BLT (01B0)      Skip next step if less
01AF 08         INX             Round up result
01B0 FF 0306    STX $0306       Store result
01B3 86 92      LDA A #$92      146
01B5 B7 030E    STA A $030E     Set nb. of measurements count
01B8 B6 0306    LDA A $0306     Load A and B w. nb. of cycles
01BB F6 0307    LDA B $0307
01BE C0 20      SUB B #$20      Substract length of subroutine
01C0 82 00      SBC A #$00      of 32 cycles
01C2 CE 030A    LDX #$030A      Set registers for division
01C5 6F 00      CLR 0,X
01C7 6F 01      CLR 1,X
01C9 A7 02      STA A 2,X
01CB E7 03      STA B 3,X
01CD 86 00      LDA A #$00
01CF C6 06      LDA B #$06
01D1 BD 0359    JSR DIVIDE      Divide nb. cycles by 6
01D4 FF 0300    STX $0300       Store result
01D7 CE 03FE    LDX #$03FE      Set first storage address
01DA B6 0323    LDA A $0323     Load A with rest of division
01DD 81 01      CMP A #$01      Select proper data acquisition
01DF 2D 0B      BLT (01EC)      subroutine for proper interval
01E1 81 03      CMP A #$03
01E3 2D 22      BLT (0207)
01E5 81 05      CMP A #$05
01E7 2D 3A      BLT (0223)
```

```
01E9 7C 0301    INC $0301       Round out 5/6 to 1

01EC B6 8000    LDA A PIA AD    Reset CA1
01EF B6 8001    LDA A PIA AC    Check for CA1-TDC signal
01F2 2A FB      BPL (01EF)      Return if no signal
01F4 B6 8000    LDA A PIA AD    Trigger pressure measurement
01F7 A7 00      STA A 0,X       Store last meas. in memory
01F9 F6 0301    LDA B $0301     Set B for delay loop
01FC 08         INX             Increment storage address
01FD 7A 030E    DEC $ 030E      Decrement nb. measurements
0200 27 3E      BEQ (023F)      Continue if zero
0202 5A         DEC B           Delay loop
0203 26 FD      BNE (0202)      Return if not zero
0205 20 ED      BRA (01F4)      Take next measurement

0207 B6 8000    LDA A PIA AD    Reset CA1
020A B6 8001    LDA A PIA AC    Check for CA1-TDC signal
020D 2A FB      BPL (020A)      Return if no signal
020F B6 8000    LDA A PIA AD    Trigger pressure measurement
0212 A7 00      STA A 0,X       Store last meas. in memory
0214 F6 0301    LDA B $0301     Set B for delay loop
0217 08         INX             Increment storage address
0218 01         NOP             Extra delay
0219 7A 030E    DEC $030E       Decrement nb. measurement
021C 27 22      BEQ (023F)      Continue if zero
021E 5A         DEC B           Delay loop
021F 26 FD      BNE (021E)      Return if not zero
0221 20 EC      BRA (020F)      Take next measurement

0223 B6 8000    LDA A PIA AD    Reset CA1
0226 B6 8001    LDA A PIA AC    Check for CA1-TDC signal
0229 2A FB      BPL (0226)      Return if no signal
022B B6 8000    LDA A PIA AD    Trigger pressure measurement
022E A7 00      STA A 0,X       Store last meas. in memory
0230 F6 0301    LDA B $0301     Set B for delay loop
0233 08         INX             Increment storage address
0234 01         NOP             Extra delay
0235 01         NOP
0236 7A 030E    DEC $030E       Decrement nb. measurements
0239 27 05      BEQ (023F)      Continue if zero
023A 5A         DEC B           Delay loop
023B 26 FD      BNE (023A)      Return if not zero
023D 20 EB      BRA (022B)      Take next measurement

023F C6 1F      LDA B #$1F      Set B for delay loop
0241 5A         DEC B
0242 26 FD      BNE (0241)      Return if not zero
0244 B6 8000    LDA A PIA AD    Reset CA1
0247 B6 8001    LDA A PIA AC    Check for CA1-TDC signal
024A 2A FB      BPL (0256)      Return if no signal
024C C6 1F      LDA B #$1F      Set B for delay loop
```

```
024E 5A        DEC B
024F CE 0410   LDX #$0410      Return if not zero
0252 7F 031F   CLR $031F       Transfer memory
0255 A6 00     LDA A 0,X       Load data
0257 E6 01     LDA B 1,X
0259 FF 031C   STX $031C       Store source address
025C FE 031E   LDX $031E       Load destination address
025F A7 00     STA A 0,X       Store data
0261 E7 01     STA B 1,X
0263 08        INX
0264 08        INX
0265 FF 031E   STX $031E
0268 FE 031C   LDX 031C
026B 08        INX
026C 08        INX
026D 8C 048F   CMPX $048F      Check for end of data
0270 26 E3     BNE (0255)
0272 7A 0310   DEC $0310       Decrement nb. of cycles
0275 27 03     BEQ (027A)      Continue if zero
0277 7E 0127   JMP $0127       Return to measurement loop
027A FE 0304   LDX $0304       Time measur. in X
027D 3F        SWI             Stop
```

Triggered data acquisition program

```
0100 5F        CLR B
0101 F7 8001   STA B PIA AC   Set PIA for DDR access
0104 F7 8000   STA B PIA AD   Set DDR as input
0107 86 3E     LDA A #$3E     00111110
0109 B7 8001   STA A PIA AC   Reset CA2
010C 86 2E     LDA A #$2E     00101110
010E B7 8001   STA A PIA AC   Set CA1 and CA2 control
0111 B7 8003   STA A PIA BC   Set CB1 control
0114 CE 01FC   LDX #$01FC     Load first storage address
0117 B6 8000   LDA A PIA AD   Reset CA1
011A C6 03     LDA B #03
011C F7 01F9   STA B $01F9    Store number of cycles
011F C6 82     LDA B #$82     130
0121 F7 01FB   STA B $01FB    Store number of measurements
0124 C6 0F     LDA B #$0F     15
0126 F7 01FA   STA B #$01FA   Store nb. of pre-TDC signals
0129 B6 8001   LDA A PIA AC   Check for CA1-TDC signal
012C 2A FB     BPL (0129)     Return if no signal
012E C6 1F     LDA B #$1F     Set B for delay loop
0130 5A        DEC B          Decrement B
0131 26 FD     BNE (0130)     Return if not zero
0133 B6 8002   LDA A PIA BD   Reset CB2
0136 B6 8003   LDA A PIA BC   Check for CB1-position signal
0139 2A FB     BPL (0136)     Return if no signal
013B 7A 01FA   DEC $01FA      Decrement nb. pre-TDC signals
013E 26 EE     BNE (0136)     Return if not zero
0140 B6 8000   LDA A PIA AD   Trigger pressure measurement
                              and read previous one
0143 A7 00     STA A 0,X      Store pressure measurement
0145 E7 01     STA B 1,X      Store time interval
0147 08        INX            Increment storage address
0148 08        INX
0149 7A 01FB   DEC $01FA      Decrement nb. measurements
014C 27 11     BEQ (015F)     Continue if zero
014E C6 0F     LDA B #$0F     Set B for delay loop
0150 5A        DEC B          Decrement B
0151 26 FD     BNE 0150       Return if not zero
0153 B6 8002   LDA A PIA BD   Reset CB1
0156 5F        CLR B          Clear B register
0157 5C        INC B          Count number of loops
0158 B6 8003   LDA A PIA BC   Check for CB1-position signal
015B 2B E3     BMI (0140)     Return to measure if signal
015D 20 F8     BRA (0157)     Return to count if no signal
015F 7A 01F9   DEC #01F9      Decrement nb. of cycles count
0162 27 0B     BEQ (0170)     Continue if zero
0164 C6 80     LDA B #$80     128
0166 F7 01FB   STA B $01FB    Reset number of measurements
0169 C6 0A     LDA B #$0A     Set B for delay loop
016B 6F 02     CLR 2,X        Delay instruction
016D 01        NOP            Delay instruction
016E 20 E1     BRA (0150)     Return to measurement loop
0170 C6 0F     LDA B #$0F     Set B for delay loop
```

```
0172 5A        DEC B          Decrement B
0173 26 FD     BNE (0172)     Return if not zero
0175 B6 8000   LDA A PIA AD   Read last pressure measurement
0178 A7 00     STA A 0,X      Store pressure measurement
017A 3F        SWI            Stop
```

1.PRO.TXT

```
            ORG $0100
PIAAC       EQU $E071
PIAAD       EQU $E070
PIABC       EQU $E073
PIABD       EQU $E072
            CLR B           Initializa PIA
            STB PIAAC
            STB PIAAD
            LDA #$3C
            STA PIAAC
            LDA #$2C
            STA PIAAC
            STA PIABC
A           LDA PIABD       Reset CB1
B           LDA PIABC       Check CB1 for position signal
            BPL B
            LDB #$0F        Delay loop
C           DEC B
            BNE C
            LDA PIABD
            BRA A           Return
            SWI
            END
```

1.PRO2.TXT

```
                ORG $0100
PIAAC           EQU $E071
PIAAD           EQU $E070
                CLR B           Initializa PIA
                STB PIAAC
                STB PIAAD
                LDA #$3C
                STA PIAAC
                LDA #$2C
                STA PIAAC
A               LDA PIAAD       Reset CA1-trigger SOC
                NOP             Delay
                NOP
                NOP
                NOP
                BRA A           Return
                SWI
                END
```

1.PRO3.TXT

```
                ORG $0100
PIAAC           EQU $E071
PIAAD           EQU $E070
PIABC           EQU $E073
PIABD           EQU $E072
PDATA           EQU $FDAE
                LDA #$82        Set number of data points per cycle
                STA $0300
                CLR B           Initializa PIA
                STB PIAAC
                STB PIAAD
                LDA #$3C
                STA PIAAC
                LDA #$2C
                STA PIAAC
                STA PIABC
                LDA PIAAD       Reset CA1
A1              LDA PIAAC       Check CA1 for TDC signal
                BPL A1
                LDX #$0000      Clear timer
                LDA PIAAD       Reset CA1
B1              LDA PIAAC       Check CA1 for TDC signal
                BMI C1
                INX             Count loops
                BRA B1
C1              STX $0302       Store time for one cycle
                LDX #$03FF      Set memory address for data
A               LDA PIAAD       Reset CA1
B               LDA PIAAC       Check CA1 for TDC signal
                BPL B
C               LDA PIABD       Reset CB1-trigger first measurement
D               LDA PIABC       Check CB1 for position signal
                BPL D
                LDA PIAAD       Trigger measurement-read previous
                                one-reset CB1
                STA 0,X+        Store measurement
                DEC $0300       Decrement number of measurements
                BNE C
                LDX #$0400      Set memory addresses for data
                LDY #$1000      conversion to ASCII
CONV            LDA 0,X         Convert left half of first byte
                JSR CONVHL
                LDA 0,X+        Convert right half of first byte
                JSR CONVHR
                LDA 0,X         Convert left half of second byte
                JSR CONVHL
                LDA 0,X+        Convert right half of second byte
                JSR CONVHR
                LDA #$0D        Issue "Return"
                STA 0,Y+
                LDA #$0A        Issue "Line Feed"
```

```
            STA 0,Y+
            LDA #$04        Issue "EOT"
            STA 0,Y+
            CPX #$0500      Check if all data converted
            BNE CONV
            LDX $0302       Put first data point in X
            SWI
CONVHL      LSR A           Conversion subroutine
            LSR A           Prepare left half for conversion
            LSR A
            LSR A
CONVHR      AND A #$F       Convert hex value to ASCII
            ADD A #$30
            CMP A #$39
            BLS OUTCHA
            ADD A #7
OUTCHA      STA 0,Y+        Store converted character
            RTS
            END
```

1.PRO4.TXT

```
                ORG $0100
PIAAC           EQU $E071
PIAAD           EQU $E070
PDATA           EQU $FDAE
                LDA #$FF        Set number of cycles to be timed
                STA $0300
                CLR B           Initializa PIA
                STB PIAAC
                STB PIAAD
                LDA #$3C
                STA PIAAC
                LDA #$2C
                STA PIAAC
                LDY #$0400
                LDA PIAAD       Reset CA1
A1              LDA PIAAC       Check CA1 for TDC signal
                BPL A1
START           LDX #$0000      Clear timer
                LDA PIAAD       Reset CA1
B1              LDA PIAAC       Check CA1 for TDC signal
                BMI C1
                INX             Count loops
                BRA B1
C1              STX 0,Y++       Store time for one cycle
                DEC $0300       Decrement number of cycles
                BNE START       Return if not zero
                LDX #$0400      Set memory addresses for data
                LDY #$1000      conversion to ASCII
CONV            LDA 0,X         Convert left half of first byte
                JSR CONVHL
                LDA 0,X+        Convert right half of first byte
                JSR CONVHR
                LDA 0,X         Convert left half of second byte
                JSR CONVHL
                LDA 0,X+        Convert right half of second byte
                JSR CONVHR
                LDA #$0D        Issue "Return"
                STA 0,Y+
                LDA #$0A        Issue "Line Feed"
                STA 0,Y+
                LDA #$04        Issue "EOT"
                STA 0,Y+
                CPX #$0500      Check if all data converted
                BNE CONV
                LDX $0400       Put first data point in X
                LDY $04FE       Put last data point in Y
                SWI
CONVHL          LSR A           Conversion subroutine
                LSR A           Prepare left half for conversion
                LSR A
                LSR A
```

```
CONVHR    AND A #$F       Convert hex value to ASCII
          ADD A #$30
          CMP A #$39
          BLS OUTCHA
          ADD A #7
OUTCHA    STA 0,Y+        Store converted character
          RTS
          END
```

Velocity fluctuation program

```
                    *BATCH FTG1CG F@GL000 F@GL (010,020)
                    ************************************************************************

FORTRAN IV G1  RELEASE 2.0              MAIN                DATE = 85103          20/29/15

0001                 REAL L,MUP,MU2P,MU3P,MU,M1,M2,M3,MCK,MR,MP,M(129),X(129),W(774),
                    *OMEGA(129),LAMBDA,MGR,LOAD,IN,INR,MAVG,SMOOTH(129),C(128,3),
                    *DATA1(2,129),DATA2(2,129),WORK(2,129)
0002                 INTEGER ICHAR(3)
0003                 INTEGER*2 DATA,INPUT(128),INPUT2(128)
0004                 DIMENSION T(129),CPHI(129),SPEED(129),SPEED1(129),
                    *SPEED2(129),YMAX(3),YMIN(3)
0005                 DATA ICHAR/'0','*','S'/
0006                 MCK=1.341
0007                 MR=0.087
0008                 MP=0.178
0009                 R=0.022225
0010                 L=0.079375
0011                 SCK=0.00504
0012                 SR=0.0165
0013                 LAMBDA=R/L
0014                 IN=0.003847849
0015                 INR=0.00009316
0016                 A=0.0028581
0017                 FRING=7.50
0018                 MUP=0.0009
0019                 MU2P=0.0005
0020                 MU3P=0.00005
0021                 MU=0.30
0022                 LOAD=0.
0023                 READ(5,100)(INPUT(I),I=1,128)
0024           100   FORMAT(Z2,127(/,Z2))
0025                 CALL RPM(SPEED,INPUT)
0026                 AMP=0.
0027                 DO 2 I=1,129
0028                 AMP=AMP+SPEED(I)
0029                 X(I)=(I-1)*5.625
0030           2     CONTINUE
0031                 AMP=AMP/129.
0032                 OMEGAM=AMP*3.141593/30.
0033                 OMEGA(1)=OMEGAM*0.95
0034                 CALL AVERAG(SPEED,SMOOTH)
               C     WRITE(6,101)
0035           101   FORMAT('1',6X,'PHI',10X,'F',9X,'R',9X,'P',9X,'Q',9X,'M',9X,'MG'
                    *,8X,'X')
0036                 DO 10 I=1,129
0037                 READ(5,102)DATA
0038           102   FORMAT(Z2)
0039                 VOLT=DATA*0.04/7.5
0040                 PRESS=((VOLT-0.35)/0.00539)
0041                 IF (I.LT.33) GO TO 6
0042                 IF (I.LT.65) GO TO 5
0043                 IF (I.LT.97) GO TO 6
0044           5     SIGN=1.
0045                 GO TO 7
0046           6     SIGN=-1.
0047           7     F=(PRESS*A*6895.)+(FRING*SIGN)
0048                 PHI=(I-1)*0.09817
0049                 XPP=(OMEGAM**2)*R*(COS(PHI)+(L/LAMBDA)*COS(2*PHI)))
```

```
0050                    R1=(F-MP*XPP)/(1-MU*LAMBDA*SIN(PHI)*SIGN)
0051                    R2=R1-(MR*XPP*SR/L)
0052                    P2=-(MR*(1-SR/L)*(OMEGAM**2)*R)+(R2*(1-LAMBDA*(SIN(PHI)**2)))
0053                    P1=R2*SIN(PHI)*(1+LAMBDA*COS(PHI))
0054                    P=SQRT((P1**2)+(P2**2))
0055                    Q1=P2-(MCK*SCK*OMEGAM**2)
0056                    Q=SQRT((Q1**2)+(P1**2))
0057                    PD=5.625*(I-1)
0058                    M1=MUP*Q*0.000127
0059                    M2=MU2P*P*0.000127
0060                    M3=MU3P*R1*0.0000762
0061                    SKRT=SQRT(((L/R)**2)-(SIN(PHI)**2))
0062                    RK=R*SIN(PHI)*((COS(PHI)/SKRT)+1)
0063                    MGR=R1*RK
0064                    M(I)=MGR-M1-M2-M3-LOAD
0065                    COSCHI=SQRT((L**2)-((R*SIN(PHI))**2))
0066                    XX=R*(1-COS(PHI))+(L-COSCHI)
                  C     WRITE(6,103) PD,F,R1,P,Q,M(I),MGR,XX
0067              103   FORMAT (5X,F7.3,6(2X,F8.1),2X,F9.6)
0068                    CPHI1=(MP+MR)*(R**2)*((SIN(PHI)+(LAMBDA*0.5*SIN(2*PHI)))**2)
0069                    CPHI2=((MR*(R**2)*(L-SR))+INR)*((LAMBDA*COS(PHI))**2)
0070                    CPHI(I)=IN+CPHI1+CPHI2
0071              10    CONTINUE
0072                    WRITE(6,106)
0073              106   FORMAT('1',10X,'THEORETICAL',4X,'AVERAGE    OMEGA(1)')
0074              12    SUM=OMEGA(1)
0075                    ENERGY=CPHI(1)*(OMEGA(1)**2)
0076                    DO 15 I=2,129
0077                    MAVG=(M(I)+M(I-1))/2.
0078                    ENERGY=ENERGY+MAVG*0.09817
0079                    OMEGA(I)=SQRT(ENERGY/CPHI(I))
0080                    SUM=SUM+OMEGA(I)
0081              15    CONTINUE
0082                    AVG=SUM/128.
0083                    WRITE(6,107)AVG,OMEGA(1)
0084              107   FORMAT(25X,2(F10.3))
0085                    IF(ABS(OMEGAM-AVG).LE.1.0) GOTO 18
0086                    IF((OMEGAM-AVG).GE.0.) GOTO 16
0087                    OMEGA(1)=OMEGA(1)-1.0
0088                    IF(OMEGA(1).LE.80.) WRITE(6,108)
0089              108   FORMAT(1X,'OMEGA(1) LE 80')
0090                    IF (OMEGA(1).LE.80.) STOP
0091                    GOTO 12
0092              16    OMEGA(1)=OMEGA(1)+1.0
0093                    IF(OMEGA(1).GT.450.) WRITE(6,109)
0094              109   FORMAT(1X,'OMEGA(1) GT 450')
0095                    IF(OMEGA(1).GT.450.) STOP
0096                    GOTO 12
0097              18    WRITE(6,110)OMEGAM
0098              110   FORMAT(' EXPERIMENTAL AVERAGE',3X,F9.2)
0099                    DO 20 J=1,129
0100                    OMEGA(J)=OMEGA(J)*30./3.141593
0101              20    CONTINUE
0102                    OMEGAM=OMEGAM*30./3.141593
```

```
0103                    YMOY=100.*INT(OMEGAM/100.)
0104                    YMAX(1)=YMOY+800.
0105                    YMIN(1)=YMOY-800.
0106                    YMAX(2)=YMAX(1)
0107                    YMIN(2)=YMIN(1)
0108                    YMAX(3)=YMAX(1)
0109                    YMIN(3)=YMIN(1)
0110                    CALL DDPLOT(3,129.0,0.,5.625,ICHAR,YMAX,YMIN,OMEGA,SPEED,SMOOTH,
                       *Y4,Y5,Y6)
0111                    WRITE(6,112)
0112          112       FORMAT('1  PHI     SPEED  OMEGA SPEED-OMEGA  (S-O)/S    DEL1     DEL2
                       *     D1-D2  (D1-D2)/D2')
0113                    AVV=0.
0114                    DO 25 I=1,129
0115                    IPHI=(I-1)*5.625
0116                    RTY=OMEGA(I)
0117                    RTY2=SPEED(I)-RTY
0118                    RTY3=RTY2/SPEED(I)
0119                    DEL1=SPEED(I)-AMP
0120                    DEL2=RTY-AMP
0121                    DEL3=DEL1-DEL2
0122                    DEL4=DEL3/DEL1
0123                    AVV=AVV+ABS(RTY3)
0124                    WRITE(6,113) IPHI,SPEED(I),RTY,RTY2,RTY3,DEL1,DEL2,DEL3,DEL4
0125                    DATA1(1,I)=SPEED(I)
0126                    DATA1(2,I)=0.0
0127                    DATA2(1,I)=OMEGA(I)
0128                    DATA2(2,I)=0.0
0129          25        CONTINUE
0130                    AVV=AVV/129.
0131                    WRITE(6,114)
0132                    WRITE(6,115) AVV
0133          113       FORMAT(1X,I5,3F9.1,F8.3,3F9.1,F8.3)
0134          114       FORMAT(' MEAN ABS((S-O)/S)')
0135          115       FORMAT(1X,F8.3)
0136                    CALL FOURT(DATA1,129,1,-1,1,WORK,129)
0137                    CALL FOURT(DATA2,129,1,-1,1,WORK,129)
0138                    WRITE(6,116)
0139          116       FORMAT('1',10X,'I',6X,'TRANSFORM SPEED',12X,'OMEGA')
0140                    DO 30 I=1,129
0141                    WRITE(6,117) I,DATA1(1,I),DATA1(2,I),DATA2(1,I),DATA2(2,I)
0142          117       FORMAT(8X,I3,4(3X,F9.3))
0143          30        CONTINUE
0144                    DO 35 I=9,129
0145                    DATA1(1,I)=0.
0146                    DATA1(2,I)=0.
0147                    DATA2(1,I)=0.
0148                    DATA2(2,I)=0.
0149          35        CONTINUE
0150                    CALL FOURT(DATA1,129,1,1,1,WORK,129)
0151                    CALL FOURT(DATA2,129,1,1,1,WORK,129)
0152                    DO 40 I=1,129
0153                    SPEED(I)=DATA1(1,I)/129.
0154                    OMEGA(I)=DATA2(1,I)/129.
```

```
FORTRAN IV G1  RELEASE 2.0                    MAIN                    DATE = 85103          20/29/15

0155              40     CONTINUE
0156                     CALL DDPLOT(3.129.0.0..5.625.ICHAR.YMAX.YMIN.OMEGA.SPEED.SMOOTH.
                        *Y4.Y5.Y6)
0157                     STOP
0158                     END

 *OPTIONS IN EFFECT*   NOTERM.ID.EBCDIC.SOURCE.NOLIST.NODECK.LOAD.NOMAP.NOTEST
 *OPTIONS IN EFFECT*   NAME = MAIN      . LINECNT =        56
 *STATISTICS*     SOURCE STATEMENTS =        158.PROGRAM SIZE =      17608
 *STATISTICS*  NO DIAGNOSTICS GENERATED
```

```
FORTRAN IV G1  RELEASE 2.0                RPM                    DATE = 85103          20/29/15

0000:                      SUBROUTINE RPM(SPEED, INPUT)
0002                       INTEGER*2 INPUT(128)
0003                       REAL SPEED(129)
0004                       DO 15 J=1,128
0005                       SPEED(J)=INPUT(J)*1.
0006                15     CONTINUE
0007                       DO 100 K=1,128
0008                       TIME=(14*SPEED(K)+142)*1.04E-6
0009                       SPEED(K)=60./(TIME*64)
0010                100    CONTINUE
0011                       SPEED(1)=(SPEED(2)+SPEED(128))/2.
0012                       SPEED(129)=SPEED(1)
0013                       RETURN
0014                       END

 *OPTIONS IN EFFECT*   NOTERM,ID,EBCDIC,SOURCE,NOLIST,NODECK,LOAD,NOMAP,NOTEST
 *OPTIONS IN EFFECT*   NAME = RPM       , LINECNT =      56
 *STATISTICS*     SOURCE STATEMENTS =        14,PROGRAM SIZE =      536
 *STATISTICS*   NO DIAGNOSTICS GENERATED
```

```
FORTRAN IV G1  RELEASE 2.0                AVERAG                DATE = 85103          20/29/15

 0001                       SUBROUTINE AVERAG(SPEED,SMOOTH)
 0002                       REAL SPEED(129),SMOOTH(129),INTER(129)
 0003                       INTER(1)=SPEED(1)*0.75+SPEED(2)*0.25
 0004                       DO 10 I=2,128
 0005                       INTER(I)=SPEED(I-1)*0.25+SPEED(I)*0.5+SPEED(I+1)*0.25
 0006                 10    CONTINUE
 0007                       INTER(129)=SPEED(128)*0.25+SPEED(129)*0.75
 0008                       SMOOTH(1)=INTER(1)*0.75+INTER(2)*0.25
 0009                       DO 20 I=2,128
 0010                       SMOOTH(I)=INTER(I-1)*0.25+INTER(I)*0.5+INTER(I+1)*0.25
 0011                 20    CONTINUE
 0012                       SMOOTH(129)=SMOOTH(128)*0.25+SMOOTH(I)*0.75
                      C     DAT4
 0013                       RETURN
 0014                       END

  *OPTIONS IN EFFECT*   NOTERM,ID,EBCDIC,SOURCE,NOLIST,NODECK,LOAD,NOMAP,NOTEST
  *OPTIONS IN EFFECT*   NAME = AVERAG  , LINECNT =      56
  *STATISTICS*     SOURCE STATEMENTS =      14,PROGRAM SIZE =     1110
  *STATISTICS*  NO DIAGNOSTICS GENERATED

  *STATISTICS*  NO DIAGNOSTICS THIS STEP


                                                        VS LOADER

OPTIONS USED - PRINT,NOMAP,NOLET,CALL,NORES,NOTERM,SIZE=204800,NAME=**GO

  TOTAL LENGTH     EA28
  ENTRY ADDRESS  118010
```

	THEORETICAL	AVERAGE	OMEGA(1)
		211.560	199.778
		210.630	198.778
EXPERIMENTAL AVERAGE		210.29	

1.GRAPH.BAS
Data analysis program

```
10 DIM D(129),D1(4,33),DS(4,33),D2(129),T(15)
12 PRINT "DATA FILE TO BE ANALYZED:"
   REM INPUT NAME OF FILE TO BE PROCESSED
13 INPUT F$
14 PRINT "DO YOU WISH TO SHIFT DATA? ANSWER BY 0, N (LEFT)
   OR -N (RIGHT)"
15 INPUT N1
   REM SHIFT TO CORRECT PHASE ERROR
16 PRINT "DO YOU WISH A VERTICAL OFFSET? ANSWER BY 0 OR N
   (LOWER)"
17 INPUT N3
   REM OFFSET AND SCALE TO OPTIMIZE OUTPUT
18 PRINT "INPUT SCALE FACTOR (NORMAL=1)"
19 INPUT N2
20 PRINT "DO YOU WANT NORMAL (N) OR LOG (L) PLOTTING?"
25 INPUT G$
26 OPEN OLD F$ AS 1
30 INPUT #1,A$
   REM READ AND DISPLAY TITLE OF FILE
40 PRINT A$
   REM READ HEX DATA AND CONVERT TO ASCII
50 FOR I=1 TO 129
60 INPUT #1,B$
70 D(I)=HEX(B$)
   REM COREECT INVALID DATA
80 IF D(I)=0 THEN D(I)=D(I-1)
100 NEXT (I)
    REM PERFORM SHIFT TO THE RIGHT
101 IF N1=0 THEN GOTO 129
102 IF N1>0 THEN GOTO 114
103 FOR I=1 TO -N1
104 T(I)=D(I)
105 NEXT I
106 FOR I=1 TO 129+N1
107 D(I)=D(I-N1)
108 NEXT I
109 FOR I=129+N1+1 TO 129
110 D(I)=T(I-(129+N1))
111 NEXT I
113 GOTO 129
    REM PERFORM SHIFT TO THE LEFT
114 FOR I=129-N1+1 TO 129
115 T(I-(129-N1))=D(I)
116 NEXT I
117 FOR I=129 TO (N1+1) STEP -1
118 D(I)=D(I-N1)
119 NEXT I
120 FOR I=N1 TO 1 STEP -1
121 D(I)=T(I)
122 NEXT I
    REM BREAK DOWN DATA INTO FOUR STROKES
```

```
129 IF D(1)=0 THEN D(1)=D(129)
130 FOR I=1 TO 33
140 I1=66-1:I2=64+I:I3=130-I
150 D1(1,I)=D(I)
160 D1(2,I)=D(I1)
170 D1(3,I)=D(I2)
180 D1(4,I)=D(I3)
190 NEXT I
195 FOR J=1 TO 4
200 GOSUB 1000
    REM SUB 1000 CONVERTS PRESSURE-ANGLE DATA INTO PRESSURE-
    VOLUME DATA
205 NEXT J
210 GOSUB 1500
    REM SUB 1500 REASSEMBLES THE FOUR STROKES INTO ONE
    VARIABLE
    REM INVOKE "BASGRAPH" TO DISPLAY P-V DIAGRAM
215 HT%=2
220 CD%=0
230 XV=0:YV=0:GOSUB 30000
240 CD%=2
250 XV=2:YV=1:GOSUB 30000
    REM PLOT FIRST STROKE
260 FOR I=1 TO 32
270 CD%=3
275 IF G$="L" THEN 292
    REM NORMAL PLOTTING
280 YV=N2*D2(I)+1-N3
290 XV=XV+0.08
291 GOTO 300
    REM LOG PLOTTING
292 YV=N2*LOG(D2(I))+1-N3
294 XV=3.66*LOG(I*0.0258+0.1742)+6.5
300 GOSUB 30000
310 NEXT I
    REM PLOT SECOND STROKE
320 FOR I=33 TO 64
330 CD%=3
335 IF G$="L" THEN 352
    REM NORMAL PLOTTING
340 YV=N2*D2(I)+1-N3
350 XV=XV-0.08
351 GOTO 360
    REM LOG PLOTTING
352 YV=N2*LOG(D2(I))+1-N3
354 XV=3.66*LOG((65-I)*0.0258+0.1742)+6.5
360 GOSUB 30000
370 NEXT I
    REM PLOT THIRD STROKE
380 FOR I=65 TO 96
390 CD%=3
395 IF G$="L" THEN 412
    REM NORMAL PLOTTING
400 YV=N2*D2(I)+1-N3
```

```
410 XV=XV+0.08
411 GOTO 420
    REM LOG PLOTTING
412 YV=N2*LOG(D2(I))+1-N3
414 XV=3.66*LOG((I-64)*0.0258+0.1742)+6.5
420 GOSUB 30000
430 NEXT I
    REM PLOT FOURTH STROKE
440 FOR I=97 TO 128
450 CD%=3
455 IF G$="L" THEN 472
    REM NORMAL PLOTTING
460 YV=N2*D2(I)+1-N3
470 XV=XV-0.08
471 GOTO 480
    REM LOG PLOTTING
472 YV=N2*LOG(D2(I))+1-N3
474 XV=3.66*LOG((129-I)*0.0258+0.1742)+6.5
360 GOSUB 30000
370 NEXT I
500 CLOSE 1
505 XV=2"YV=0:GOSUB 30000
510 INPUT C$
520 CD%=4
530 YV=2:YV=0:GOSUB 30000
540 IF C$="YES" THEN GOTO 12
550 STOP
```

SUBROUTINE 1000

```
1000 DS(J,1)=D1(J,1)
1010 DS(J,2)=.815*D1(J,4)+.185*D1(J,5)
1020 DS(J,3)=.462*D1(J,5)+.538*D1(J,6)
1030 DS(J,4)=.391*D1(J,6)+.609*D1(J,7)
1040 DS(J,5)=.471*D1(J,7)+.529*D1(J,8)
1050 DS(J,6)=.640*D1(J,8)+.360*D1(J,9)
1060 DS(J,7)=.868*D1(J,9)+.132*D1(J,10)
1070 DS(J,8)=.147*D1(J,9)+.853*D1(J,10)
1080 DS(J,9)=.461*D1(J,10)+.539*D1(J,11)
1090 DS(J,10)=.793*D1(J,11)+.207*D1(J,12)
1100 DS(J,11)=.146*D1(J,11)+.854*D1(J,12)
1110 DS(J,12)=.515*D1(J,12)+.485*D1(J,13)
1120 DS(J,13)=.890*D1(J,13)+.110*D1(J,14)
1130 DS(J,14)=.273*D1(J,13)+.727*D1(J,14)
1140 DS(J,15)=.659*D1(J,14)+.341*D1(J,15)
1150 DS(J,16)=.045*D1(J,14)+.955*D1(J,15)
1160 DS(J,17)=.428*D1(J,15)+.572*D1(J,16)
1170 DS(J,18)=.808*D1(J,16)+.192*D1(J,17)
1180 DS(J,19)=.179*D1(J,16)+.821*D1(J,17)
1190 DS(J,20)=.537*D1(J,17)+.463*D1(J,18)
1200 DS(J,21)=.886*D1(J,18)+.114*D1(J,19)
1210 DS(J,22)=.214*D1(J,18)+.786*D1(J,19)
1220 DS(J,23)=.518*D1(J,19)+.482*D1(J,20)
1230 DS(J,24)=.800*D1(J,20)+.200*D1(J,21)
```

```
1240 DS(J,25)=.050*D1(J,20)+.950*D1(J,21)
1250 DS(J,26)=.249*D1(J,21)+.751*D1(J,22)
1260 DS(J,27)=.399*D1(J,22)+.601*D1(J,23)
1270 DS(J,28)=.481*D1(J,23)+.519*D1(J,24)
1280 DS(J,29)=.472*D1(J,24)+.528*D1(J,25)
1290 DS(J,30)=.331*D1(J,25)+.669*D1(J,26)
1300 DS(J,31)=D1(J,27)
1310 DS(J,32)=.220*D1(J,28)+.780*D1(J,29)
1320 DS(J,33)=D1(J,33)
1330 RETURN
```

SUBROUTINE 1500

```
1500 FOR I=1 TO 33
1510 D2(I)=DS(1,I)
1520 NEXT I
1530 FOR I=34 TO 65
1540 J=66-1
1550 D2(I)=DS(2,J)
1560 NEXT I
1570 FOR I=66 TO 97
1580 J=I-64
1590 D2(I)=DS(3,J)
1600 NEXT I
1610 FOR I=98 TO 129
1620 J=130-I
1630 D2(I)=DS(4,J)
1640 NEXT I
1650 RETURN
```